UCRL-19300

THE CHARGED PION LIFETIME MEASURED IN FLIGHT

Arthur J. Greenberg
(Ph. D. Thesis)

August 1, 1969

AEC Contract No. W-7405-eng-48

LAWRENCE RADIATION LABORATORY
UNIVERSITY of CALIFORNIA BERKELEY

UCRL-19300

DISCLAIMER

THE CHARGED PION LIFETIME MEASURED IN FLIGHT

Contents

THE CHARGED PION LIFETIME MEASURED IN FLIGHT

Lawrence Radiation Laboratory
University of California
Berkeley, California

ABSTRACT

The lifetime of the charged pi meson was found by determining as a function of distance the number of surviving pions in a narrow beam. Measurements for both π^+ and π^- were made along a 36-ft decay path, equivalent to 0.6 lifetime, using a movable pion detector. The monitor counters defining the beam were designed so that the measured attenuation with distance was due solely to pion decay and not to loss of scattered particles. The attenuation together with the pion velocity, derived from a precise time-of-flight measurement, determined the lifetime. The movable counter and the pion detector in the monitor system were differential Cerenkov counters with a liquid hydrogen radiator. The lifetime measured in this experiment with pions in flight, 26.02 ± 0.04 nsec, is in agreement with other equally precise experiments with positive pions at rest. Comparison of the lifetimes measured with pions in these two states of motion is relevant to the question of microcausality in field theory.

I. INTRODUCTION

A. Different Experimental Methods

Since the discovery of the charged pi meson, its mean life has been measured by a variety of procedures. The most frequently used method consists of stopping positive pions in a scintillator and measuring the timing of the decay muon in the same, or an adjacent, scintillator. In early experiments of this type, photographs of oscilloscope traces were measured by hand to determine the timing for each event. With the use of a time-to-height converter and a multichannel, pulse-height analyzer, the statistical error can be easily reduced. The two most precise measurements of the positive lifetime were made with stopping pions and employed such electronics.

The negative lifetime can not be measured by the same technique. When a negative pion slows down in matter, it enters a Bohr orbit and interacts with a nucleus. Capture by the nucleus, a strong interaction, has a rate far exceeding the rate for free decay, a weak interaction. (In contrast, negative muons interact weakly with nuclei, and their lifetime can be determined from stopping measurements.) There has been recent interest in testing CPT invariance by experiments comparing the lifetimes of pions of both signs. In order to measure both lifetimes by the same method, these experiments used a pion beam which could be changed in sign and compared the attenuation as a function of distance along the beam path. The measurements determine the absolute lifetime in addition to the lifetime ratio.

The experiment described here is of this type.[1] In previous beam measurements the emphasis was on the test of CPT, and because of the design of the experiments the lifetime ratio was more free of systematic errors

than the absolute lifetime. The quoted errors in the lifetime for these earlier beam experiments were much greater than the errors for experiments with stopping pions, and the values for the lifetime disagreed not only with each other but with the stopping measurements. Table I gives the results for experiments of both types.

Table I. Measurements of the charged pion lifetime. (Values are in nanoseconds.)

Most precise experiments with stopping pions	
Eckhause et al.[2]	26.02±0.04
Nordberg et al.[3]	26.04±0.05
Experiments with pions in flight	
Bardon et al.[4]	25.6±0.3
Lobkowicz et al.[5]	26.67±0.24
Ayres et al.[6]	26.6±0.2
Petrukhin et al.[7]	24.8±0.4
This experiment	26.02±0.04

One motivation for determining the lifetime by a different technique is that all recent experiments with stopping pions used such similar arrangements of counters and electronics. Thus, while they all shared the advantages of this approach, they conceivably also shared unknown systematic difficulties. Systematic errors in the method can indeed be significant. The recent Rochester measurement with stopping pions (Ref. 3) was motivated by an earlier experiment which disagreed with the William and Mary result (Ref. 2) by some four standard deviations.[8]

This experiment and that of Ref. 6, both performed at the Lawrence Radiation Laboratory's 184-in. cyclotron, used the same technique. The

author and several of the collaborators who carried out the present experiment participated in the earlier one. The first experiment had an error comparable to the other beam measurements and was just as much in disagreement with the stopping measurements. Nevertheless, its method was potentially more suitable for a precise measurement of the lifetime of pions in flight than were the other beam techniques. The experience of the first experiment and the increased understanding of the system during the course of the later one enabled systematic errors in the technique to be discovered. It is felt that the difficulties in the first experiment are now understood and that the present experiment has eliminated or properly taken into account, the major systematic limitations of the method.

A measurement of a time interval must be calibrated against some standard of sufficient accuracy. Experiments with pions at rest typically use a high-frequency oscillator. Calibration of the frequency of the oscillator presents no difficulty. In experiments with pions in motion, the velocity of the particles is needed to convert the observations at different distances from the point of production to corresponding times. Because of the velocity dependence of the time-dilation factor, a more precise value of the velocity is required to calculate the lifetime in the pion rest frame--the fundamental quantity--than the lifetime in the laboratory frame. Assuming pure exponential decay, the probability a pion existing at $t = 0$ has not decayed at time t in the laboratory is $\exp(-t/\gamma\tau)$, where τ is the lifetime in the rest frame. In terms of x, the distance of the pion from its position at $t = 0$, the exponent can be rewritten as

$$\frac{t}{\gamma\tau} = \frac{x}{\beta c\gamma\tau} = \frac{mx}{p\tau} .$$

The observed attenuation depends on the product of the momentum p and the lifetime; thus the relative error in the lifetime can be no smaller than that of the momentum. Because $dp/d\beta$ is large for relativistic particles, a given relative uncertainty in τ requires a much greater precision for the velocity.

A beam experiment can derive the lifetime from the observed attenuation with distance by determining either the velocity or the momentum of the beam. This experiment relied on a time-of-flight measurement of the beam velocity. The calibration of the time-of-flight system used a high-frequency oscillator. Thus the fundamental time standard was essentially the same as for experiments with stopping pions.

One feature all beam experiments require is a monitor system of counters establishing a beam whose lateral extent is sharply defined over the entire decay path. The difference in the number of pions at the beginning and at the end of this distance must be due solely to particle decay. Any pions which miss the final detector cause the measured lifetime to be too short. Measuring the number of surviving pions at two or more positions along the decay path determines the lifetime.

It is not essential that <u>both</u> the monitor system and the final detector be able to distinguish pions from other particles in the beam. In fact, only this experiment and its earlier version used a final detector that distinguished pions. The other experiments identified pions at some point ahead of the decay path. Data from the final detector had to be corrected by calculating the effect of pion decay products which counted. The calculation is simplified by the fact that pions decay primarily by a two-body mode with a single charged particle. Predicting the effect of detecting decay muons, however, requires knowing the spatial

distribution of pions along the decay path. To determine this distribution experimentally requires a downstream pion detector, which is lacking in these other experiments.

There are other disadvantages in not being able to distinguish pions from decay muons along the decay path. The maximum lateral extent, the envelope, of the pions in the beam can not be directly measured to test whether this envelope is smaller than the aperture of the downstream counter at all positions along the decay path. Also, if decay muons count in the detector, the total number of counts depends on its precise lateral position. The number of decay muons decreases with radial distance from the beam center line. Thus, with the detector off center, the number of counts decreases even if all pions are still intercepted. A counter which responds only to pions and whose effective aperture is larger than the beam envelope is insensitive to small lateral displacements of its position.

In the earlier version of this experiment the monitor system did not distinguish pions. As long as a constant fraction of the particles defined by the monitor is pions, it is sufficient if only the final counter is a pion detector. If the monitor rejects particles which are not pions, however, the experiment becomes insensitive to fluctuations in the relative intensity of these other particles.

The present experiment is the only one which employed pion detectors both in the monitor and along the decay path. These were differential Cerenkov counters using either liquid hydrogen or deuterium as the radiating medium. The counting rate in the experiment was high enough so that statistical error was not the dominant uncertainty in the final result. Systematic errors associated with the final detector were the major

limitation. A large fraction of the running time involved investigations of systematic difficulties in this counter, and much of the subsequent analysis was concerned with these problems.

B. Relation to Theory

There are two features of theoretical interest in the measurements of the pion lifetime: the value of the lifetime and the possible difference between results obtained for pions at rest and for pions in flight. Goldberger and Treiman were able to express the pion decay rate in terms of the weak-interaction coupling constant and the pion-nucleon coupling constant. The theory of the weak interaction had successfully related reactions involving nucleons and leptons. It was remarkable that the theory could be extended to include another strongly interacting particle, the pion, with the addition of a single parameter. Although the Goldberger-Treiman relation was originally deduced from a dispersion relation calculation, at the present time it can be derived within the framework of other theories. In particular it follows from the partially conserved axial vector current (PCAC) hypothesis.[9]

From the V-A theory of the weak interaction, the expression for the pion decay rate, calculated by the usual techniques of field theory, is

$$\Gamma = \frac{m_\pi}{8\pi}\left(1 - \frac{m_\mu^2}{m_\pi^2}\right)^2 \left(\frac{m_\mu}{m_\pi}\right)^2 f^2 .$$

The rate depends on one parameter, the dimensionless coupling constant f. With conventions consistent with the above equation, the Goldberger-Treiman relation has the form

$$f = \sqrt{2}\ \frac{m_\pi}{M}\ \frac{C_A}{C_V}\ \frac{GM^2}{g} .$$

C_A/C_V, the ratio of the A and V terms in the weak Hamiltonian, is 1.18. g is the pion-nucleon coupling constant; $g^2/4\pi = 15$. The product of the weak-interaction coupling constant G and the square of the proton mass M is 1.01×10^{-5}. The pion lifetime determined by these values is 33 nsec.

For a calculation which involves a strong-interaction vertex, the prediction is quite good. Nevertheless, the theoretical value is 27% too high. Experimental measurements have a far greater precision than is needed for testing existing theories of the decay process.

The second relation of the lifetime measurements to theory concerns special relativity. At present no violations of this theory have been observed. It may be that the structure of space-time is different over very small distances, but that experiments to date have not probed this region. Since high energy phenomena are required to test interactions at small distances, experiments in high energy physics must be used for this type of verification of special relativity. Blokhintsev has examined the degree to which present data of various types support the theory.[10]

Local field theory, which is based on microcausality, assumes that special relativity is valid at arbitrarily small distances. If the theory is to be modified so that the structure of space-time is different for points closer in space than some universal length α, this comparison must be made in an invariant fashion. The usual invariant interval x between the points $x_1 = (t_1, \underline{x}_1)$ and $x_2 = (t_2, \underline{x}_2)$ satisfies $x^2 = (x_1 - x_2)^2 = (t_1 - t_2)^2 - (\underline{x}_1 - \underline{x}_2)^2$. The condition $x^2 \approx 0$ does not ensure $|\underline{x}_1 - \underline{x}_2|$ is small since $x^2 \approx 0$ can occur if $|t_1 - t_2|$ and $|\underline{x}_1 - \underline{x}_2|$ are each small, or $|t_1 - t_2| \approx |\underline{x}_1 - \underline{x}_2|$ although neither is small.

To define nearness in space for two world points it is necessary to introduce a certain time-like unit vector n. The invariant expression $R^2 = (nx)^2 - x^2$ is formed from n and x, the difference between the vectors describing the two points. nx is the (four-dimensional) scalar product of n and x. In contrast to x^2, R^2 is positive-definite, and in the coordinate system for which n = (1, 0, 0, 0), $R^2 = (\underline{x}_1 - \underline{x}_2)^2$. The nearness

of two events is determined by comparing R with α.

Two classes of theories can be developed depending on how the vector n is incorporated into the theory. It can be associated with the elementary particles or with space-time itself. In the first case the vacuum remains homogeneous and isotropic, and the motion of free particles still obeys Lorentz invariance. Within small distances from particles, however, causality can be violated, and this assumption leads to predictions concerning the scattering of particles. Nonlinear field theory is one example of this first class of theories.

The comparison of lifetimes measured for particles at rest and in flight has been treated by a theory of the second type, in which the vector n is associated with the vacuum. In such theories microcausality is again violated. In addition, relativistic invariance is violated because the vector singles out a particular coordinate system, the one in which the space-time inhomogeneities are at rest.

Experimental tests of the homogeneity and isotropy of space-time are of several types. If these symmetries of space-time were not valid, the conservation laws following from them would be violated. Direct tests of conservation of energy, momentum, and angular momentum have not provided a very precise check. Another technique is to compare the scattering cross sections measured in two different coordinate systems.[11] One is the usual system in which one particle is at rest in the laboratory; in the other system, achieved by a colliding-beam experiment, the center of mass of the two particles is at rest. In the future this technique may be a useful test.

Rédei has noted that the form of relativity violation presented by Blokhintsev predicts a deviation from the usual velocity dependence of

particle lifetimes. This deviation was calculated for muons[12] and pions.[13] The procedure was essentially the same in both cases. Noncausality was introduced in the weak interaction of the four fermions involved. For the muon the violation occurs at the $\mu e \nu_\mu \bar{\nu}_e$ vertex and for pions at the $N\bar{N}\mu\bar{\nu}_\mu$ vertex. (Pion decay is assumed to proceed via the $N\bar{N}$ virtual state.) The Hamiltonian for pion decay was written in the form

$$\int\int d^4x\, d^4y\ \bar{\psi}_N(x)\ (1 - \gamma_5)\,\gamma_\lambda\,(1 + \gamma_5)\,\psi_N(x)\,F(x - y)$$

$$\times\,\bar{\psi}_\nu(y)\,(1 - \gamma_5)\,\gamma_\lambda\,(1 + \gamma_5)\,\psi_\mu(y).$$

If the form factor $F(x - y)$ is $\delta(x - y)$, the y integration can immediately be performed, and the Hamiltonian reduces to its usual form, expressing a point interaction. In the calculation of Rédei $F(x - y)$ is non-zero if the two world points have the same time coordinate and have a spatial separation less than the universal length α. The comparison with α is formulated with the vector n as described above.[14]

C. Some Mathematical Considerations

1. Statistical Accuracy

To see the relationship between the accuracy of the determination of τ and the statistical accuracy of the measured attenuation, consider first the case in which measurements are made at only two positions. At the first position the ratio of the number of surviving pions to the number of monitor counts is R_1. At the second position, a distance x from the first, the ratio is R_2. If x is n times the mean decay length (to be denoted by x_o), then $R_2 = R_1 \exp(-n)$. Assuming that R_1 and R_2 have the same relative error $\delta R/R$, this equation implies $\delta n = \sqrt{2}\ (\delta R/R)$. From $n = x/x_o = mx/p\tau$ it follows that $\delta\tau/\tau = \delta n/n = \sqrt{2}\ (1/n)(\delta R/R)$.

In the more general case observations are made at N positions, R_i being measured at position x_i. One seeks the values of R_o and x_o in $R_i = R_o \exp(-x_i/x_o)$ which give the best fit in the least-squares sense. It is convenient to consider the logarithm of the above equation, $\ell n\, R_i = \ell n\, R_o - (1/x_o)x_i$, since the computation for the linear problem $y_i = a + bx_i$ is much simpler. The lifetime is inversely proportional to the parameter b. If all the y_i have the same absolute error (equal weight), the best value for b is

$$b = \frac{N \Sigma\, x_i y_i - \Sigma\, x_i\, \Sigma\, y_i}{N \Sigma\, x_i^2 - (\Sigma\, x_i)^2} = \frac{(1/N)\, \Sigma\, (x_i - \bar{x})y_i}{(1/N)\, \Sigma\, x_i^2 - \bar{x}^2}\ , \text{ where } \bar{x} = \Sigma\, x_i/N,$$

and all sums are for $1 \leq i \leq N$. The expression in the denominator, $(1/N)\, \Sigma\, x_i^2 - \bar{x}^2 = (1/N)\, \Sigma\, (x_i - \bar{x})^2$, has the form of the variance of the x_i and will be denoted by σ_x^2. It is not a statistic, however, since the x_i are assumed to be precisely known. To find the variance of b note that the numerator has been written as the sum of N independent random variables y_i. If all the y_i have the variance σ_y^2,

$$\sigma_b^2 = \frac{(1/N^2)\,\Sigma\,(x_i - \bar{x})^2\,\sigma_y^2}{\sigma_x^4} = \frac{\sigma_y^2}{N\sigma_x^2} \quad .$$

Thus the error in b is minimized if $N\sigma_x^2 = \Sigma\,(x_i - \bar{x})^2$ is maximized. Least error results if all measurements are made at the two extreme positions. In this case the general expression for the error can be shown to reduce to the form originally found for a two-position measurement.

For a given relative error in measurements of R at two positions, the greater the value of n, the number of mean decay lengths between positions, the smaller the relative error in τ. (R is the ratio of detected pions to monitor counts.) Because of the attenuation of the counting rate, however, the farther downstream the second measurement is made, the longer it takes to achieve a given relative error in R. Thus, for a fixed number of monitor counts M (a fixed measurement time), there is an optimum value for n. Determining this value makes use of the fundamental statistical relationship for this experiment: The error in the measurement of the number of surviving pions is $\sqrt{MR(1 - R)}$. This expression follows from the fact that the number of pions detected is a binomial random variable. Its variance is MR(1 - R) since there are M "trials," and R is the probability of "success." Dividing by M gives the absolute error in R: $\delta R = \sqrt{R(1 - R)/M}$. The relative error is $\delta R/R = \sqrt{(1 - R)/MR}$.

We can now express the error in τ if R_1 is determined from the number of pions detected at x_1 for M_1 monitor counts. R_2, x_2, and M_2 are similarly related, and $(x_2 - x_1)/x_o = n$. Applying $\delta\tau/\tau = (1/n)(\delta R/R)$ to each of the two positions, we find

$$(\delta\tau/\tau)^2 = \frac{1}{n^2}\left(\frac{1 - R_1}{M_1R_1} + \frac{1 - R_2}{M_2R_2}\right) = \frac{1}{n^2}\left(\frac{1 - R_1}{M_1R_1} + \frac{1 - R_1\exp(-n)}{M_2R_1\exp(-n)}\right).$$

Given R_1 and the constraint that $M_1 + M_2$ = a constant, there are unique values for n and for the ratio M_2/M_1 which minimize $\delta\tau/\tau$. In the limit $R_1 = 1$ (the beam is known to be entirely pions at x_1), the optimum value of n is 1.6; M_1 can be zero since it is not necessary to take any data at x_1. For R_1 small, $\delta\tau/\tau$ is minimized for $n \approx 2.6$ and $M_2/M_1 \approx 3.6$. The solution varies monotonically for intermediate values of R_1.

If all experimental error is statistical, it is most efficient to acquire data at just two points on the decay path. Observations at intermediate points, however, are of value in detecting systematic errors. To test the fit to an exponential attenuation with distance, $\delta R/R$ (rather than δR) should be the same at each point, since it is $\ell n\ R$ that is linear in x. Since $\delta R/R = \sqrt{(1 - R)/MR}$, runs must be made for a different number of monitor counts M for each data position. If all runs have the same M, farther downstream the statistical error will be greater since R decreases. If at each position data is accumulated until the same number of pions have been counted, MR is kept constant. Again the measurements at downstream data positions are comparatively less accurate, although in this case the variation is less than if M is kept constant.

The possible presence of certain systematic errors makes it unwise to try to make $\delta R/R$ strictly the same at every data position since the data-taking time would vary greatly from position to position. If data at upstream points is acquired too rapidly, fluctuations which might have averaged out over a longer time period could contribute error. Since M is proportional to time, if $\delta R/R = \sqrt{(1 - R)/MR}$ is to be the same at each point, the measurement time must vary as $(1 - R)/R$. In our experiment

this quantity was 3.7 times as great at the end of the decay path as at the start. As a compromise between equal statistical accuracy at each position and equal data-taking time at each position, a given number of pions were detected at each point (MR constant). For this choice the statistical accuracy at the most downstream position was 16% less and the data-taking time was 30% more than the mean values for all data positions.

2. The Effect of Systematic Errors

It is instructive to consider the error in τ introduced by systematic errors having various functional forms. Let $R = R_o \exp(-n)$, where $n = x/x_o$, be the true ratio of surviving pions at x to monitor counts.

(a) Suppose the measured ratio has some constant relative error (an absolute error proportional to R). Then the measured value of R becomes $R' = R_o \exp(-n) + \epsilon R = (1 + \epsilon) R_o \exp(-n)$, where ϵ is the relative error in R. Any error of this form does not lead to an error in τ at all. The fit to the data simply gives a different value for R_o; it is x_o that determines the lifetime.

There are several examples of this type of systematic effect. Suppose the movable counter, although responding only to pions, fails to detect every entering pion. (In the above equation ϵ would be negative.) As long as this pion inefficiency is not a function of distance, there is no error in the lifetime measurement. Similarly, suppose some constant fraction of monitor coincidences are caused by particles other than pions. If these other particles are rejected by the movable counter, the lifetime is not affected.

Another example concerns the muons from pions decaying immediately in front of the movable counter. Because the number of these muons is

proportional to the number of pions in the beam in front of the counter, the change in R caused by counting some fraction of the muons is proportional to R. In general, however, the number of decay muons entering the counter is not strictly proportional to R, and spurious counting of these particles does cause error in the lifetime. (See Sec. VI-D.)

Since the number of accidental coincidences in the monitor system is some fraction of the number of monitor counts, this systematic error is proportional to R. A similar relation holds for accidentals in the coincidence between the signals from the monitor system and the movable detector. (This second accidental rate is assumed not to be significantly affected by the variation with distance of the rate in the movable detector.)

(b) Now consider the case of a constant absolute error in R (a relative error inversely proportional to R). Such an error does affect the measured lifetime. The observed value of R can be written $R' = R_o \exp(-n) + \epsilon R_o$. Here ϵ is the relative error at $x = 0$. If τ is determined from two measurements n mean decay lengths apart,

$$\delta\tau/\tau = (1/n)(\delta R/R) = (1/n)\epsilon \exp(n) = \epsilon(1 + n/2 + \ldots).$$

This dependence on n is reasonable because as x increases, the constant error becomes a larger fraction of the true value of R. A systematic effect of this type results if the monitor coincidence includes muons or electrons and these particles count in the movable detector.

(c) Another class of systematic error may be viewed as a distance-dependent efficiency of the final counter. Perhaps the simplest example is $R' = R_o \exp(-n)(1 + \epsilon n)$. This form represents some effect linear with distance which causes a relative error in R of ϵ at one mean decay length.

The last factor may be rewritten as follows:

$$(1 + \epsilon n) = \exp[\ell n(1 + \epsilon n)] = \exp[\epsilon n - (\epsilon n)^2/2 + \ldots] .$$

Thus

$$R' = R_o \exp[-n(1 - \epsilon) - (\epsilon n)^2/2 + \ldots] = R_o[1 - (\epsilon n)^2/2 + \ldots] \exp[-n(1-\epsilon)].$$

The first-order effect of a systematic error linear in distance is simply to change the apparent lifetime. Here then is the most important argument in favor of as long a decay path as possible. For a given statistical accuracy in R, the larger the value of n, the smaller the systematic error that can be detected by virtue of the apparent non-exponential decay it induces. (Conversely an experiment cannot readily search for true non-exponential decay if the number of decay lengths is small.) If n is too small, this type of systematic error will not cause significant deviations from an exponential fit to the data, and the χ^2 test of goodness of fit will not serve to indicate its presence. A "good" value of χ^2 still has significance by implying that fluctuations are not more than expected from counting statistics and that there are no gross deviations from exponential decay.

(d) Finally, consider the error caused by a counter efficiency dependent on R. Although this case will be shown to be similar to the previous one, it will be treated separately since one source of experimental error, a rate dependence of the efficiency, did in fact have this form. Let $R' = R[1 + \epsilon(R_o - R)/R_o]$. This form assumes that the change in efficiency from its value at $x = 0$ is linear with R. Substituting $R = R_o \exp(-n)$, we find $R' = R_o \exp(-n)[1 + \epsilon(n - n^2 + \ldots)]$. For a small value of n this form is identical to that describing an error linear with distance with ϵ being the relative error. Again, for small enough n, the effect changes the apparent lifetime without noticeably altering the quality of the fit to an exponential.

II. THE BEAM AND ELECTRONICS

The monitor counters of the beam transport system had to meet several requirements. The most fundamental was that the envelope of the particles in the monitor coincidence had to be smaller than the entrance aperture of the movable pion detector the entire length of the decay path. The length of the path over which the measurement could be made was limited by this consideration.

Another requirement of the monitor was that it minimize fluctuations in the quantity being measured, the fraction of pions in the beam. Ideally, only the statistics of particle decay should contribute to fluctuations in the pion fraction. The composition of the particles emerging from the pion production target could vary, however. In order to provide a stable pion intensity monitor, the beam system included one detector sensitive only to pions and one which detected electrons.

The pion detectors in the experiment, both the movable one and the one in the monitor system, were differential Cerenkov counters. For good resolution in these detectors it was important that the momentum distribution of the beam be narrow and have sharp limits. In this way the counters could be adjusted so that the efficiency was the same for all pions in the beam. Stable operation would not have been possible if the distribution had a "tail" of off-momentum pions which failed to count (or counted with reduced efficiency). The full width at half maximum of the momentum distribution was 0.5%. Because the momentum distribution was narrow, the lifetime calculated from the observed attenuation of the beam depended only on the mean momentum. The dependence on higher moments of the momentum distribution was negligible. (The calculation is given in Appendix A.)

A diagram of the beam system is shown in Fig. 1. The important counters, the pion detectors, are CM and CP. CM is the Cerenkov counter in the monitor system, and CP is the movable counter. Figure 2 is a photograph of part of the beam system, the decay path, and CP. Pions were produced in a beryllium target placed in the external proton beam of the cyclotron. Beryllium was used to reduce the difference in yield between positive and negative pions; π^+ were still produced five times more copiously than π^-. The magnet elements between the production target and the counter M_4--two bending magnets and two quadrupole doublets--were symmetric about the collimator. An image of the target with high dispersion was formed at the collimator, whose slit width determined the momentum width of the emerging beam. At M_4, the point symmetric with the target, a dispersionless image was formed. The final magnet, a 12-in.-diameter quadrupole triplet, focused M_4 to a point near the end of the decay path. The beam thus had a "waist" in the middle of the decay path: The lateral dimensions of the beam went through a minimum between the quadrupole and the end of the beam line.

Particles which scattered failed to behave according to the beam optics described above. To reduce scattering in air, the beam traveled in vacuum wherever possible. There was vacuum pipe from a point immediately after the beryllium target up to the movable counter. The diameter of the vacuum pipe along the decay path was 8 in.; the beam diameter never exceeded 6 in. The vacuum system was continuous except for air gaps provided for CM and the scintillation coincidence counters--M_1, M_2, M_3, and M_4. To minimize scattering, the scintillators were only 1/16-in. thick and were covered by thin aluminized Mylar.

The M counters were all outside the wall shielding the proton beam.

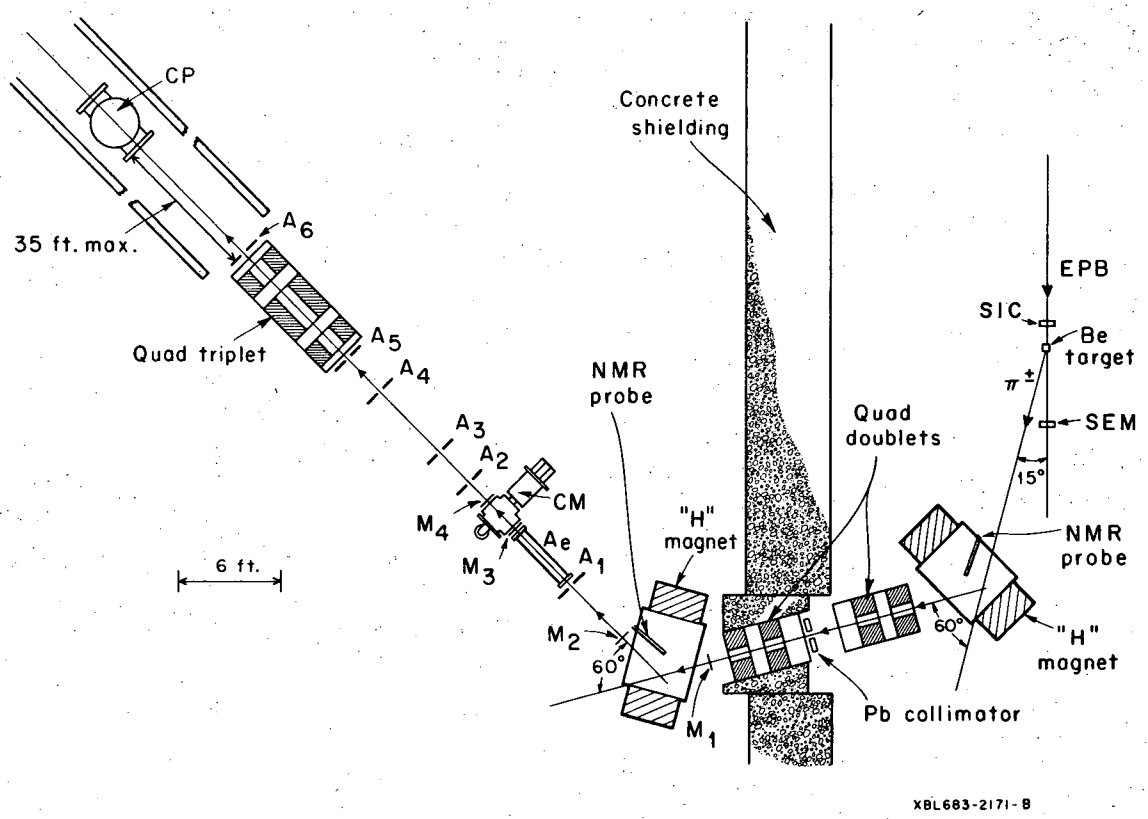

Fig. 1. Diagram of the beam system. Pions were produced at the beryllium target by the external proton beam (EPB) of the cyclotron. The lifetime was measured by detecting surviving pions with counter CP positioned different distances from the last beam-defining counter, A_6.

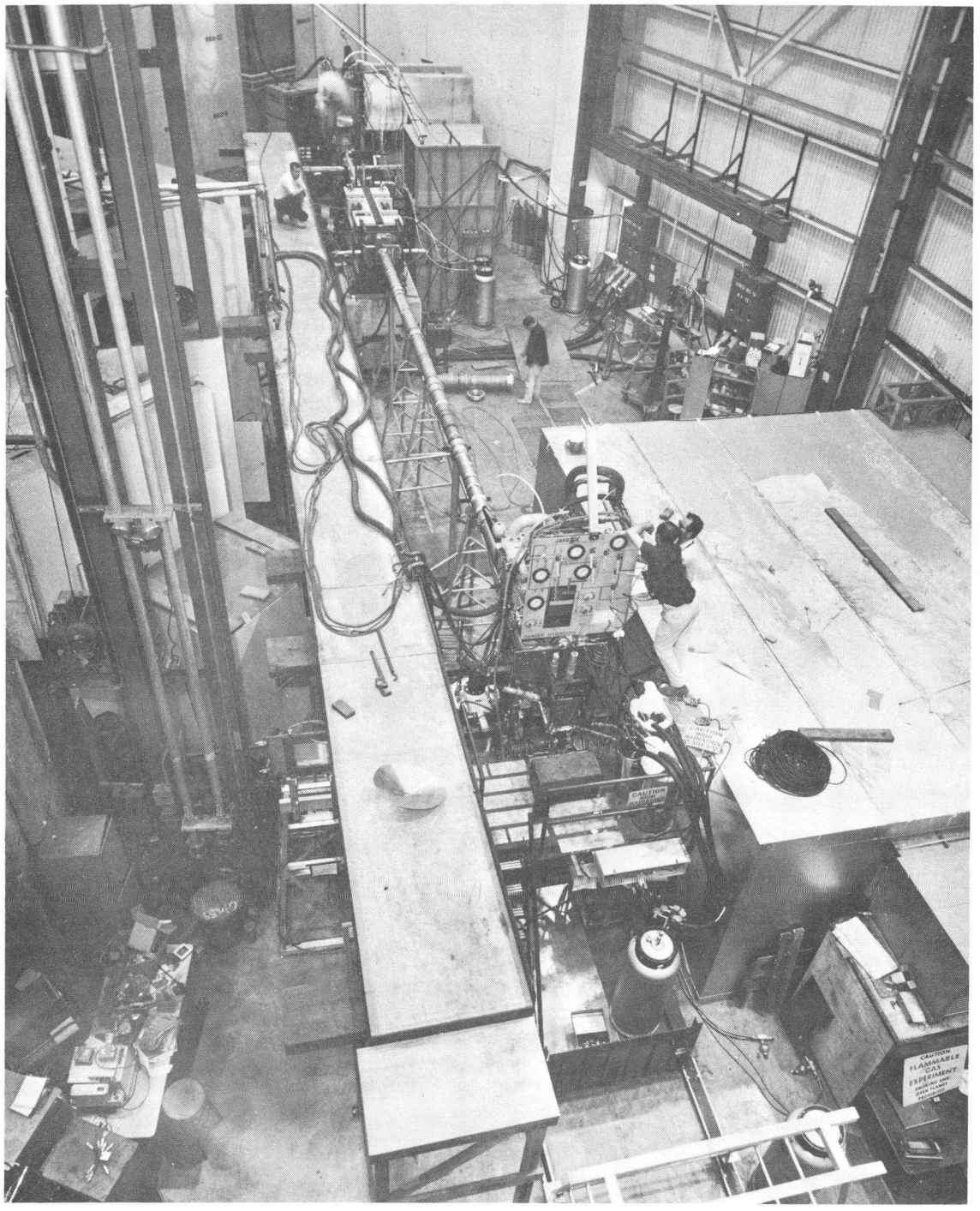

XBB 679-5660

Fig. 2. The experimental area outside the cyclotron shielding wall. The pipe in the center is the beam vacuum pipe. All the aparatus in the foreground, at the end of the pipe, is part of the movable Cerenkov counter and traveled as a unit on the tracks. The second bending magnet and final quadrupole can be seen in the background. The elevated platform at the left supported various lines serving the movable counter. The house at the right contained the electronics for the experiment.

The high particle background behind the wall would have prevented satisfactory operation of counters. Four scintillation counters in the beam were sufficient, however. The first bending magnet determined the beam momentum since the target, the collimator, and M_1 defined a trajectory through the magnet. The entrance trajectory to the second bending magnet was defined by the collimator and M_1, and the exit by M_2 and M_3. Requiring a coincidence with M_4 ensured that pions traversed CM without undergoing large-angle nuclear scattering.

Since the observed attenuation of the beam depended inversely on the product of the pion lifetime and the beam momentum, it was essential that this momentum be stable and reproducible. The momentum was determined primarily by the two bending magnets. The field at the center of each was monitored by a nuclear magnetic resonance gaussmeter which enabled setting the fields to an accuracy of 0.005%. The quadrupole magnets were set by means of current shunts and a potentiometer.

In order to define a pion beam whose lateral extent was sharply limited, a series of anticoincidence counters was used to electronically eliminate particles with undesired trajectories. Each of these counters, A_1 through A_6, consisted of a thick sheet of scintillator with a hole in the center. Particles in the monitor coincidence had to pass through the hole; particles striking the scintillator were vetoed. A_2 through A_6 had to veto with nearly perfect efficiency pions deflected in M_4, the last source of scattering in the beam. The anticounters themselves did not have any material directly in the beam. Since they were mounted inside the beam vacuum pipe, no light-tight wrapping was needed over the holes. Particles going all the way through the scintillator were readily detected. The critical requirement, however, was that particles which scattered from the

edge of one of the holes be detected efficiently. The inside surface of the holes had no wrapping since otherwise a particle could scatter from the wrapping and produce no light. The counters which performed most of the vetoing--A_3, A_5, and A_6--had a scintillator viewed by two photomultipliers, one on each side of the hole. The outputs of the two tubes were added before pulse-height discrimination.

There were two reasons for having a series of these anticounters. The overall efficiency for rejecting particles with unsuitable trajectories was increased since such particles often passed through more than one counter. Also, by detecting muons from pions decaying after M_4, the counters served to increase the fraction of monitor particles which were still pions at the start of the decay path. If there were fewer anticounters, more muons would be missed, and this fraction would be smaller.

Electrons in the beam were identified by the counter A_e, a threshold Cerenkov counter, shown in Fig. 3. Its radiating medium was carbon dioxide at a pressure of 45 psia, which provided a threshold velocity of $\beta = 0.999$. (Pions in the beam had $\beta = 0.912$.) Electrons produced Cerenkov light at about 3 deg. A cylindrical mirror, 36-in. long and 5-in. in diameter, improved the light collection for electrons whose trajectories were displaced from the axis. The 45-deg mirror, through which the beam had to pass, was made from 0.001-in. aluminized Mylar. The use of a quartz side window and a quartz-faced photomultiplier increased transmission of Cerenkov light in the ultraviolet region. Monitor particles which might have scattered from the edge of the entrance aperture of A_e were vetoed by A_1. This anticounter preceded A_e and had a hole slightly smaller than the entrance aperture.

The beam setup included two important monitors of the cyclotron

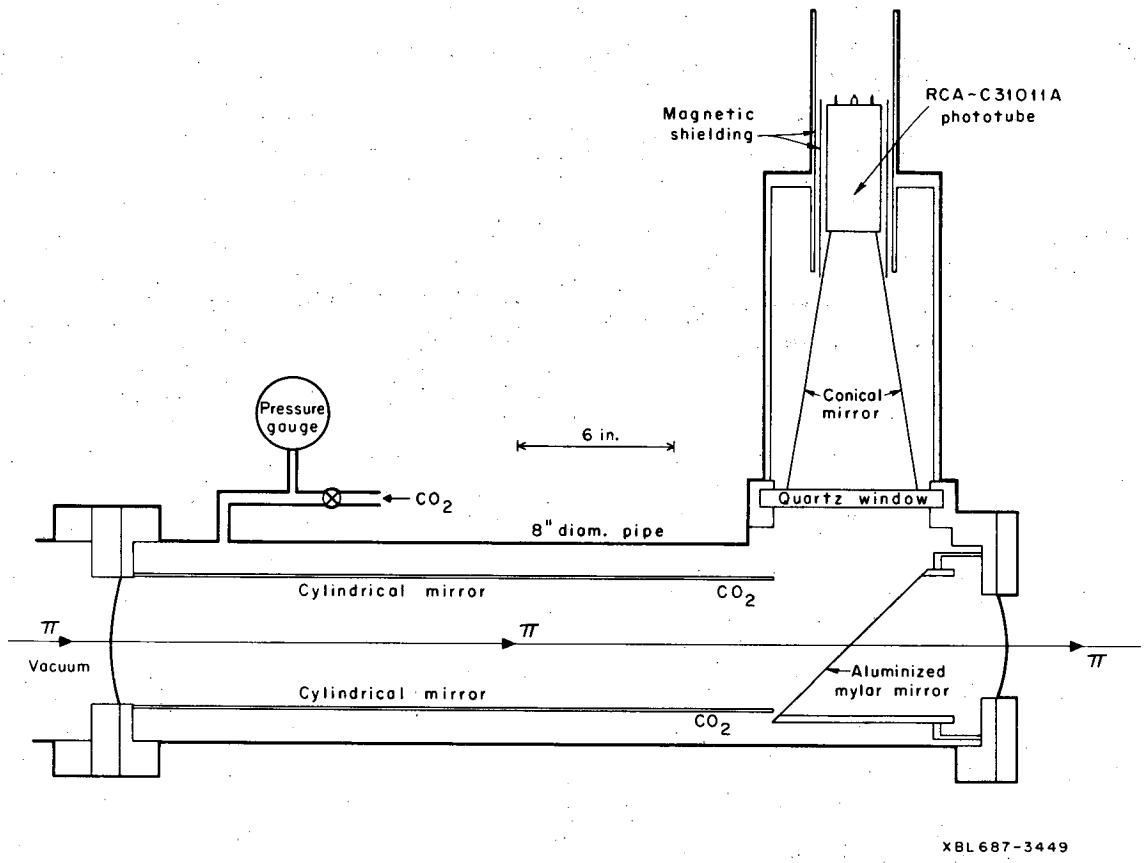

Fig. 3. The gas Cerenkov counter, A_e, which identified electrons in the beam. The cylindrical mirror has been shortened in the drawing; it was 36-in. long.

proton beam. A secondary emission monitor (SEM in Fig. 1) located behind the beryllium target measured the relative intensity of the beam. A split ionization chamber (SIC) in front of the target recorded the lateral position of the beam. A small change in beam position was of significance since it altered the ratio of pions and electrons in the secondary beam. (The electrons in the beam arose from neutral pions produced at the target. The more target material the decay gamma rays traversed, the more electron pairs were produced.) The ionization chamber permitted correcting the steering of the proton beam when necessary.

During π^+ running, protons could scatter from the target and enter the beam transport system. They were stopped by the liquid hydrogen in CM, however, and did not exist in the subsequent part of the secondary beam.

Logic signals from the many counters were used in a great number of coincidence circuits. Some 19 different coincidences were normally scaled during data taking and others were temporarily set up for tests of the beam or the movable counter. Actually, the lifetime measurement required only two coincidences. Others served as monitors of the performance of various counters, measured accidental coincidences, and so on. One of the two primary coincidences, denoted M ("monitor"), was proportional to the number of pions at the start of the decay path. Explicitly, the M coincidence was $M_1M_2M_3M_4\bar{A}_1\bar{A}_e CM\ \overline{CMA}\ \overline{\Sigma A}$. The bar denotes anticoincidence; $\overline{\Sigma A}$ stands for $\bar{A}_2\bar{A}_3\bar{A}_4\bar{A}_5\bar{A}_6$. CMA is the signal from an anticoincidence system of the monitor pion detector which will be described later. A "count" in the detector means a CM signal with none from CMA. The D ("data") coincidence, the other essential one, identified particles which satisfied the M coincidence and also counted in the movable detector.

Symbolically it was M CP $\overline{\text{CPA}}$; CPA was analogous to CMA.

The ratio of the number of D coincidences to M coincidences as a function of x, the distance of the movable counter along the beam line, determined the lifetime; D/M was proportional to $\exp(-mx/p\tau)$. Each of these two important coincidences was counted by two independent scalers so that malfunctioning of any scaler would be immediately apparent.

The action of the anticounters, A_1 to A_6, in the electronic logic was critical. For example, if a pion passed through A_6 and missed the movable counter, unless it was vetoed by A_6 it would have the appearance of a pion which decayed before reaching the final counter. To ensure that every particle with a coincident anticounter signal was properly vetoed, each anticounter discriminator was operated in a "no dead time" mode: Its logic output remained in effect during the recovery time of the unit. In addition, the signals from each discriminator were 40 nsec long, so that there was no question of imperfect timing. The occasional vetoing of acceptable pions only decreased the M-coincidence rate slightly and thus had no effect on the measured lifetime.

RCA-8575 phototubes were used for the thin counters M_1, M_2, M_3, and M_4. Because of the low level of scintillation light, the high quantum efficiency of these tubes was valuable. Amperex-56AVP tubes were used for the thick anticoincidence counters.

III. THE PION DETECTORS

A. Design

1. Principles of Operation

The experiment used two differential Cerenkov counters to distinguish pions from other particles in the beam.[15] Basically, the counters identified pions by responding only to particles traveling parallel to the beam axis and having the correct velocity. The optical system allowed Cerenkov light from these particles to reach a photomultiplier tube. Light from other particles was stopped by a baffle.

The choice of the radiating medium in a Cerenkov counter depends on the fundamental relation between Cerenkov angle, index of refraction, and particle velocity: $\cos \theta = 1/n\beta$. If there is little freedom in the choice of θ and β, then n is constrained. Although a small Cerenkov angle has the advantage of better resolution (greater $d\theta/d\beta$), light output increases with Cerenkov angle. For a focusing counter such as ours, however, too great an angle would require excessively large lenses and cause increased difficulty with optical aberrations. Our counters were designed for a Cerenkov angle of about 11 deg. The pion velocity was constrained because of the importance to the experiment of a high pion flux. Pion production at the cyclotron was greatest for β about 0.92.

This angle and velocity require an index of around 1.1 A gas having an index this high must be at high pressure. Beam particles would have to pass through thick windows in order to traverse the radiator. Coulomb scattering and nuclear interaction of pions make this approach unsuitable for our counter. Hydrogen, in liquid form, has a refractive index about 1.1. Although hardly a convenient liquid to use, its low Z and low A minimize scattering and interaction in the liquid.

A diagram of the movable counter CP is shown in Fig. 4 and the monitor counter CM in Fig. 5. The design of the counters was similar; CP was essentially a larger version of CM. The larger counter used 5-in., RCA-4522 phototubes; the smaller one used 2-in., RCA-8575 phototubes. The radiating liquid was contained within a flask constructed with thin domes at the beam entrance and exit. The plane mirror within the liquid (0.0005-in.-thick aluminized Mylar stretched on a frame) allowed the subsequent elements of the optical system to be out of the beam. Light reflected from this mirror left the flask through a quartz side window. Immersed in the liquid, coaxial with the beam line, was a cylindrical mirror, of diameter 7-in. in CP and 4-in. in CM. This mirror was essential in making the counter efficiency independent of the radius at which a particle entered. All the light from all particles which passed through the mirror was collected. Because light reflected from the mirror did not change its angle with respect to the axis, the Cerenkov light from a particle had a distribution in this angle which was independent of the radial distance of the particle trajectory from the beam axis.

After leaving the liquid through the side window, light was focused by two lenses. The image produced by this doublet depended on the velocity of the particle and its angle to the optic axis. Cerenkov light at angle θ from a particle traveling parallel to the axis produced a ring of light at the focal plane. The ring was centered on the axis and had a radius f tan θ, where f is the focal length of the doublet. The relation for the radius of the ring can most easily be seen by first considering the effect of the lenses on a collection of rays parallel to one another. If the rays are parallel to the optic axis ($\theta = 0$), they are focused to a point ($r = 0$). If these parallel rays make an angle θ with the axis, this point

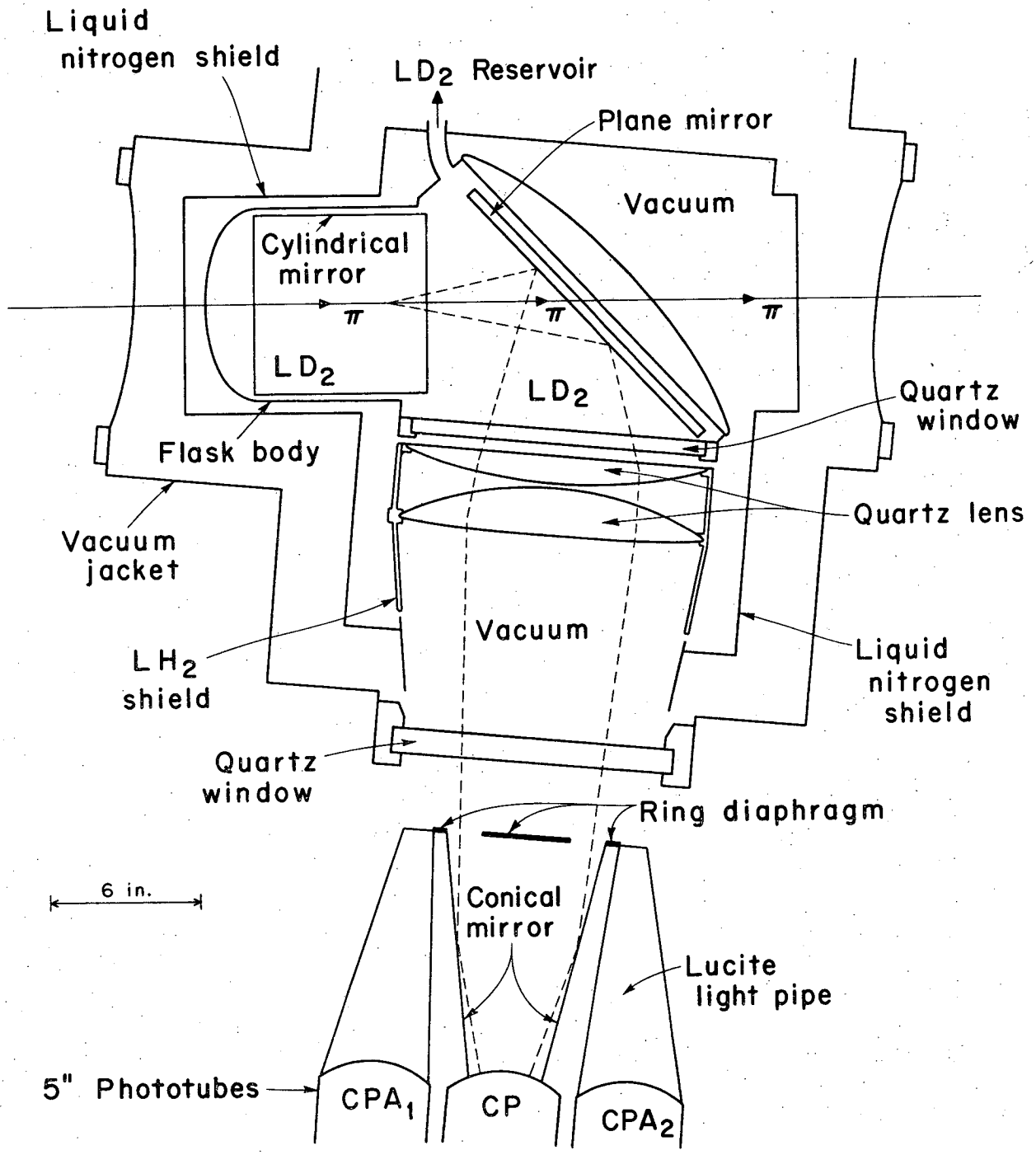

Fig. 4. The cryogenic and optical systems of CP, the movable Cerenkov counter. The dotted lines show two rays of the Cerenkov light emitted by a pion of the correct velocity. The photomultiplier assembly was a separate, removable unit. It is shown in Fig. 6.

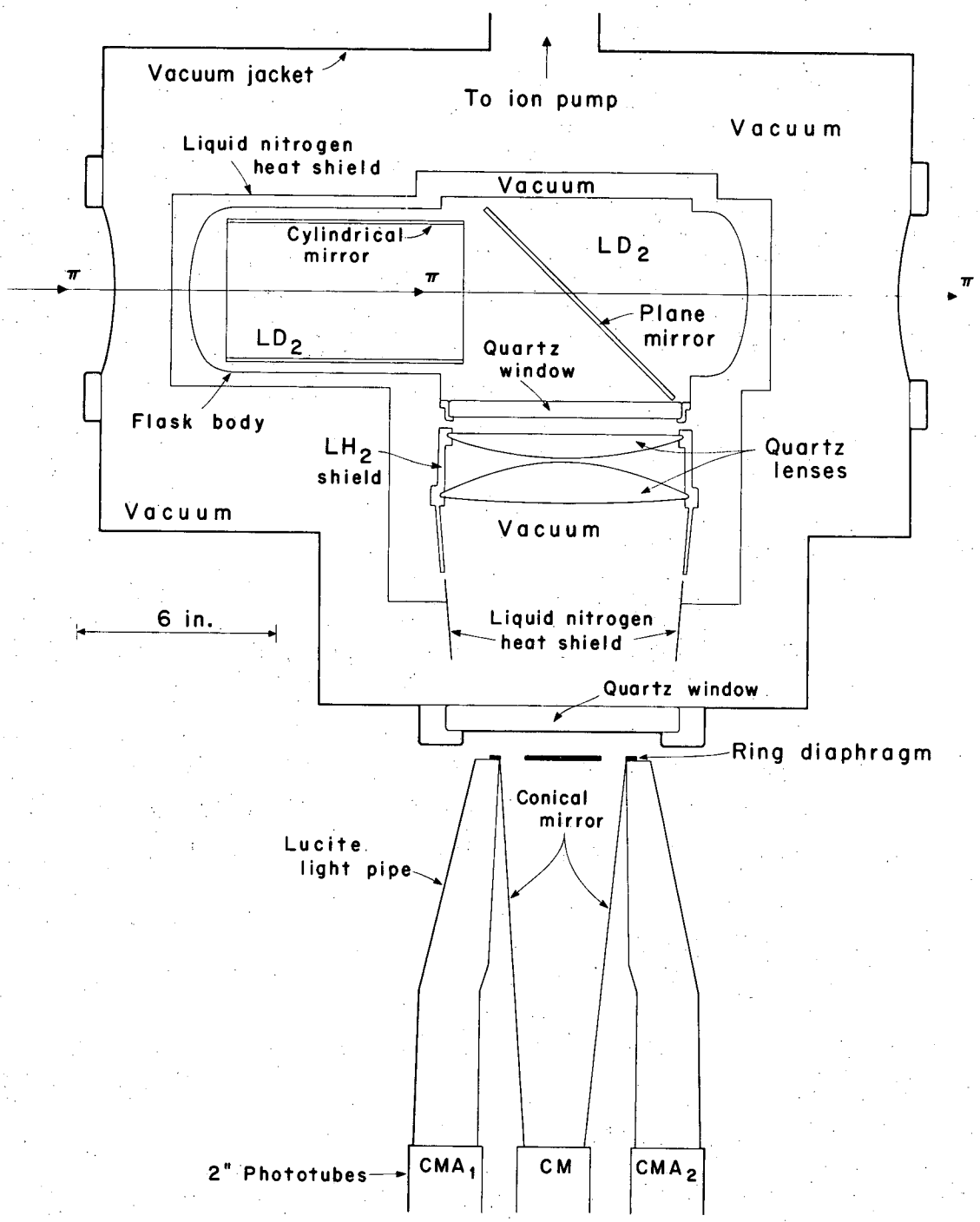

XBL6812-7471

Fig. 5. The monitor Cerenkov counter CM. Note that the domes at the ends of the liquid hydrogen flask were parallel, in contrast to CP which had a wedge-shaped volume of hydrogen.

is displaced laterally by f tan θ. By symmetry, a cone of incident light produces a ring at the focal plane.

The cylindrical mirror had no effect on the radius at which light crossed the focal plane; however, it could alter the distribution of light intensity around the ring. For a particle traveling parallel to, but not along, the optic axis, the ring was not illuminated uniformly. One region received light from both sides of the particle's Cerenkov cone--from one side directly and from the other after a reflection.

If the particle trajectory made an angle θ with the optic axis, the ring image was simply displaced laterally by f tan θ. Actually for our optics, this thin-lens approximation was true only for angles less than about 10 deg. For larger angles parts of the image were distorted.

Discrimination against particles having the wrong velocity was accomplished by an opaque diaphragm in the focal plane. Its ring-shaped aperture allowed rays from particles having the right velocity to pass through. Light from slower particles struck the central disc; the ring image for faster particles had too large a radius and missed the opening. The conical mirror immediately behind the aperture "funneled" the light to the photomultiplier at the exit of the mirror. (A reduction in area has disadvantages: Reflections reduce light intensity, and the angles of rays entering the phototube become greater. Without any reduction, however, a large radiating volume requires a large diameter phototube, or several phototubes.)

Since particles having an angle with respect to the optic axis produced a displaced ring image, much less of their light was able to pass through the aperture, and such particles should fail to count. If the sensitivity of the photomultiplier was high enough, however, it was possible that some

off-angle particles might count. To improve the rejection, two additional photomultipliers detected light falling within an annulus surrounding the opaque annulus of the diaphragm. An ultraviolet-transmitting, Lucite light pipe conveyed the light from each half of the annulus to one of the phototubes. The photograph of the photomultiplier assembly for CP (Fig. 6) shows these light pipes and the diaphragm. For the movable counter the output pulses from the two tubes, CPA_1 and CPA_2, were added and discriminated to produce the logic signal CPA. This signal was used in anticoincidence with the central photomultiplier signal, CP. The same procedure was used for the monitor counter CM.

At this point it is useful to be more specific and consider the Cerenkov light produced by the various particles in the beam used in this experiment. Nominal values of parameters will be used in the discussion; the results will then be approximately correct for both CM and CP. (There were geometrical differences between the two counters, and the beam velocity entering each was not precisely the same.) In a Cerenkov radiator with an index of refraction of 1.1, pions with $\beta = 0.92$ produced Cerenkov light at 11 deg. Electrons with the same momentum as the pions had $\beta = 1$ and radiated at the maximum Cerenkov angle, 25 deg. Muons of this momentum had $\beta = 0.95$ and radiated at 17 deg.

In addition to the momentum-analyzed particles, the muons from pion decay must be considered. Their velocities ranged from 0.85 for "backward" muons (those emitted backward in the pion rest frame) to 0.95 for "forward" muons. Muons having these two limiting values were of special importance because they were emitted forward in the laboratory and remained in the beam. Many of those with intermediate values left the beam before reaching the movable counter. Backward muons posed no problem since their velocity

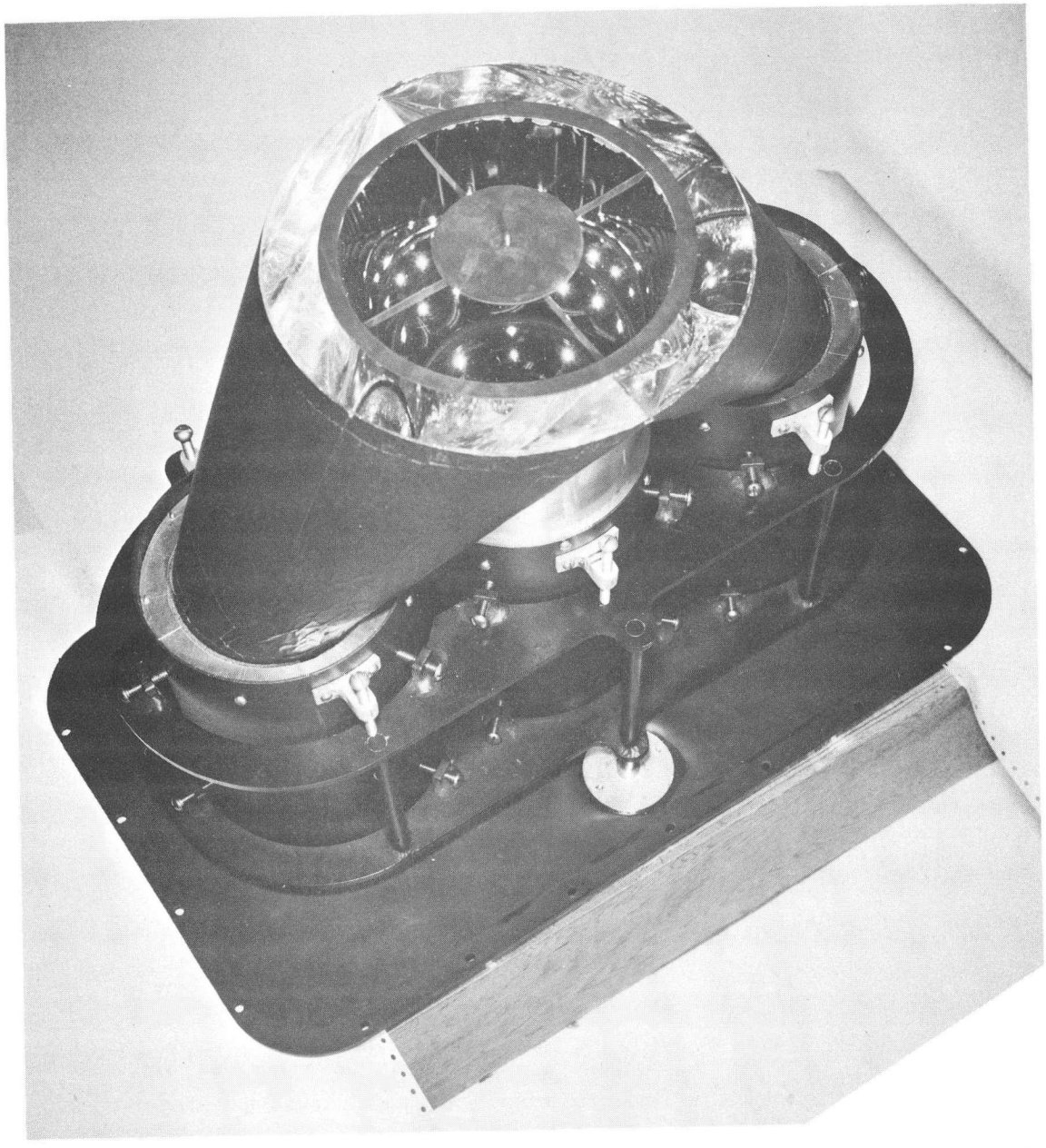

XBB 670-5770

Fig. 6. The photomultiplier assembly for the movable counter. The three parallel cylinders contain the phototubes. The light-collecting cone and the central phototube can be seen through the aperture, formed by a metal annulus supporting a central disk.

was less than $\beta = 0.91$, the threshold for producing Cerenkov light. Forward muons had about the same velocity as beam muons and were rejected to the same degree. Some decay muons had the same velocity as pions, although their angle with respect to the beam line was 7 deg. In principle, the counter distinguished them from pions because too little of their light reached the central phototube or because they were vetoed by the anticoincidence phototubes.

For the counter to have sufficient resolution, the angular distribution of radiated light for each particle type had to be narrow. (The Cerenkov angle of beam pions and muons differed by only 6 deg.) The distribution in angle of particle trajectories in the beam was necessarily narrow, since the beam was designed to travel a long distance with limited radial extent. The trajectories of particles in the monitor coincidence had angles with respect to the beam axis no greater than 1/2 deg. The width of the momentum distribution of the beam, 0.5%, led to a variation of Cerenkov angle of only 1/4 deg. Multiple Coulomb scattering in the radiator smeared the image of pion Cerenkov light about one deg. (The rms, projected scattering angle for 25 cm of liquid hydrogen, radiation length 970 cm, is 1/2 deg.) The last significant effect detrimental to counter resolution was dispersion in the radiator, by which light of different wavelengths was emitted at different Cerenkov angles. It is much more difficult to estimate this effect since the loss of resolution depends not only on the variation of index of refraction with wavelength, but on the spectral response of the phototube and the frequency dependence of the light attenuation in reaching the phototube. Dispersion is mentioned later in connection with the counting of decay muons.

2. Cryogenic Features

There were important practical problems encountered in using liquid hydrogen in the Cerenkov counters. The hydrogen vessel had to be insulated especially well since boiling would cause scattering of Cerenkov light. Precautions were needed to prevent gradual fogging of the optical windows and lenses which would make the counter efficiency decrease with time. Control of the pressure and temperature of the liquid was necessary if the index of refraction was to be constant and reproducible. Purity of the liquid hydrogen was important so that repeated filling of the flask did not leave deposits on the internal mirrors.

The cryogenic system incorporated the standard laboratory deuterium condenser designed to condense gaseous deuterium internally by means of a reservoir of liquid hydrogen. (This indirect procedure was necessary because available deuterium was in gaseous form.) The system had the advantage that, with few changes, runs could be made with either liquid hydrogen or deuterium in the Cerenkov counters. Also, condensing the liquid within the counter permitted filtering the gas to ensure the purity of the liquid.

To reduce heat flow to the flask and fogging of optical surfaces, the flask and lenses were completely surrounded (except for openings for the beam and outgoing Cerenkov light) by a metal structure maintained at liquid nitrogen temperature, the "liquid nitrogen shield" indicated in the figures. A "liquid hydrogen shield" around the lenses was connected to the liquid hydrogen reservoir. The lens region was especially critical, in terms of heat flow, because of the direct optical path between the flask and the photomultiplier assembly, which was at room temperature. Since the hydrogen shield was cooled before the flask was filled, the contamina-

tion from warmer surfaces migrated to this shield rather than to the flask. To further reduce heat transfer, the flask was covered with 20 layers of 0.00025-in. aluminized Mylar.

The flask was designed to minimize the effect of any boiling that did occur. Since the cylindrical mirror was not part of the boundary of the hydrogen volume but rather was immersed in the liquid, bubbles tended to form outside the mirror instead of inside it. In the movable counter bubbles originating at the exit of the cylindrical mirror were directed around the outside of the mirror so that they did not cross the path of Cerenkov light.

Temperature stability of the liquid in the flask was achieved by maintaining a constant gas pressure in the deuterium reservoir with a self-relieving pressure regulator. (The independent hydrogen system was at atmospheric pressure.) With the regulator set for 3 psig, gas continued to enter the reservoir and condense until liquid partially immersed the condensing surfaces. Whenever the pressure exceeded 3 psig, the regulator allowed gas to escape. Operation with the deuterium reservoir almost full made the equilibrium of the system less sensitive to perturbations such as filling of the hydrogen reservoir. Platinum resistance thermometers, which recorded continuously on a strip chart, were used to monitor temperatures in the flask and reservoirs. As indicated by temperature measurements, the variation in the index of refraction of the flask liquid was less than that corresponding to a 0.02-deg change in Cerenkov angle.

To keep the internal surfaces of the flask free from deposits, the gas used for condensing passed through a filter (5-Å molecular sieves at liquid nitrogen temperature) trapping contaminants such as water, air,

oil. To minimize condensation on the outside of the cold flask, the insulating vacuum was maintained by an ion pump, rather than a diffusion pump from which oil might migrate to the flask. A diffusion pump was used only for the initial pumping and there was a liquid nitrogen trap between it and the insulating vacuum. The ion pump maintained a vacuum of 5×10^{-8} torr.

Slight differences in the properties of ortho- and para-hydrogen could have caused a significant time variation in the index of refraction of the radiating medium. The liquid hydrogen in the counters initially had the same ortho-para ratio, three to one, as the gas from which it was condensed. To accelerate the conversion to pure para-hydrogen, the low-temperature equilibrium state, the liquid passed through a catalyst to reach the flask. Conversion was essentially completed between the time the counter was filled and any lifetime data were taken.

B. Photomultiplier Pulse-Height Spectrum

The fact that some pions entering the Cerenkov counter underwent a nuclear interaction before completely traversing the radiator had very important consequences in the experiment. To illustrate the resulting difficulty, consider a typical scintillation counter. It is desirable to be able to "plateau" such a counter: to make its detection efficiency insensitive to small changes in the level of the scintillation light or the gain of the photomultiplier. This situation can be achieved if the output of the phototube always exceeds some minimum pulse height. The threshold of a pulse-height discriminator can then be set below this minimum, and an output will be generated for every particle entering the counter.

The situation was quite different in our Cerenkov counters. By design their efficiency was dependent on both the velocity of the entering particle and the angle of its trajectory with the beam line. Thus the Cerenkov light collected from a pion was proportional to the distance it traveled in the radiator without changing its velocity or angle. At any given depth in the radiator some pions underwent nuclear scattering. Such scattering changed the angle of the pion trajectory, and--by imparting energy to the proton--reduced the pion velocity. For a large enough scattering angle, the final velocity was below threshold and no further Cerenkov light was produced. (In liquid hydrogen a pion with $\beta = 0.912$ scattered at a lab angle greater than 18 deg does not radiate.) Because some pions interacted after penetrating only a short distance into the liquid, there was no minimum light level reaching the phototube and no minimum pulse height for the output. It was impossible to plateau the counter. (Of course a single photon constitutes a minimum light level; however, the system gain was such that tens of photons were required

to produce a count.)

The most convincing demonstration of the validity of this description was pulse-height analysis of the central photomultipliers of CM and CP. Because an output from the last dynode was used for analysis, the functions of the anode output in the electronic logic did not have to be disturbed. A stretcher made the fast pulses from the phototube compatible with the pulse-height analyzer. The stretcher was gated to obtain the pulse-height distribution only for particles satisfying a certain coincidence. Figure 7a shows the pulse-height spectra obtained from CP under three different conditions of gating. The curve labeled "no counter" was for particles which satisfied the monitor coincidence. The two lower curves were for particles which, in addition, counted in a 12-in.-square or 3-in.-diameter scintillation counter immediately following CP. Of the three curves, normalized so that their peaks have equal height, the distribution obtained without an additional coincidence counter has the most counts in the valley. Note that use of the larger counter gave less improvement than the smaller one. The reason is that the pions could nuclear scatter and still intercept the downstream counter. A larger counter detected more pions which scattered at large angles and thus had produced less usable light.

Figure 7b gives added evidence that the shape of the distribution depended greatly on pion interactions. The spectra obtained for positive and negative pions with the counter filled with hydrogen or deuterium were consistent with the cross sections for πp and πd scattering. The interaction of pions in hydrogen was dominated by the first pion-nucleon resonance since the pion momentum gave a center-of-mass energy very close to 1236 MeV. The $\pi^+ p$ total cross section (195 mb) is about three times

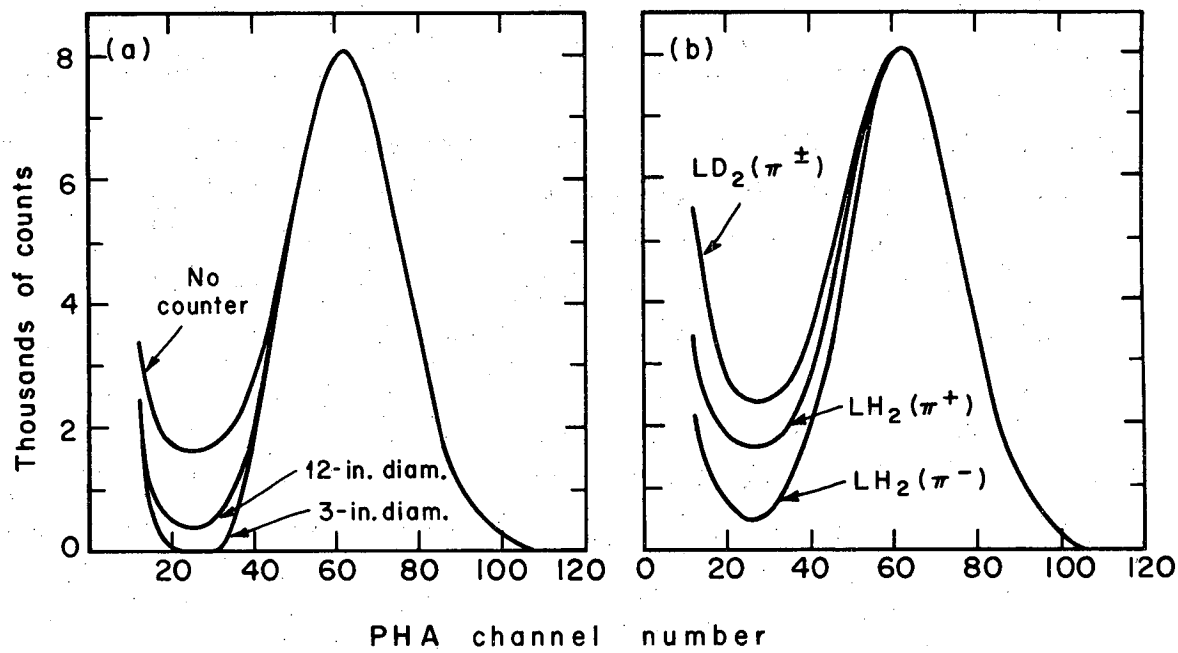

XBL689-6830

Fig. 7. Pulse-height spectrum of the central phototube of the movable counter under different conditions. The distributions have been normalized to have the same maximum value.

(a) The spectrum obtained by requiring coincidence with a downstream counter and the spectrum with no coincidence requirement.

(b) The spectra observed with the π^+ and π^- beam when the counter was filled with liquid hydrogen and the spectrum, for either beam, when deuterium was used.

π^-p (65 mb), and indeed the π^+ pulse-height distribution exceeded π^- in the valley. With deuterium the spectra were the same for plus and minus--as expected from charge independence--and indicated more interactions than for π^+ with hydrogen--in agreement with the fact that the πd cross section (250 mb) exceeds π^+p.

For particles satisfying the monitor coincidence there was a great difference between the pulse-height distributions obtained from the central phototubes of CM and CP. For positive pions the peak-to-valley ratio was around 500 for CM, while it rarely reached 10 for CP. The difference is to be expected. The trajectory of a pion in the monitor had to be sufficiently parallel to the beam axis to pass through M_4 and through the holes in all the anticounters which followed. Thus particles undergoing large-angle scattering in CM were excluded. It was just such scattering in CP, however, that caused the poor peak-to-valley ratio in that counter.

Although operating CP in coincidence with a downstream counter improved the pulse-height spectrum, it was not possible to take lifetime data in this manner. Scattering in the radiator caused the beam size at the exit of CP to be larger than the downstream counter. If a coincidence was required with this additional counter, the detection efficiency depended critically on the beam size entering CP and the precise lateral position of CP with respect to the beam. The dependence on the position of CP was exaggerated because the radiator was wedge-shaped (see Fig. 4). Pions crossing the counter high in the flask traversed less absorber and were less likely to interact before reaching the downstream counter. If coincidence with the 12-in.-square counter was required, the counting rate increased 2% for each inch CP was lowered. (The fact that an

unscattered pion crossing high in the flask produced less Cerenkov light than one low in the flask was not of importance; for either trajectory the absence of scattering ensured sufficient light to produce a count.)

Because of the shape of the pulse-height spectrum from CM or CP, there were always pions which produced a photomultiplier output below the discrimination threshold and thus failed to count. The precise counting efficiency depended on the intensity distribution of the light reaching the phototube, the tube gain, and the discrimination level. The few tenths of a percent inefficiency of CM was of little consequence since the only effect was to reduce slightly the rate of monitor coincidences. The smaller peak-to-valley ratio of the pulse-height spectrum for CP made it more susceptible to changes in conditions. Variation of efficiency of this counter could lead to serious systematic errors. Four sources of error will be discussed: (a) random fluctuations in the tube gain and discrimination level, (b) changes in beam size and lateral counter position, (c) rate dependence of the tube gain, and (d) attenuation in the cable delay between tube and discriminator.

C. Systematic Errors in the Movable Counter

1. Fluctuations in Phototube Gain and Discrimination Level

Variation of the photomultiplier gain or the threshold of the associated discriminator caused changes in the efficiency of CP. Consideration of the pulse-height distribution shows that the two effects are essentially equivalent. If the tube gain increases, the abscissa of any point of the distribution is scaled up; the threshold pulse height is unchanged. If the discrimination level decreases, the threshold is at a smaller abscissa; the distribution is unchanged. In both cases the fraction of pulses above threshold increases; i.e., the efficiency increases.

Ideally it would have been desirable to monitor directly the tube gain and the discrimination level and to make adjustments to keep the counter efficiency constant. This was not done, however, because of the difficulty of making sufficiently precise measurements of the efficiency. The amplitude of available light pulsers was not stable enough for the purpose. Also, because of the inherent variation in the phototube pulse height, a light pulser--even if perfectly stable--must be capable of a high enough repetition rate. The rate must permit making statistically reliable measurements in a time short compared to the time interval in which the efficiency might change significantly.

In a sense the best indication of changes in CP efficiency was the data itself, the ratio of pions detected at a given point downstream (D coincidences) to pions in the monitor (M coincidences). It was concluded that fluctuation in D/M, in excess of that expected on the basis of statistics, was primarily due to variation of the CP efficiency. Although erratic behavior of the monitor system could have been responsible, various

properties of the monitor (e.g., fraction of electrons, fraction of particles vetoed) showed no abnormal variation, and fluctuations in D/M were not correlated with fluctuations in the monitor.

The counter M_5, a 12-in.-square scintillation counter immediately behind CP, gave additional confirmation that D/M fluctuations--exceeding those expected statistically--were caused by efficiency variations. As explained earlier, the pulse-height spectrum for particles which counted in a downstream counter, as well as in CP, had a greater peak-to-valley ratio than the spectrum obtained with no coincidence requirement. Thus the measured fraction of monitor particles counting both in CP and in M_5 (the ratio of DM_5 coincidences to M coincidences) should have been less sensitive to gain changes of the photomultiplier in CP. Indeed it was found that excessive fluctuation in the D coincidence was not accompanied by similar fluctuation in DM_5.

If the variations in phototube gain were strictly random and had a time scale much shorter than the time between changes of data position, they had a minor effect on the lifetime determination. Slow, monotonic drifts in gain posed a more serious problem. Such a drift occurred following the initial application of high voltage to the tube or when the voltage was removed and then restored. In the latter case the perturbation was especially severe if the tube was exposed to light while the voltage was off. When it was necessary to exchange one phototube for another, for example, at least 12 hours were required for the new tube to become sufficiently stable. To minimize long-term drifts the high voltage was applied to the tube many days before the start of a run.

2. Changes in Beam Size and Position

Factors which would cause variation in the level of Cerenkov light

reaching the phototube constituted a second class of systematic errors that would have been absent if the pulse-height spectrum had been ideal. The principal concern was a dependence of the light level on the position at which a pion entered the Cerenkov counter--in other words, a non-uniform efficiency across the entrance aperture. In such a case data at any position of the counter along the decay path would depend on the precise centering of the counter with respect to the beam. Even worse, variation in beam size would cause a systematic difference in counter efficiency from one position along the decay path to the next.

One possible source of nonuniform efficiency across the counter aperture was the cylindrical mirror. For pions having a trajectory farther from the beam axis a larger fraction of their Cerenkov light reflected from the cylindrical mirror to reach the phototube. If this mirror was not a perfect reflector, the light level at the phototube would be a function of the pion entrance trajectory. There was no evidence, however, that the mirror did have a significant effect on the efficiency. As pointed out earlier, the fact that the radiator was wedge-shaped did not cause nonuniformity of response because the light produced by any pion traveling even the shortest dimension of the radiator was well above threshold if the particle did not interact.

The major source of nonuniformity of response was far from obvious, and its discovery greatly increased understanding of the performance of the counter. The problem lay in the variation of efficiency across the face of the central photomultiplier of the counter. Despite the fact that part of the Cerenkov light of a particle reflected from the cylindrical mirror and part did not, and that the light underwent different numbers of reflections from the conical mirror, there was still a significant

correlation between the entrance trajectory of the particle and the portion of the face of the phototube illuminated by its Cerenkov light. As a result nonuniformity of response across the phototube caused nonuniformity of efficiency across the counter aperture.

When the importance of using a phototube with a uniform response was realized, an apparatus was set up to measure the variation of efficiency over the face of the tube. A light pulser, illuminating only a small region of the tube, was moved from one point to another. A map of the relative efficiency over the face of the tube was made by observing the amplitude of the output pulses with an oscilloscope. Because of the great variation among photomultipliers, even among those of the same type, a large number were tested to find the most uniform ones available. The procedure was made more lengthy because uniformity depended greatly on the voltage of the focusing grid, and different values were tried for each tube. As might be expected, regions near the perimeter of the tube face often showed the greatest deviation in efficiency. In order to make use of only the central, more uniform, portion of the tube, a new conical mirror was constructed with an exit diameter of 3.5 in. (The original diameter was 4.5 in.)

These improvements gave the movable counter a more uniform response over the central region of its aperture. The region over which it had high efficiency was reduced to a 5.5-in.-diameter circle, however. (The cylindrical mirror had a 7-in. diameter.) Outside the central circle the efficiency was several percent lower. The explanation involves the optics of the cylindrical mirror and lenses. Although the radius at which Cerenkov light crossed the focal plane was independent of the radius of the particle trajectory, the angle of the light at this point was

partially correlated. At the focal plane, light from pions with trajectories farther from the axis included more rays with large angles. The new cone, because of its more acute apex angle, less efficiently conveyed large-angle light to the phototube. Thus the counter efficiency for pions far from axis was reduced.

3. Rate Dependence of the Phototube Gain

The effect of random variations in phototube gain has been discussed. To a large degree, measurements made over a long period of time are not biased by such variations. Systematic changes in gain from one data position to another could have a serious effect on the accuracy of the experiment. For example, when the movable counter was at the most upstream data position, adjacent to the final quadrupole, the fringe field could impair the phototube response. Similarly, differences in the ambient magnetic field along the decay path could lead to systematic variations in tube gain. These fields were weak, however, and measurements indicated that the magnetic shielding around the tube was quite adequate.

One systematic gain variation did have an important effect in the experiment. The gain of the tube exhibited a slight dependence on the counting rate. Origins of such an effect are discussed in Appendix B. In a scintillation spectrometer such a gain variation is always of concern, since the variation in pulse height leads directly to errors in energy measurements. On the other hand, a typical scintillation counter is insensitive to small gain variations. In CP, however, any gain change necessarily altered the counting efficiency. A rate-dependent efficiency was the type of error not readily revealed by the goodness of fit of the data. As explained in the Introduction, if the decay path is short, the fit to an exponential can be good, although the measured lifetime is in

error. The gain of the central phototube of CP was less at lower rates, so that the counter efficiency monotonically decreased as the counter was moved downstream. The measured beam attenuation was too great and the calculated lifetime too short. This rate effect is discussed further in Analysis.

4. Attenuation in the Cable Delay

There was another important systematic error which, like the rate-dependent gain, had an approximately linear dependence on the distance along the decay path, so that the goodness of fit of the measured beam attenuation did not suggest its presence. The problem concerned the manner in which the timing of pulses in the electronic logic was preserved when the position of the movable counter was changed. Suppose the counter was at the most downstream position, and its pulses were properly timed with respect to signals from the monitor system. As the counter was moved upstream, the delay contributed by particle time of flight was reduced, and cable delay had to be added to the signals.

Initially this variable cable delay preceded the pulse-height discriminator for each signal from the counter. This is the arrangement for a typical counter. The fact that the signal undergoes some degree of attenuation in the cable is usually unimportant. Since the approximate delay is found before the voltage is adjusted, the only effect of the attenuation is that a slightly higher voltage is needed. In the case of CP, however, the delay was not constant. By varying the attenuation of the phototube signals, the change in cable delay caused a systematic change in counter efficiency from one position to the next. Because the efficiency was higher at positions farther downstream, the effect caused the measured lifetime to be too long.

Once the problem was recognized, it was readily corrected. For each phototube of the movable counter, the variable delay was placed after the discriminator so that standard logic pulses, for which the slight changes in amplitude were less critical, traveled through the delay cable. As additional precaution the logic pulses were restandardized by a second discriminator following the cable. Now, as the counter position was changed, the length of cable between the two discriminators changed, but the length from the phototube to the first discriminator was constant.

In the earlier version of this experiment (Ref. 6) the variable delay preceded the discriminator. It is now believed that this systematic error had a significant effect on the results of that experiment. The measured π^+ lifetime was anomalously long, and the lifetime-ratio calculation suggested that the π^+ lifetime was greater than π^-. The cable-delay error would cause the apparent lifetimes to be too long and, because liquid hydrogen was the radiator, would affect π^+ more than π^-.

C. Operating the Counters

Much of the running time was devoted to optimizing the performance of the Cerenkov counters. Any alteration of the flask or the parts of the optical system which were inside the vacuum jacket was a major undertaking. Changing the ring diaphragm, the central phototube, or the light-collecting cone was relatively easier. After any of these changes, the high voltage and discrimination levels for the phototubes had to be carefully chosen.

One of the first parameters to be determined was the width of the annular opening in the diaphragm. If the opening was too wide, the counter resolution would decrease. Past a certain point, however, narrowing the opening would only limit the admitted light without improving resolution. A diaphragm was chosen which accepted Cerenkov light with angles $\pm$ 3 deg from the central value.

One test of counter resolution was to measure the efficiency of the counter, the fraction of beam particles detected, as a function of the beam momentum, which was varied by changing all the magnet currents from their normal values by some scale factor. Such a momentum-response curve for CM is shown in Fig. 8. At some lower value of momentum the muons in the beam had the correct velocity to count, and the curve shows a peak for these particles. At a momentum above the operating point, the light from pions was centered on the anticoincidence ring, and the efficiency was especially low.

An increase in efficiency occurred when the momentum was raised still higher. In this region the Cerenkov angle was so great that part of the light made a spurious reflection from some surface and passed through the ring aperture. At the central momentum, light from beam electrons probably

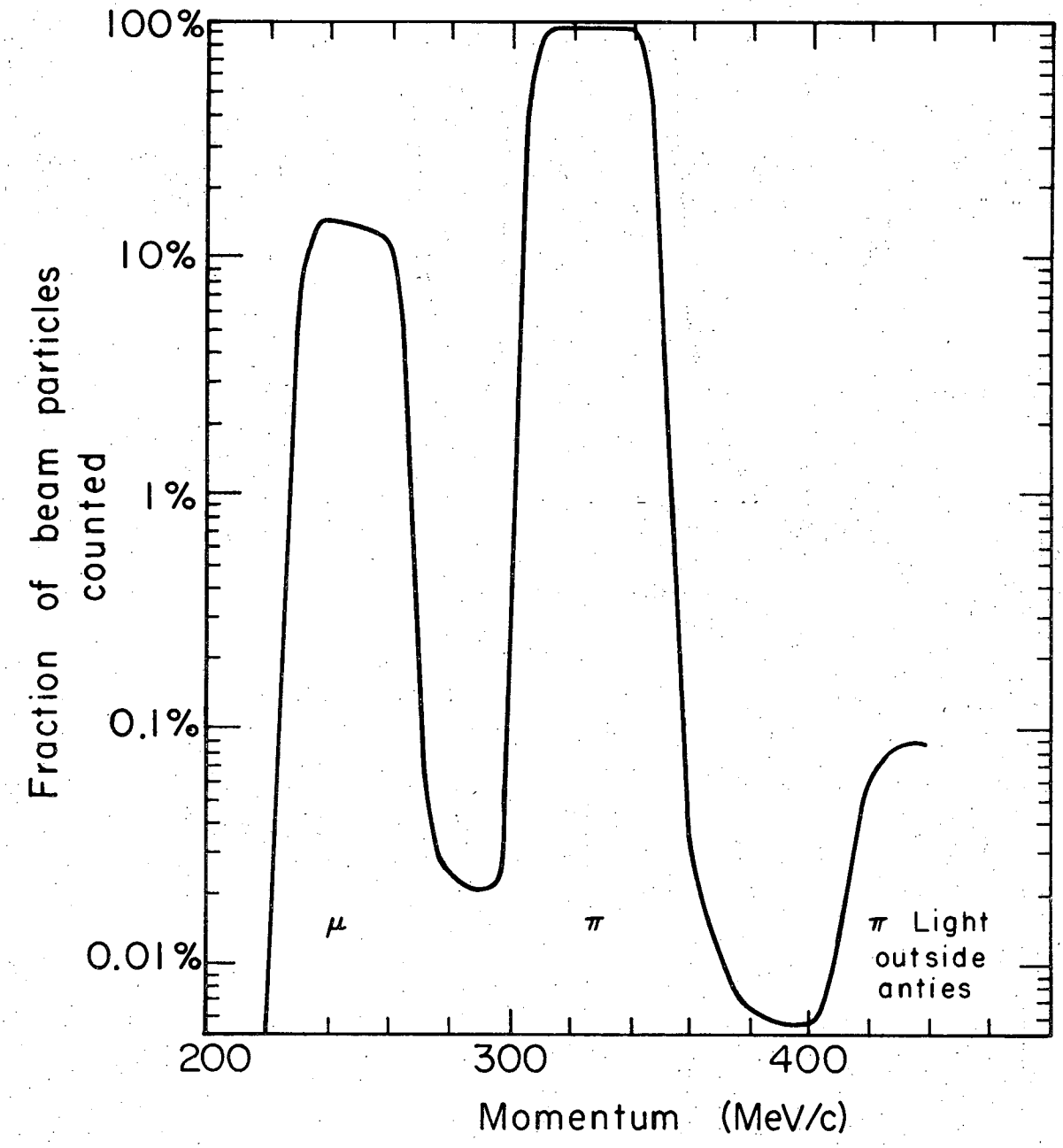

XBL687-3161

Fig. 8. The response of CM as a function of the beam momentum. Peaks occurred when muons and pions had the correct velocity. The background at high momentum resulted from spurious reflections of the wide-angle Cerenkov light.

behaved in this manner causing a small fraction of these particles to produce pulses in the central photomultiplier above the discrimination level. (As explained later in this section, electrons which counted in the Cerenkov counters caused negligible error in the measured lifetime because of the efficient operation of the electron veto counter A_e.)

The important feature of the pion peak was its flat top, indicating that over a range of about 15 MeV/c the counter efficiency was independent of momentum. (Actually, in the central region the apparent efficiency increased slightly with momentum because the higher the velocity, the smaller the fraction of pions which decayed before reaching the counter.) Momentum-response curves were used to determine the best operating momentum for the beam. It was more convenient, of course, to make small changes in the magnet currents than in the dimensions of the ring diaphragms. The diaphragm for CP took into account the 14 MeV that pions lost in traversing CM. Thus the beam momentum could be optimized for both counters simultaneously.

The performance of the Cerenkov counters depended greatly on the settings of the discriminators for the central photomultiplier and for the tubes of the anticoincidence ring. The discrimination level for the central photomultiplier was set according to the following considerations. If it was too low, rejection of undesired particles would not be satisfactory. If it was too high, the counter efficiency would be more sensitive to those systematic problems causing gain variation which have been discussed.

For CP the most important of these systematic effects was the variation of efficiency over the face of the central photomultiplier. The resulting variation in the efficiency of the counter over its aperture

was examined by making a series of precise measurements of D/M with CP displaced with respect to the beam line, either laterally or vertically. One such "profile" of the beam is shown in Fig. 9. The shape of the observed curves depended on both the counter and the beam. If the extent of the beam was well-defined and the counter efficiency was uniform over an area larger than the beam, then there would have been a range of displacements for which D/M was constant. A discussion of the profile in terms of beam containment will be given later. The effect of nonuniform counter efficiency was revealed by repeating the test with a different setting of the discrimination level for the central photomultiplier. For a higher threshold the width of the (approximately) constant portion of the curve was reduced, indicating that the effective counter aperture was smaller. The width of the curve allowed predicting how far down the decay path the beam would be contained within this aperture.

The counter efficiency was not sufficiently uniform if the threshold was too high. A convenient test of whether the threshold was too low involved the response of CP to electrons and muons. Two logic circuits identified these components of the beam. Recall that the monitor coincidence M was $M_1M_2M_3M_4\bar{A}_1\bar{A}_e CM\ \overline{CMA}\ \overline{\Sigma A}$. Particles satisfying $M_1M_2M_3M_4\bar{A}_1A_e\overline{\Sigma A}$ had the same trajectories as the pions in M but were electrons since they counted in the threshold Cerenkov counter A_e. Similarly, particles satisfying $M_1M_2M_3M_4\bar{A}_1\bar{A}_e\overline{CM}\ \overline{\Sigma A}$ were muons because they failed to count in either A_e or the central phototube of CM. Two additional circuits recorded those electrons or muons which counted in CP.

Identification of muons relied on correctly vetoing the pions in the beam. Note that the requirement was anticoincidence with CM rather than with CM $\overline{CMA}$, the logic signal which was used in coincidence to identify

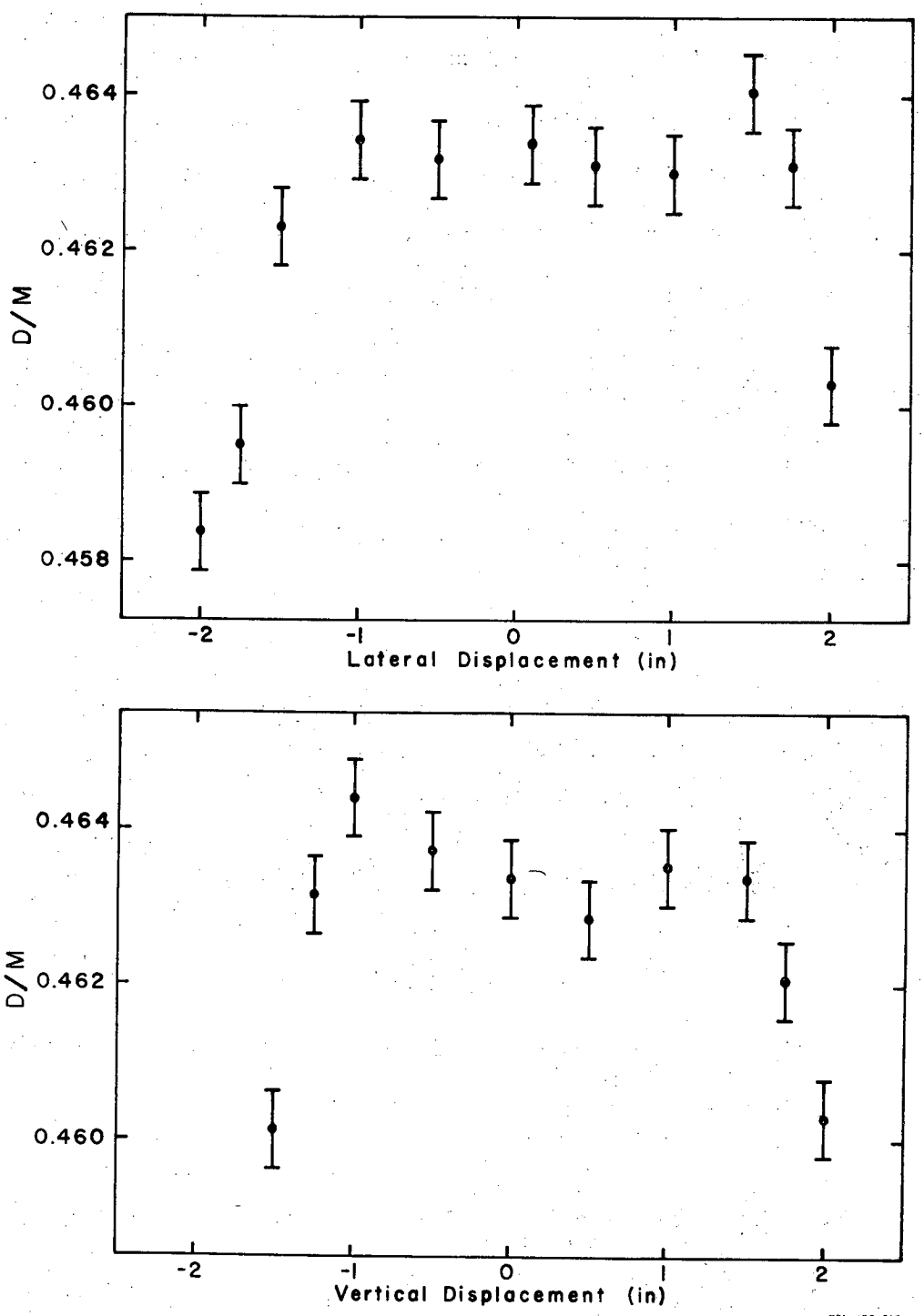

Fig. 9. Measurements of D/M made with CP, the movable Cerenkov counter, displaced from beam center. D/M is the fraction of the particles in the monitor coincidence which counted in CP.

pions. The reason was that some 0.2% of pions, which otherwise would have satisfied the monitor coincidence, produced enough light to be vetoed by CMA. For these pions the logic signal CM $\overline{\text{CMA}}$ would be absent. Thus with the alternate form of the anticoincidence requirement, these pions would not be vetoed.

At the discrimination level chosen for data taking, CP typically responded to 5% of the electrons and 0.2% of the muons. It must be emphasized that these efficiencies do not directly indicate a systematic error in the experiment. Error resulted only when CP responded to a particle which was not a pion and this particle spuriously satisfied the monitor coincidence. A measurement of the A_e efficiency, using a time-of-flight identification of electrons, showed that less than 1% of the beam electrons failed to count in A_e. The efficiencies of CM for beam electrons and muons were 0.5% and 0.02%, respectively. Consideration of the appropriate products of these efficiencies shows that the actual error was negligible. The fraction of electrons and muons which counted in CP was of significance because it was an indication of the fraction of decay muons that counted. Because the monitor system could not aid in rejecting decay muons, as in the case of electrons and beam muons, the error from these particles was not negligible. The problem of decay muons is discussed in Sec. VI-D.

The procedure for adjusting the anticoincidence system of one of the Cerenkov counters will now be described. The voltages applied to the photomultipliers which viewed each half of the anticoincidence ring were adjusted so the tubes had equal sensitivity as indicated by similar pulse-height spectra. There was only one discrimination level to set because the outputs of the two tubes were added before discrimination.

As was the case for the central photomultiplier, the choice of threshold was a compromise. If the threshold was too high, the anticoincidence ring did not fully perform its function of vetoing particles which were not pions. If the ring was made too sensitive, however, pions which should have counted were vetoed. Pions with higher momentum were more likely to count in the ring since their Cerenkov angle was greater. Momentum-response curves aided in setting the discrimination level. An excessively low threshold was indicated by a decrease in the counter efficiency for pions with momentum above the central value.

IV. THE DATA RUNS

With all the experimental apparatus performing optimally, a measurement of the positive and negative lifetimes with sufficient statistical accuracy required only about a week of continuous running. There were some 12 months, however, between the installation of the beam magnets and the completion of the experiment. Clearly most of the effort in the experiment was not devoted to routine data taking. Tuning of the beam transport system and the two Cerenkov counters and making various tests of their performance consumed a large portion of the running time. Eventually the stage was reached at which the best test of the performance of the system was how well it made the desired measurement. Several independent runs were carried out. Not all of these provided usable data, and some change in the movable Cerenkov counter was often made between these runs to improve its performance. One other phase of the experiment involved determining the velocity of the beam. This measurement was made in two different ways. The first used a magnetic spectrometer technique: an auxiliary bending magnet and four spark chambers. The second, a time-of-flight measurement, proved to be the more reliable. It will be described in detail in Sec. V.

A data run consisted of recording the number of pions detected by the movable counter (D coincidences) for some number of monitor counts (M coincidences). Measurements were made at seven positions along the decay path. The distance between each position was about six ft, the length of the sections from which the beam vacuum pipe was constructed. The first position, for which the CP was as far upstream as possible, was denoted DP1 (Data Position 1). The others were similarly named, DP7 being the position about 36 ft downstream of DP1. There was a gate valve

in the beam vacuum pipe at the start of the decay path, just after the last monitor counter, A_6. When the counter position was changed, the gate valve was first closed to keep evacuated and light-tight the section of vacuum pipe containing A_2 through A_6. High voltage could thus remain on these counters. After the length of the beam pipe was changed and vacuum restored, the gate valve was opened. A transit, situated on the beam line beyond the end of the decay path, was used to align the beam pipe. The Cerenkov counter was aligned by means of the beam-profile measurement previously described. This was the most reliable method since the precise location of the flask with respect to the exterior of the counter (the vacuum jacket) was not known. In addition, this method did not require knowing the lateral position of the beam as a function of distance along the decay path.

For π^- data the maximum intensity of the external proton beam was used; for π^+ this intensity was reduced so that the rate of monitor coincidences was the same for both beam polarities, about 1000 per second. (The maximum π^+ beam was used only for tests of the beam or Cerenkov counters.) Data were taken for both π^+ and π^- during the same run, the beam polarity being changed 6 to 12 times at each position. Frequent alternation of polarity was of particular value in determining the lifetime ratio. While the absolute lifetime measurement required that the counter efficiency be sufficiently constant during the entire run, the ratio calculation relied only on the constancy of the ratio of the plus and minus counter efficiencies. If the efficiency varied slowly compared to the rate of polarity reversal, the plus-minus ratio for sequential measurements would not change greatly.

In order to provide more statistical information about fluctuations,

the contents of all scalers were recorded and cleared more frequently than the polarity was reversed. For example, on one polarity the scalers might be recorded four times, each time 200 000 D coincidences were reached. The great quantity of numbers generated (there were 37 scalers) was not a hindrance because the scaler contents, besides being printed out on a typewriter, were written on magnetic tape to facilitate the subsequent computer analysis.

In the course of the experiment eight separate data runs were made.[16] There were important experimental differences between any two runs, and the range of validity of the results varied. Five of the runs used liquid deuterium in CP, and three used liquid hydrogen. The radiating liquid in CP was of great significance because of the nature of the π^+ and π^- pulse-height spectra for the two different media. (See Sec. III-B and Fig. 7b.) The effect of gain changes was greater, the greater the number of pulses having amplitude near the discrimination threshold. With hydrogen the π^+ distribution was greater at this point than π^-. With deuterium the plus and minus distributions were the same and were higher at threshold than either of the hydrogen distributions. Because the rate dependence of the gain of the central CP photomultiplier affected the π^+ efficiency more than the π^- when hydrogen was the radiating medium, the best measurements of the lifetime ratio were the deuterium runs, in which the rate effect was the same for π^+ and π^-.

For several reasons only the hydrogen runs were considered for the measurement of the absolute lifetime. Three of the systematic problems related to pion interactions in CP made hydrogen the preferable radiating medium. One was the rate-dependent phototube gain. Because of the limited data on the dependence of counter efficiency on rate, the most

suitable analysis of the hydrogen runs took advantage of the fact that the efficiency variation was greater for π^+ than for π^-. Such an analysis would not have been possible for the deuterium runs. (The different analyses are discussed in Sec. VI-A.)

The second systematic difficulty was variation in the efficiency of the CP phototube from one region of its face to another. Because of the difference in the pulse-height spectra, this problem was more serious when deuterium was the radiator than when hydrogen was used. Nonuniformity in the response of the counter across its entrance aperture, a result of this variation, was tested by beam-profile measurements. The results presented in Fig. 9 were obtained with the π^+ beam during the best hydrogen run. Although measurements with π^- were not carried out, they surely would have indicated an even more uniform response. In contrast, none of the profiles obtained during deuterium runs indicated as uniform a response as that shown in Fig. 9.

Similarly, because of the pulse-height spectra, the third systematic problem, random gain fluctuation, was more severe when CP was filled with deuterium. For example, the absolute lifetime calculation for one of the best deuterium runs had a poor goodness of fit: χ^2 per degree of freedom (χ^2/D) was 2.0. In contrast, for the best hydrogen run, χ^2/D was 1.0 for π^- and 1.3 for π^+. (The fact that the lifetime ratio calculation depended less critically on the stability of the counter efficiency was illustrated in the above deuterium run. Despite the poor absolute lifetime fit, the ratio fit had χ^2/D of 1.1, and this run was one of three upon which the best value of the ratio was based.)

In addition to these systematic difficulties with the use of deuterium, the beam momentum for the deuterium runs was not known well enough. Since

the index of refraction of liquid deuterium is slightly higher than that of liquid hydrogen, a lower beam velocity was needed to produce the same Cerenkov angle.[17] The operating momentum was 312 MeV/c for liquid hydrogen and 285 MeV/c for deuterium. The magnetic spectrometer measurement of the deuterium momentum surely had a large error, since it indicated a 0.7% difference between positive and negative momenta while all other tests showed good equality between the two beams. The best value of the hydrogen momentum came from the time-of-flight velocity mesurement performed at the end of the experiment. Since CP had been removed to increase the available flight path, no further lifetime data could be taken. A deuterium time-of-flight measurement would have required condensing deuterium in CM solely for this purpose. By this time it was apparent that hydrogen data were preferable for the absolute lifetime analysis, and the measurement was not made.

Of the three liquid hydrogen runs, one was far superior to the other two, and the absolute lifetime has been derived from the data of this run only. One of the two unsatisfactory runs was troubled by tube-gain instability. Poor reproducibility made the problem evident during data taking. The other run was the only one in the experiment which used a 2-in. phototube (an RCA 8575) in CP. To use this tube the reflective cone had to have a more acute angle, and thus the effective diameter of CP was reduced. (The relation between cone angle and the usable area of the counter was explained in Sec. III-C-2.)

The quality of the data from the best hydrogen run can be appreciated by comparing the 2-in.-tube data. For π^-, χ^2/D was worse for the latter run, and although χ^2/D was comparable for both π^+ fits, more data points were many standard deviations from their fitted values for the run with

the 2-in. tube. Confidence in the validity of the best run came from the fact that, within statistics, the same lifetime resulted from calculations which omitted different data positions. In the other run, however, omission of DP1 made a significant difference. Finally, the chosen run was the most complete. Data were taken at every position at two different times. (The order of positions was 4, 7, 6, 5, 4, 3, 2, 1, 7, 6, 5, 3, 2, 1.) Reproducibility, which tested the stability of the whole system, was excellent.

III. THE TIME-OF-FLIGHT MEASUREMENT

A. The Necessary Precision; the Problem of Calibration

Determining the lifetime from the observed beam attenuation required a measurement of the beam momentum--more precisely, the product $\gamma\beta$. The most reliable value was from a time-of-flight measurement of the pion velocity.

The time-of-flight technique directly measures the velocity of a particle by determining the time delay between the responses of two detectors, separated a known distance, through which the particle passes. The difficulty in determining the momentum p of a relativistic particle from its time of flight t is apparent from the equation

$$\frac{\delta p}{p} = \gamma^2 \frac{\delta \beta}{\beta} = \gamma^2 \frac{\delta t}{t} .$$

The relation shows how much smaller the relative error in β must be to achieve a given relative error in p. In principle, β can be determined to arbitrary accuracy by making the flight path sufficiently long. The major practical restriction to this approach is the reduction in counting rate from particle decay and beam divergence.

The beam of this experiment was well suited for a time-of-flight measurement. Its limited divergence made a long flight path possible. Its small lateral extent permitted using small timing counters. (Precise timing is difficult for large counters.) The flight path had a length which gave a pion transit time of 97 nsec. Since γ^2 was 6.0, the equation above shows that an accuracy of, say, 0.1% in p requires that t be known to 0.02 nsec. At first sight this may appear to be an impossible demand because of the many sources of time jitter in the electronics. For example, fluctuations in the secondary-electron transit time in most photomultiplier

tubes is more than ten times the required timing accuracy. The important point is that our application of the time-of-flight technique only sought to determine the mean transit time of pions in the beam, not that of individual particles as is often done in experiments with neutrons. If the nature of the fluctuations is understood, the accuracy in determining the mean can be increased by simply observing more particles.

The basic electronic arrangement consisted of a scintillation counter at each end of the path over which particles were to be timed. The output pulses entered discriminators, which in turn drove the START and STOP inputs of a time-to-amplitude converter (TAC), a device with output amplitude proportional to the difference between arrival times of the two inputs. The TAC output went to a pulse-height analyzer (PHA); by means of analog-to-digital conversion the PHA memory accumulated a velocity histogram.[18]

The limitation of the technique is the precision in determining the calibration of the system: the relation between time difference and PHA channel number. A sufficient procedure is to establish the time difference corresponding to some channel, and secondly the "scale factor" for the system, the number of channels per nanosecond. The great difficulty in precise calibration is that random variations in the performance of the electronics alter the calibration during the course of the measurement.

The number of channels per nanosecond changes with the gain of the TAC and PHA. Equally important are effects which shift the whole scale without changing the scale factor; in effect the channel corresponding to zero time difference changes. Such a shift can result from variations of the thresholds of either the discriminators following the scintillation counters or the START and STOP discrimination circuits internal to the TAC.

(The time delay between the input pulse to a discriminator and the output is a function of the threshold; unless the input pulse has an infinitely short rise time, a higher threshold causes an increased delay.) Another cause of shifts of the time scale is variation of the mean electron transit time in the photomultipliers caused by slight changes in the applied voltage. A change of one volt produces a significant change in transit time, about 0.01 nsec.

Despite these electronic fluctuations an accurate calibration is possible if it is carried out simultaneously with the primary measurement. Because systematic changes in the data are revealed by changes in the observed calibration, correction is possible. For one part of the calibration procedure, establishing a reference time interval, the criterion of simultaneous measurement was fulfilled by recording the time of flight of the momentum-analyzed electrons in the beam as well as the pions. To sufficient accuracy the electron velocity was that of light ($1 - \beta \approx 10^{-6}$), and thus knowledge of the flight distance determined the transit time. Variation in phototube time delay could broaden the peaks corresponding to the two particles but would not affect the separation between them.

An important added advantage of making use of the difference between pion and electron flight times, rather than measuring directly the total flight time, was that a greater precision in p could be obtained with given relative errors in the measured time interval t and in the flight distance d. If t is the pion time of flight, then $\beta = d/ct$. If instead, t is the difference between pion and electron flight times, then $\beta = 1/(1 + ct/d)$. The uncertainty in β caused by a given relative error in t or d in the first case is larger than that in the second by the

factor $\gamma^2(1 + \beta)$, about 11 in this experiment. Uncertainty in the flight distance was negligible if momentum was derived from the pion-electron difference: A 0.1% momentum measurement required an accuracy of only 5 cm.

The effect of random shifts in the electronics has to be considered in choosing a method for carrying out the second part of the calibration, determining the number of channels per nanosecond. One simple method consists of delaying one of a pair of identical outputs from a pulse generator to produce START and STOP pulses having a fixed, although unknown, time difference. Used as inputs to the TAC, these pulse pairs make a peak around some channel of the PHA. If an additional known time delay is added, the position of the peak changes some number of channels corresponding to this time interval. The difficulty is that the two measurements are done at different times, and any spurious shifts in timing cause error. In an ideal arrangement the time difference between the two inputs to the TAC alternates rapidly to minimize the effect of short-term changes. In addition, the calibration as a whole is performed continuously during acquisition of the primary data, so that slow changes in calibration can be recorded.

The procedure actually used in this experiment did not fully satisfy these criteria. The systemawas calibrated against the time delay in two cables, which in turn had to be measured. A more satisfactory direct calibration, a modification of the setup used to measure the two cable delays, is proposed below.

B. The Timing Counters and Electronics

The existing scintillation counters in the beam (M_1, M_2, M_3, and M_4) were only 1/16-in. thick and were not suitable for timing purposes. A scintillator thickness of about 1/2 in. was desired in order to produce more photons and thus more photoelectrons. Increasing the number of photoelectrons reduces the time jitter in two related ways. The statistical fluctuation in the secondary-electron transit time in the photomultiplier decreases. Secondly, because pulse-height variation is reduced, jitter from the subsequent pulse discrimination decreases. One disadvantage of a thick scintillator was that the momentum deduced from time of flight had to be corrected for ionization energy loss in the upstream counter. The thicker the counter, the more accurately energy loss per unit thickness would have to be known for the scintillator.

The first timing counter, denoted T_1, was positioned just after CM. It was undesirable to put T_1 anywhere in the beam ahead of CM since the momentum distribution entering the Cerenkov counter would be changed. The scintillator of T_1, 2.25-in. square, was adjacent to the scintillator of M_4, a 2-in. circle, so that every particle in the monitor traversed T_1. A simple, Lucite light pipe coupled the scintillator to the photomultiplier. To improve photoelectron yield an RCA-8575 photomultiplier was used because of its high quatum efficiency.

The ideal second counter would have been CP since the particles to which it responded were precisely those we wished to time. It was unsuitable, however, because the lack of uniformity of the phototube pulses made accurate timing difficult. A counter like T_1 placed in front of CP could have provided the timing pulse with appropriate logic requiring that the particle traversing the timing counter also count in CP. The

problem with such an arrangement was that a thick scintillator in front of CP would alter the momentum and angular distribution of the beam entering the counter. In addition, the use of CP, a rather long counter, would have significantly reduced the flight path that could be readily obtained. For these reasons CP was not used in the measurement.

The downstream counter T_2 was a scintillation counter identical to T_1. Since the movable Cerenkov counter was not to be used, it was removed from the decay path. T_2 was mounted on the beam line 87 ft from T_1, about 1.1 mean decay lengths from DP1. There was a continuous vacuum from M_4 to T_2. The extended beam is shown in Fig. 10.

The measurement was made by accumulating particle data, recording the results, and then calibrating the system with the two delay cables. This procedure was repeated 18 times so that the degree of internal consistency among the data could permit estimating the effect of systematic drifts.

A simplified logic diagram is shown in Fig. 11. The important feature of the setup for particle data (the top diagram) was that the PHA was operated in a coincidence mode: A signal at the data input was ignored unless there was a level at the coincidence input. Such operation permitted rejection of particles which traversed both timing counters yet failed to satisfy a given coincidence requirement. The PHA accepted timing data only for those particles counting in T_1 and T_2 and satisfying either the M coincidence or the coincidence identifying electrons.

By gating the PHA, rather than one of the fast logic components, there was less danger of introducing a timing bias from the coincidence requirement. Because of the 300-nsec internal-conversion delay in the TAC, the enabling gate reached the PHA much earlier than the data signal.

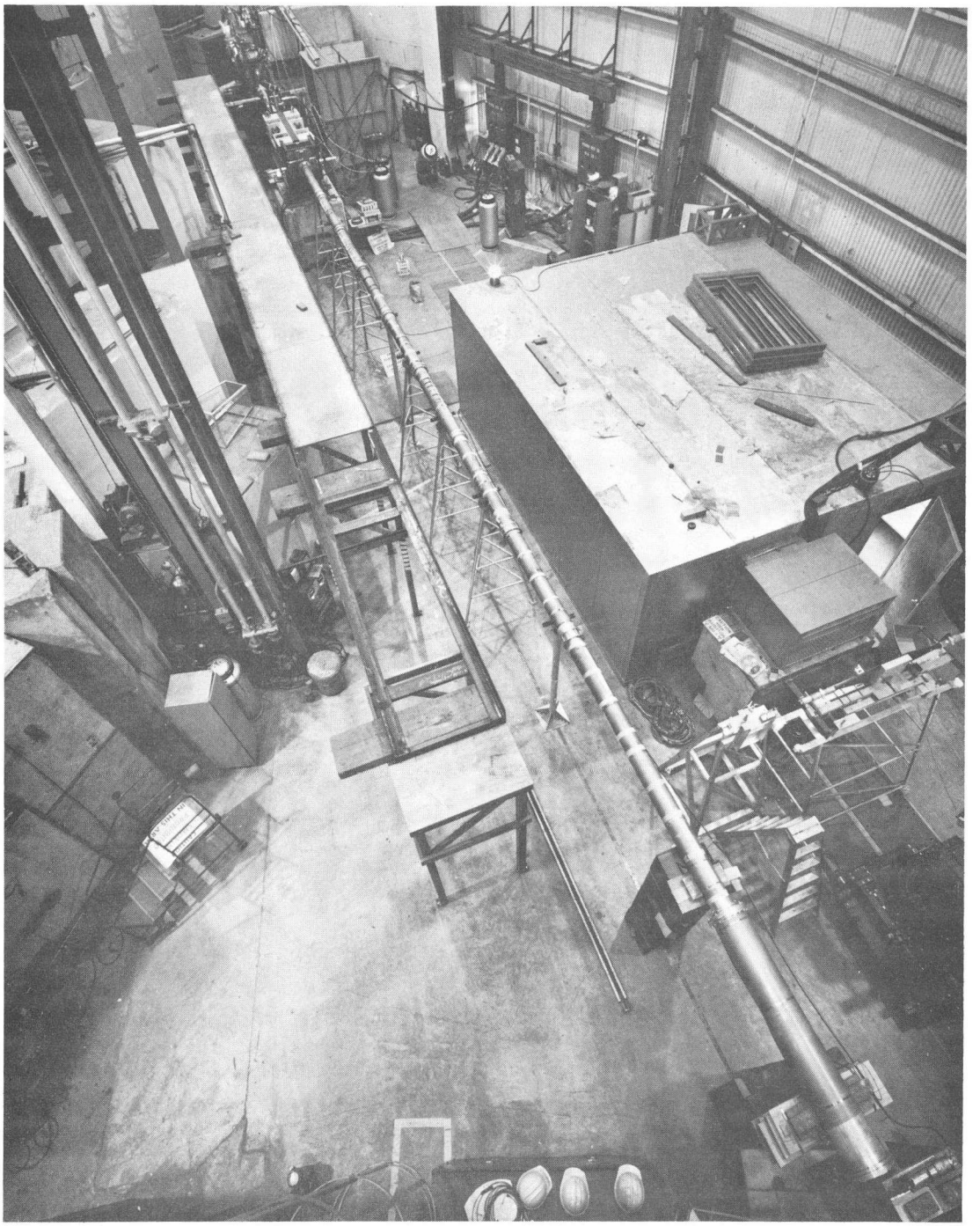

XBB 684-2314

Fig. 10. The experimental setup for the time-of-flight measurement. The movable Cerenkov counter has been removed and the beam vacuum pipe extended. (Compare Fig. 2.) T_2, the final timing counter, is in the lower right corner of the photograph.

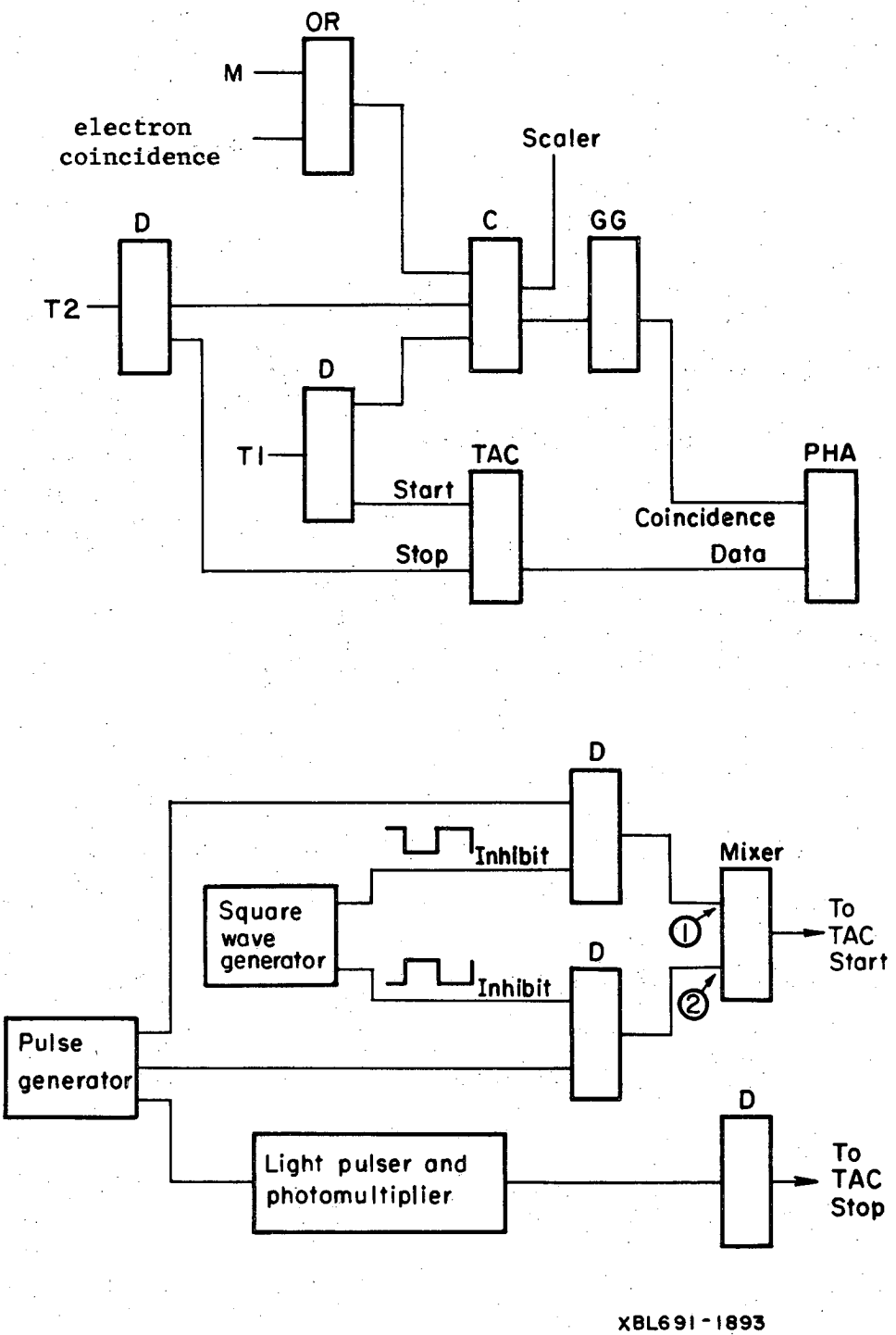

Fig. 11. Logic diagrams for the time-of-flight measurement. To record particle flight times, the inputs to the TAC were signals from counters T_1 and T_2 as shown in the upper figure. To calibrate the system, the TAC inputs were generated by the arrangement in the lower figure. Cables of known time delay were inserted at point 1 or point 2. D labels discriminator modules; C, coincidence; and GG, gate generator.

The width of the gate was adjusted so it ended well after the data signal.

The bottom diagram in Fig. 11 shows the setup used to calibrate the TAC-PHA system between runs. The pulse generator operated at a rate compatible with the TAC and PHA ($\approx$ 2 kHz) and simultaneously drove two discriminators and a light pulser.[19] The light pulser was viewed by a photomultiplier whose output after discrimination served as the STOP input for the TAC. The purpose of the light pulser and photomultiplier was to introduce time jitter in the STOP pulses. Without it the TAC pulse-height distribution fell in a single channel of the PHA, and it was impossible to obtain resolution better than one channel. With the use of the photomultiplier, the calibration system produced Gaussian peaks similar to those of the time-of-flight data.

The two discriminators driven directly by the pulse generator were alternately inhibited by complementary outputs from a slow ($\approx$ 10 Hz) square wave generator. Thus only one or the other sent pulses to the mixer. With no added calibration cables, the time difference between START pulses from either discriminator and STOP pulses was approximately the pion transit time.

The basic calibration procedure consisted of a run with a calibrated cable at point 1 in the figure and a run with the same cable at point 2. Because of the action of the square wave generator, two peaks were simultaneously acquired in the PHA during each run. One, at the approximate location of the pion peak, resulted from START pulses which reached the mixer without added cable delay; the other, corresponding to a smaller time difference, resulted from pulses delayed by the calibrated cable before reaching the mixer. After each time-of-flight run, this procedure was carried out for each of the two calibration cables. Their nominal

delays were 10 and 20 nsec; the time-of-flight difference between electrons and pions was about 9 nsec.

C. Analysis

1. Time-of-Flight Data

The mean channels for the electron and pion peaks in the TAC pulse-height distribution were found by a least-squares fit to some function. The variance in the contents of any channel was taken to be the number of counts in that channel. It was necessary to consider what functions should be used for electrons and pions, and how many channels in any peak should be used in the fit. For a group of particles with a unique velocity, the shape of the observed peak reflects just the instrumental resolution. The electron peak shape is expected to be Gaussian because timing fluctuations, principally those in the photomultipliers, have this shape.

The pions have a distribution of velocities. Since this distribution is determined by the beam transport system, essentially a momentum-defining system, it might be expected that the pion momentum distribution--rather than the velocity distribution--is Gaussian. The observed time-of-flight distribution should be an intermediate case, since it results from the true velocity distribution folded into the Gaussian instrumental resolution. Because of these considerations the pion data were fit assuming a Gaussian distribution in either momentum or velocity to allow comparing the two limiting cases.

For each peak only those channels whose contents exceeded a given fraction of the maximum of the fitted curve were considered. The number of channels used in the fit was varied by changing this cutoff fraction. If too few channels are used, the mean of the fitted curve may be in error because of variation from one channel to the next of the effective channel width; if more channels are used, the effect is minimized. If

too many channels of the peak are used, the "tails" of the distribution may receive undue weight. Far from the mean, the system resolution function may not be strictly Gaussian, and in addition a larger fraction of the counts may arise from some background. Fits were also made which allowed for the possibility of a constant background.

The analysis considered most meaningful was fitting all peaks to a Gaussian plus constant background. Figure 12 shows the fitted curves for electrons and pions for one run. Table II gives the mean number of channels between pions and electrons for the 18 runs as a function of the cutoff fraction used for pions and that for electrons. The best value was taken as 107.54 channels.

Table II. Mean number of channels between pions and electrons.

	Electron cutoff			
Pion cutoff	0.1	0.2	0.3	0.4
0.1	107.58	107.59	107.59	107.59
0.2	107.56	107.56	107.56	107.56
0.3	107.54	107.54	107.54	107.54
0.4	107.53	107.54	107.54	107.54

Chi-square per degree of freedom averaged 1.3 for electrons and 0.8 for pions with this form of fit. If the fits did not allow for background, the mean separation (for cutoffs of 0.3) was 107.57 channels; goodness of fit was 1.9 and 1.0 for electrons and pions, respectively. Lastly, if the pion peaks were fit assuming their shape resulted from a Gaussian distribution in momentum, the computed separation was 107.56; goodness of fit was essentially unchanged. This last method of fitting was the least realistic. The fact that the pion peaks were only 15% wider than the electrons shows that the width was contributed mainly by instrumental resolution, not by the width of the momentum distribution.

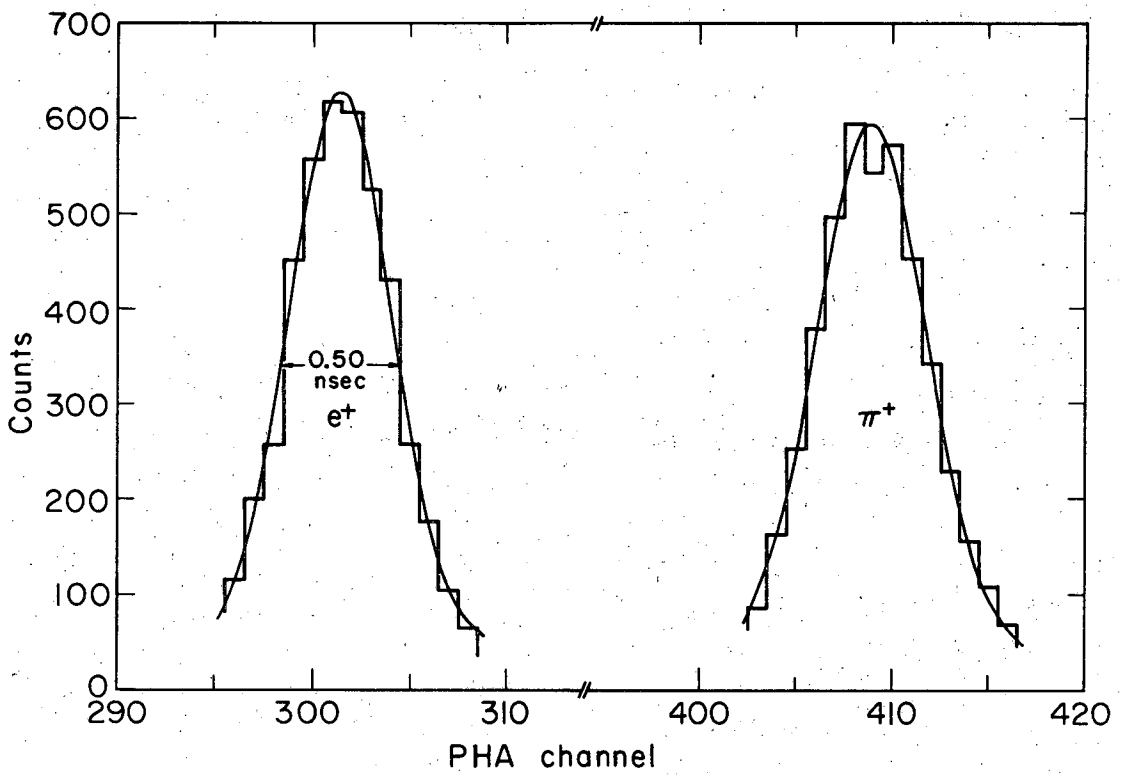

Fig. 12. Time-of-flight spectrum for one of the 18 runs. The histograms show the observed distributions for electrons and pions. The curves are least-squares fits to a Gaussian plus constant background. χ^2 per degree of freedom is 1.2 for the electron peak, and 1.3 for the pion peak.

The major source of uncertainty in the number of channels separating pions and electrons was fluctuations in the electronics which caused the observed separation to vary from run to run. Based on the internal consistency of the 18 runs, the error is estimated to be 0.11 channel.

2. Calibration Data

For one of the two reference cables the data from the calibration procedure consisted of the mean channels for four PHA peaks: two for each of the positions for the cable. (Refer to Fig. 11.) The mean for each peak was found by a least-squares fit to a Gaussian shape. To derive the expression used to calculate channels/nsec for the system, define channel numbers and corresponding START-STOP time differences for the four peaks as follows:

		Low peak	High peak
Cable at point 1	PHA channel	C_1^{in}	C_2^{out}
	time difference	$T - T_1$	$T + \Delta T$
Cable at point 2	PHA channel	C_2^{in}	C_1^{out}
	time difference	$T - T_2 + \Delta T$	T

For the PHA channels the superscripts indicate whether the cable was "in" or "out" of the position indicated by the subscript. Because the cable acted to delay the START input of the TAC, the "low peak" corresponded to the leg of the network which included the cable. The inherent time difference between START pulses proceeding via point 1 and STOP pulses was T; for point 2 the time was $T + \Delta T$. T_1 was the time delay added by inserting the cable at point 1. The same cable at point 2

caused a delay of T_2. (T_1 did not precisely equal T_2 because of differences in the response of the two input circuits of the mixer.) T and ΔT were unknown quantities; T_1 and T_2 were known. If G is the "gain" of the system (channels/nsec), these quantities are related by $(C_2^{out} - C_1^{in}) = G(T_1 + \Delta T)$ and $(C_1^{out} - C_2^{in}) = G(T_2 - \Delta T)$. Eliminating ΔT, we find

$$G = \frac{\left(C_2^{out} - C_1^{in}\right) + \left(C_1^{out} - C_2^{in}\right)}{T_1 + T_2} .$$

To understand the motivation behind this method of calculating G, consider the more straightforward procedure of comparing the positions of the peaks observed with and without the cable at <u>one</u> point in the setup. In this case

$$G = \frac{C_1^{out} - C_1^{in}}{T_1} \quad \text{or} \quad G = \frac{C_2^{out} - C_2^{in}}{T_2} .$$

Because C_1^{out} and C_1^{in} were measured in two <u>different</u> runs, a change in the transit time of the phototube, for example, could introduce error. The more involved expression for G, however, consists of differences in channel numbers for peaks observed in the <u>same</u> run, and error from electronic changes was minimized.

The average of the 32 separate calibrations was 12.454±0.005 channels/nsec, where the uncertainty is based on the internal consistency among the measurements. The 15 measurements using the "10" nsec cable were consistent with the 17 based on the "20" nsec cable. The two cases gave 12.456 and 12.453 channels/nsec, respectively. The calibration was also obtained by the alternative procedure, comparing the peaks found with and without a calibration cable in one leg of the setup. Although the calculated mean was essentially the same as that obtained by the more

involved method, the "internal consistency error" was 0.010 channels/nsec instead of 0.005.

The values for the cable delays used in the calculations were 10.335 nsec for the "10" nsec cable in position 1 and 10.345 for position 2. The corresponding values for the "20" nsec cable were 20.251 and 20.265 nsec. Each value was the average of some 30 independent measurements whose internal consistency implied an uncertainty of 0.007 nsec. Thus the greatest relative uncertainty was that for the shorter cable, 0.07%. It is felt that the only systematic error in the cable delays was from nonlinearity of the TAC and PHA when these were used to calibrate the cables. This error is included in the calculation of the uncertainty in momentum given below.

Additional confidence in the values of the cable delays is gained by comparing the ratio of the time delays claimed for the two cables to the ratio of the number of channels each cable shifted the calibration peaks during the time-of-flight measurement. During data taking the ratio of the shift for the "20" nsec cable to that for the "10" averaged 1.9591. The ratio of the assumed time delay for the "20" nsec cable to that of the "10" is 1.9592 (an average for the two positions in the calibration setup). Because of the nature of the method used to calibrate the cables, systematic error could have affected the measurement of the longer cable much more than the shorter. In view of this possibility, the agreement of the above ratios is indeed encouraging.

3. Momentum Calculation

The calculated difference between the pion and electron flight times, 8.635±0.014 nsec, implies a momentum of 308.46±0.27 MeV/c. The error in the time difference reflects the uncertainty in calibration cable delays

(0.07%) and in the number of channels between calibration peaks (0.04%) and between particle peaks (0.10%). Nonlinearity of the TAC-PHA system is estimated to contribute no more than 0.10% to the error. (Evaluation of this nonlinearity is described below.) Calibration of the reference cables and the time-of-flight measurement itself made use of the TAC and PHA in a similar fashion; the above nonlinearity error covers both cases.

Since the lifetime data were taken without T_1 in the beam, the appropriate momentum is higher by an amount corresponding to the energy loss in the 1.49 cm of scintillator. This energy loss was calculated assuming the plastic scintillator has a density of 1.02 g/cm^3 and is composed of hydrogen and carbon with atomic ratio of 1.10.[20] With stopping powers of 4.27 and 1.86 MeV-cm^2/g for hydrogen and carbon,[21] respectively, the effective stopping power is 2.06 MeV-cm^2/g, and the energy loss is 3.13 MeV. The estimated uncertainty is 5%. The atomic stopping powers have an accuracy of order 1%.[22] Other small sources of error are departure from Bragg's rule (the effective energy loss is the sum of the losses of the constituent elements), error in the effective thickness of the scintillator if it was not precisely perpendicular to the beam, and small energy losses in counter wrapping. The calculated stopping power is insensitive to the hydrogen-carbon ratio; a 10% change in the ratio changes dE/dx only 0.5%.

The final result, the momentum of the beam with which the lifetime was measured, is 311.89±0.32 MeV/c.

D. Systematic Errors

1. Decay Muons

Since T_2 did not distinguish pions from decay muons, a systematic error could result from these background particles. Momentum-analyzed electrons and muons formed peaks well separated from the pion peak, but the time-of-flight distribution of decay muons which registered in the counter was hidden under the pion peak. If this distribution was not symmetric about the true pion peak, the observed "pion" peak would appear shifted in position.

An estimate of the magnitude of this error showed that it was negligible. The time-of-flight distribution for decay muons was calculated with several simplifications. The pion beam was assumed to have no angular divergence and no lateral extent--a beeline of particles. T_2 was represented as a circle of radius 3.5 cm. Since the lab angle between a decay muon trajectory and the beam axis was always small, the transit time between the decay point and the counter was computed using the projected distance along the beam axis.

If the velocity of the decay muon is greater (less) than the pion velocity, the effective time of flight is shorter (longer) than if the pion had not decayed. For a given value of this difference, there are contributions from decays occurring over some interval of the decay path. The limits of the interval are determined by the maximum and minimum muon lab velocity and by the requirement that the muon intercept the counter. The kinematic relationship between the time-of-flight difference, the center-of-mass decay angle, and the distance between the decay and the counter is shown in Fig. 13. The decays corresponding to the open region of the figure are those in which the muon misses the counter. The

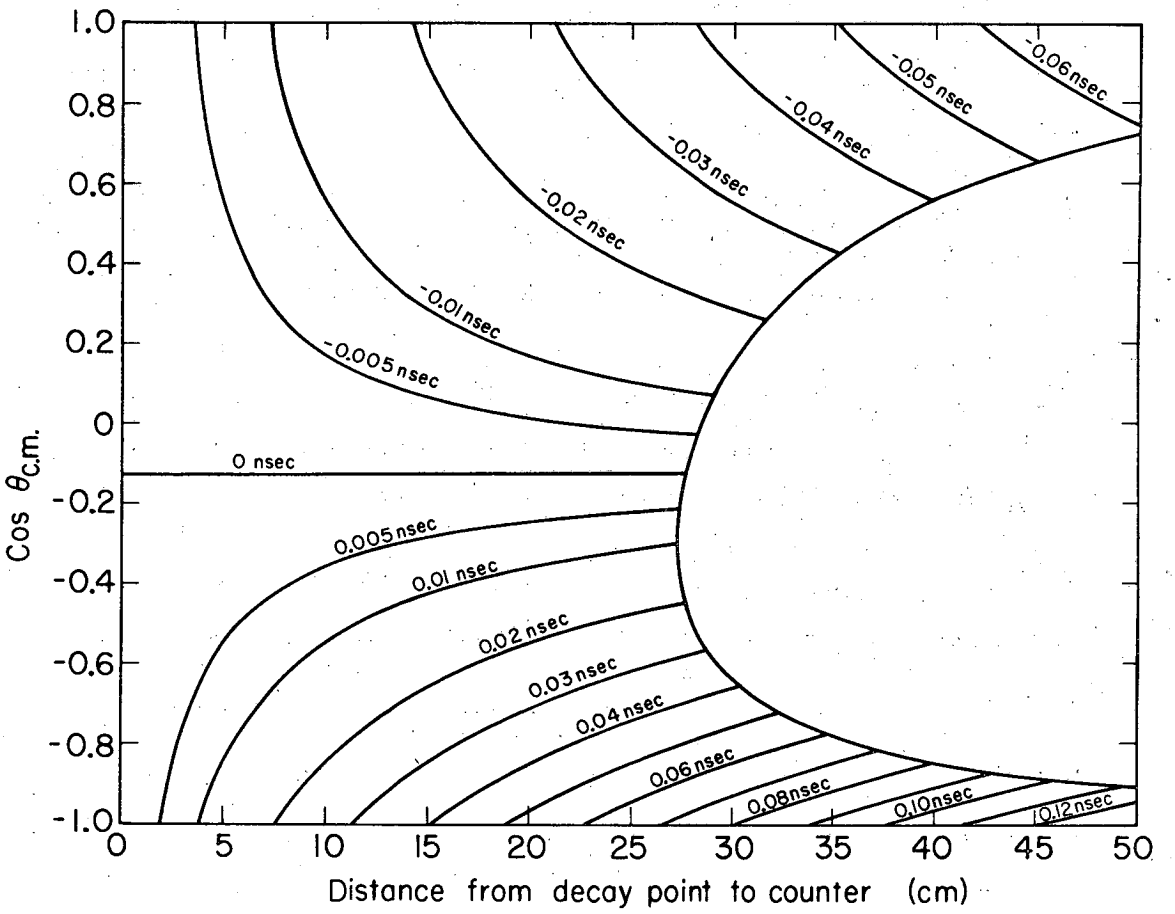

Fig. 13. Kinematics of the decay muons which intercept a 3.5-cm circle perpendicular to the pion beam. Each curve corresponds to a given value of the difference between the time of arrival of the decay muon and the time the pion would have arrived had it not decayed. Muons decaying forward in the pion rest frame arrive "early"; those decaying backward arrive "late."

horizontal line labeled "0 nsec" indicates decays in which the muon velocity is the same as the pion velocity; this relationship occurs for a fixed decay angle. Note that for larger time differences smaller ranges of decay distances and decay angles are possible. Thus the resulting time-of-flight distribution, shown in Fig. 14, is strongly peaked about the mean pion time of flight. (The actual distribution is, of course, much broader because of the finite experimental resolution.)

The error caused by the detected decay muons is estimated as follows. In the analysis of the time-of-flight data, the mean of each pion PHA peak was found by fitting to channels corresponding to a time interval of approximately a nanosecond. The above calculation shows that 0.024 of the particles arriving within this interval were actually decay muons. The mean arrival time of these muons is 0.017 nsec earlier than pions which did not decay. The muon background thus causes the "pion" time of flight to appear 0.0004 nsec too short. By assuming the incident pion beam is a line of particles this approximate calculation underestimates the ratio between the decay muons and pions intereepted by T_2; nevertheless, for any reasonable estimate of the actual magnitude of the background, the error is still negligible.

2. Spurious Cerenkov Light

It was essential that the timing counters respond in the same manner for both pions and electrons. Although scintillation light was sufficiently similar for both particles, the weak Cerenkov light from particles traversing the thick, cylindrical part of the light pipe had different intensities for electrons and pions. Since the Cerenkov light originated closer to the phototube than scintillation light, it was an asymmetric background in the time distribution of the phototube pulses. The problem

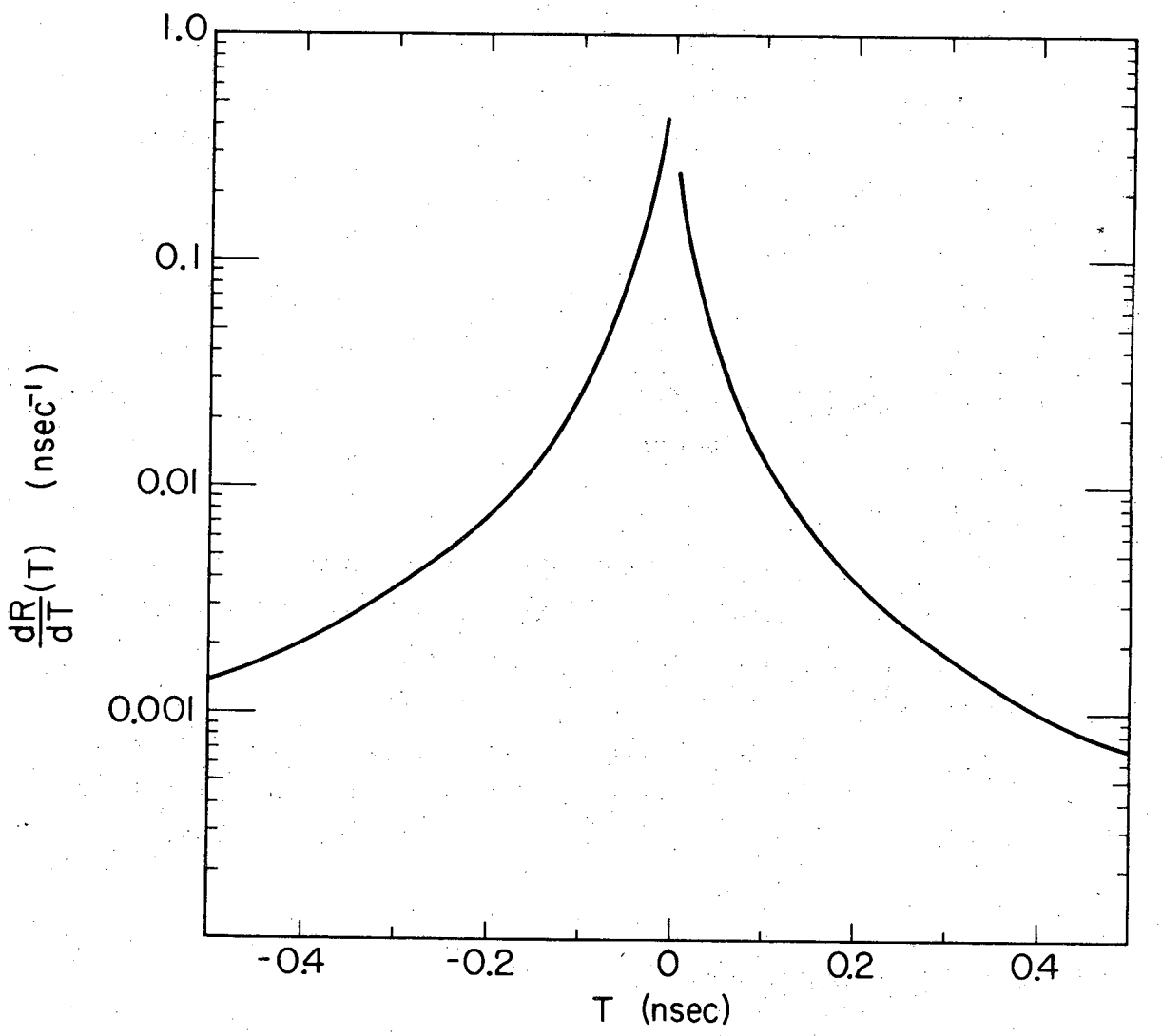

XBL691-1894

Fig. 14. The calculated time-of-flight distribution of decay muons detected by counter T_2. $\frac{dR}{dT}(T)$ is the number of muons arriving in the time interval dT divided by the total number of pions detected. T = 0 corresponds to the mean pion time of flight. The integral of the function over the interval shown in 0.024, the ratio of detected muons to detected pions.

affected only T_2; particles counting in M_3 and M_4 could not have passed through the light pipe of T_1.

If the threshold of the discriminator following T_2 was set exceptionally low, the time-of-flight distribution for electrons showed a small peak from Cerenkov light as well as the main scintillation peak. Tests were made to determine if under normal data-taking conditions Cerenkov light significantly altered the shape of the electron peak. An additional scintillation counter, T_3, was placed behind T_2. Its scintillator overlapped the scintillator, but not the light pipe, of T_2. The shape of the peak for electrons counting in both T_2 and T_3 was compared to that for electrons counting in T_2 alone. No significant difference was seen. In a more critical test, T_3 was used in anticoincidence with T_2 so that only particles producing light in the light pipe were considered. The observed Cerenkov background was relatively flat over the region of the desired light and was only 2% of the maximum of the scintillation peak which would have been observed without the anticoincidence requirement. Thus the small background had negligible effect on the measured position of the scintillation peak.

3. Dispersion in the Beam

The area of T_2 was much smaller than the cross section of the beam. Dispersion in the beam could have caused the measured momentum to depend on the lateral position of the counter. If Cerenkov light had not been a problem, the dispersion could have been investigated by simply changing the position of T_2. One reason this light was such a small background during normal data taking was that the thick aluminum flange for the vacuum window at the end of the beam pipe shielded the T_2 light pipe. If T_2 was displaced with respect to the beam line, the effective

shielding was altered. The magnitude of the Cerenkov background changed greatly, obscuring any small variation in the shape of the peak resulting from dispersion.

The optics of the beam transport system could have caused dispersion in the beam arriving at T_2. The first bending magnet and quadrupole produced an image of the target at the collimator. The second bending magnet and quadrupole then formed an image at M_4, and the third quadrupole a final focus at a point upstream of T_2. Except for the effect of chromatic aberration, there was no dispersion at the last two foci. Because of the dispersion introduced at the collimator image, at the last two foci there might have been a correlation between the momenta of beam particles and their angles with respect to the axis. Such a momentum-angle correlation would cause a momentum-space correlation (dispersion) in the beam downstream of the final focus.

Multiple Coulomb scattering in the liquid hydrogen radiator of CM effectively destroyed the angular correlation and made the momentum error from dispersion at T_2 negligible. The problem was analyzed by the conventional matrix description of beam optics. For a given momentum the various counters determined what portion of the phase space of particles emitted by the production target was accepted by the system (passed through all counters). If there were no scattering in CM and T_2 was one inch from the true beam center line, the error in the observed mean momentum would have been significant. The trajectory of a particle was displaced one inch at T_2 if it was off-momentum 0.12%. Taking the finite sizes of T_2 and the target into account, one finds the error in the measured momentum would have been 0.09%.

To incorporate CM scattering in the phase-space calculation, a

larger effective size was used for each aperture downstream of CM. As an approximation, the dimensions were increased by $L\Delta\theta$, where L was the distance from CM to the counter and $\Delta\theta$, the rms scattering angle, was 0.7 deg. The result was that the counters following CM did not limit the transmitted phase space at all; the limits were determined by the apertures ahead of CM. Thus the position of T_2 could not bias the momentum distribution of particles passing through all the counters including T_2.

The result can be expressed another way. In the presence of scattering in CM, T_2 would have to be at least 13 in. off center for its position to have an effect on the momentum distribution of beam particles counting in it. There was no beam at this radius, however; M_4 and A_6 geometrically limited the beam radius to 9 in. at T_2. The difference results because the counters following CM had two distinct effects. In restricting the momentum distribution of the beam, the effective dimensions of these counters were larger because of the scattering in CM. On the other hand, restriction on what possible trajectories could pass through the counters was not affected by this scattering. (Scattering in CM did have the effect of reducing the rate of monitor coincidences because particles with unsuitable trajectories were vetoed.)

The mixing of trajectories of different momentum made another possible source of error negligible: a difference in the position at T_2 between the positive and negative beams. The stray magnetic field of the cyclotron--leakage from the return flux of the magnet--did not change when the beam polarity was changed. This field, already very weak at such a large distance from the machine, was reduced to less than 0.2 gauss by magnetic

shielding around the vacuum pipe the whole length of the flight path. A field of 0.2 gauss along the decay path would cause a separation between the beams of 1.5 cm. The previous arguments show that a displacement of this size had no significant effect on the measured momentum.

4. Linearity of the System

Tests were performed to find the integral linearity of the TAC-PHA system: the degree to which a linear relationship held between PHA channel number and the time difference between START and STOP inputs of the TAC. This integral linearity was calculated from a measurement of the differential linearity of the system: the variation from channel to channel of the corresponding incremental time differences. The technique used was to generate START and STOP pulses having a random time separation. Statistically significant differences in the number of counts accumulated in each PHA channel indicated the differential nonlinearity.

Random START pulses were generated by a radioactive source viewed by a scintillator and photomultiplier. STOP pulses were produced by a pulse generator whose period was greater than the maximum time difference accepted by the TAC. (This period was nominally 150 nsec; the TAC produces an output only if a STOP pulse occurs within 110 nsec after the START.) This arrangement ensured that a random START pulse could be followed by no more than one STOP during the time the TAC was ready. If two STOP pulses had been allowed to follow a START within this time, the TAC output would always correspond to the earlier one, and the time distribution would be biased toward low values.

If the system had no differential nonlinearity, each channel would correspond to some constant incremental time difference $\overline{\Delta T}$, and the time interval represented by channel C would be simply $C\,\overline{\Delta T} + T_o$. In practice

the ith channel corresponded to some incremental time interval $(\Delta T)_i$ and the true time interval represented by channel C was of the form

$$\sum_{i=1}^{C} (\Delta T)_i + T_o'.$$

(T_o and T_o' are constants.)

The quantities of interest in this experiment were differences between two time intervals. The data analysis effectively assumed the system was linear: $\overline{\Delta T}$ was determined for some range of channels, and this same mean value was applied to a different interval. From the above expressions the discrepancy between the true time difference from channel C_1 to C_2 and the value calculated assuming linearity is

$$\sum_{i=C_1}^{C_2} (\Delta T)_i - (C_2 - C_1)\,\overline{\Delta T}.$$

To illustrate the observed integral nonlinearity for our system Fig. 15 is a plot, as a function of channel number C, of the quantity

$$E(C) = \sum_{i=150}^{C} (\Delta T)_i - (C - 150)\,\overline{\Delta T}.$$

The range of channels covers all the intervals used during the time-of-flight measurement, the associated calibrations, and the later cable measurements. The error in the computed time difference between channels C_1 and C_2 is given directly by $E(C_1) - E(C_2)$. It can be seen that over this region of the PHA the error could have been no larger than 0.009 nsec. The greatest relative error in the data analysis would occur for the smallest time interval calculated, the 8.6 nsec difference between the pion and electron times of flight. Thus it is concluded that the relative error arising from nonlinearity was less than 0.10%.

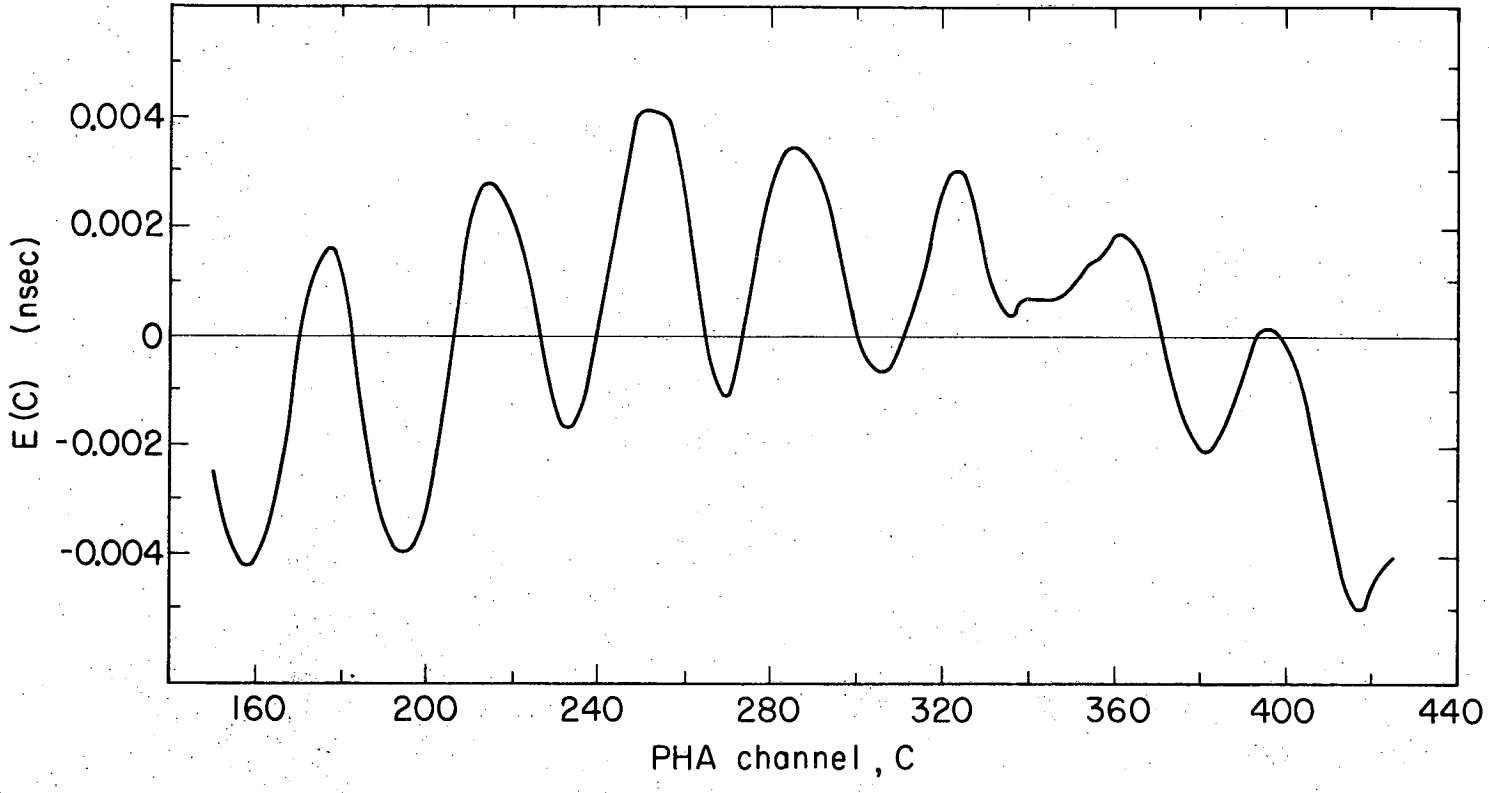

XBL691-1895

Fig. 15. Linearity of the TAC-PHA system. $E(C) = \sum_{i=150}^{C} (\Delta T)_i - (C - 150)\,\overline{\Delta T}$. $(\Delta T)_i$ is the time increment corresponding to the ith channel. $\overline{\Delta T}$ is the mean value. $E(C_1) - E(C_2)$ is the sum of the time deviations for the channels between C_1 and C_2 and is thus the total time error between these two channels.

E. Calibration of Reference Cable Delays

The technique compares the shift in arrival time of pulses delayed by the cable with a shift corresponding to a known change in the period of a pulse generator. An arrangement of fast-logic modules extracts a pair of sequential pulses from the wave train of a high-frequency pulser, routes the first to the START input of a TAC, and the second to STOP. At the TAC these pulses are separated in time by $\Delta T_1 = 1/\nu_1 + C$, where ν_1 is the frequency of the pulse generator, and C is the inherent time difference between the paths from the pulser to the two inputs of the TAC. Pulse pairs generated in this way produce a peak in the pulse-height distribution of the output of the TAC.

The generator frequency is then changed to ν_2. A new peak is produced corresponding to $\Delta T_2 = 1/\nu_2 + C$, where C is unchanged. The time scale of the system (channels/nsec) is thus determined since the number of channels between the peaks corresponds to a known time difference: $1/\nu_1 - 1/\nu_2$. If, instead of changing the frequency, a cable is inserted at some point before the TAC, the number of channels the peak changes determines the time delay of the cable.

In principle, knowledge of the linearity of the TAC and PHA is not needed. If the second frequency is varied until the time shift corresponds exactly to that caused by the cable, the TAC and PHA serve merely as a bridge circuit sensing equality between the two cases. Our TAC-PHA system was sufficiently linear so that after finding a second frequency which gave approximate equality, we could then calculate the cable delay by simple proportion.

A simplified logic diagram is shown in Fig. 16. As previously discussed, to make an accurate comparison it is necessary to minimize the

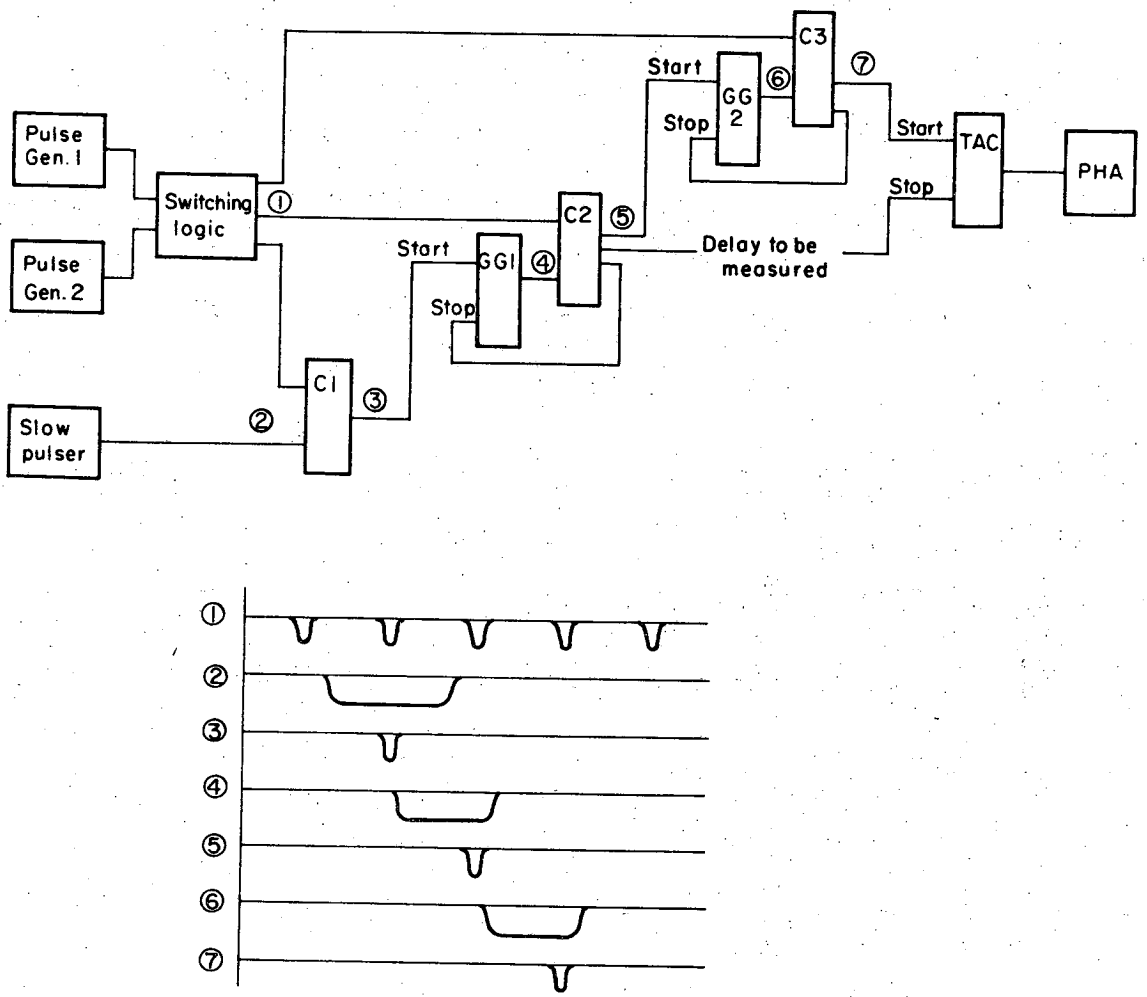

XBL691-1892

Fig. 16. Logic diagram for the setup used to measure the time delay of the calibration cables. The timing relationships at the points indicated in the diagram are shown below. C modules are coincidence units; those labeled GG are astable gate generators.

delay between observations made under the two conditions. For this reason, rather than change the frequency of one pulse generator, two similar generators were used with a system for rapidly switching from one to the other. The box labeled "switching logic" consisted of modules which effectively enabled Pulse Generator 1 and inhibited Pulse Generator 2, then inhibited 1 and enabled 2. The alternation rate was about 10 Hz.

Since $T = 1/\nu$ implies $\delta T = \frac{1}{\nu} \frac{\delta \nu}{\nu}$, using a high frequency minimizes the error in T caused by drifts in ν during the measurement. On the other hand the lower the frequency, the smaller the relative change in frequency that is required to measure a given time delay. A low frequency thus minimizes the effect of spurious timing shifts associated with changes in pulsing rate. The primary consideration in the circuit design was to prevent such shifts.

The frequencies used were between 5 and 10 MHz (periods between 200 and 100 nsec). Since such a repetition rate far exceeded the capabilities of the TAC or PHA, during each cycle of the slow electronics a system of gating ensured the following conditions.

(a) Only one pulse reached the START input of the TAC and only one reached STOP.

(b) Pulses never reached the TAC or PHA when the unit was "busy."

Depending on the state of the switching logic, the three coincidence units in Fig. 16 were driven in parallel by one or the other of the high-frequency pulse generators. The unit labeled "slow pulser" operated at a rate compatible with the TAC and PHA ($\approx$ 2 kHz) and produced pulses of width a little greater than the period of either generator. For each cycle of the slow pulser, at least one pulse from a fast pulser appeared at point 3, the output of the first coincidence unit (C1). Because the

slow and the fast pulsers were asynchronous, the coincidence was sometimes marginal, resulting in jitter in the timing of the output pulse. This pulse was unsuitable for direct use with the TAC and was used instead to generate a gate to pick out the next cycle of the fast pulser.

The two gate generators were operated in a bistable mode: The output gate began when a pulse arrived at START and lasted until one reached STOP. The pulse from C1 turned on the first gate generator (GG1) producing a logic level at point 4. When a pulse from the fast pulser reached the second coincidence unit (C2), one output turned off the previous gate generator (GG1), so that subsequent inputs to C2 were ignored, and one output turned on the next gate generator (GG2). The sequence of events at the last gate generator and coincidence (C3 and GG2) was identical. In fact this chain of modules can be extended indefinitely with the output of the nth coincidence unit in time with the nth cycle of the fast pulser.

The method for calibrating a cable was as follows. Initially the cable was not in place. The two pulse generators were set to approximately the same frequency. As the switching logic alternated between the two generators, the TAC pulse-height distribution appeared as peaks R and A in the sketch below. Peak R served as a reference point; the frequency of Pulse Generator 1 which produced it was never changed. A run was then made with the cable inserted in the setup. Peaks corresponding to R and B were accumulated. Lastly the cable was removed, and the frequency of Pulse Generator 2 changed so that peaks R and C were observed.

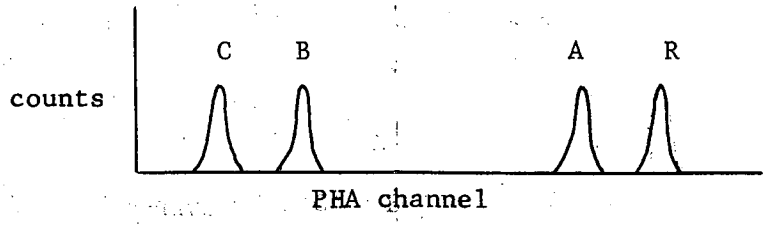

The pulse-height distributions were printed out, and the PHA memory cleared after each of the three runs. In this way the reference peak was recorded each time. By using the difference in channels between R and the second peak (A, B, or C), rather than the absolute position of the second peak, we minimized the effect of shifts in the electronics. If the system was linear, the time delay of the cable was

$$\frac{\left(R_B - B\right) - \left(R_A - A\right)}{\left(R_C - C\right) - \left(R_A - A\right)} \left(\frac{1}{\nu_A} - \frac{1}{\nu_C}\right) ,$$

where A is the mean channel of peak A, and R_A is the mean channel of the reference peak accumulated at the same time. B, R_B, C, and R_C are defined analogously. ν_A is the frequency of Pulse Generator 2 during runs A and B; ν_C is the frequency during the C run. (The frequency of Pulse Generator 1 does not enter.)

To be sure that there was no frequency-dependent systematic error, measurements were made using three separated frequency intervals. Four runs were made at each frequency range. Finally, to check for long-term shifts in the measured delay, the entire procedure was carried out on three different days. Results for one cable are presented in Table III. Each entry is an average of the four runs.

To test for spurious timing shifts when the frequency was changed, runs were made with Pulse Generator 1 fixed and Pulse Generator 2 set at different frequencies. As required for the validity of the cable measure-

Table III. Measured delay for one cable (nsec).

	Frequency interval (MHz)		
	7.25 - 8.85	5.88 - 6.77	4.93 - 5.56
First day	10.335	10.328	10.332
Second day	10.340	10.335	10.338
Third day	10.338	10.336	10.340

ments, the number of channels between the reference peak and the variable peak was linear with $1/\nu$ for frequencies below 20 MHz. The deviation observed above 20 MHz can be understood by considering the timing relationships in Fig. 16.

The coincidence at C2 is between one pulse from the high-frequency generator and a gating signal from GG1 which begins with the preceding fast pulse. (Refer to timing sketches 1, 4, and 5.) At low frequencies, the gating signal reaches C2 almost a full period before the arrival of the fast pulse. At high frequencies, however, the internal delay of the gate generator (13 nsec) and the delay in connecting cables becomes important. As the period decreases, there is less time between the arrivals of the gate and the fast pulse. At very high frequencies the gate follows the fast pulse and fails to make a coincidence. Well before this happens, however, there occurs a slight spurious time delay in the output of the coincidence unit.

This undesired timing shift did not occur in calibrating the reference cables. The frequencies used for the tests were in a range far removed from where the effect was first seen. Further confirmation comes from the fact that the measurements at the three different frequency intervals were in adequate agreement. The small, apparent correlation with frequency interval--measurements for the second interval gave the lowest values--can be attributed to nonlinearity in the TAC and PHA. This

nonlinearity was in fact the primary limitation to the precision of the measurement.

The most important elements in the calibration setup were the high-frequency pulse generators. They were actually sine wave generators whose output was converted to logic pulses as follows. First the sine wave was limited in amplitude so that it became approximately a square wave of reduced amplitude. This clipping was accomplished by the use of semiconductor diodes as shown below.

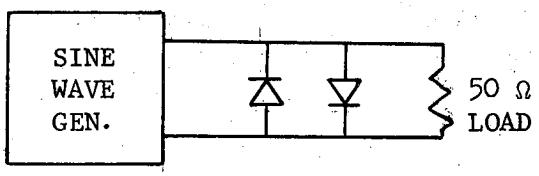

The limiting effect resulted from the voltage-dependent forward impedance of the diodes. For small applied voltages the diode impedance was large compared to the load; most of the sine wave amplitude appeared at the load. For larger voltages the diode impedance decreased, and the output amplitude became a smaller fraction of the input amplitude. The clipped since wave was differentiated to obtain pulses of alternating polarity. Finally a discriminator served to produce standardized pulses of one polarity.

The most suitable sine wave generator found was the Tektronix Model 190. Its frequency range is wide, and it is stable enough during the time required for a measurement. In addition it has a large enough output amplitude to permit the above clipping technique. (If the voltage is too low, the forward diode is not driven into its nonlinear region and no limiting occurs.) It was extremely valuable to be able to control the extent of the limiting by varying the amplitude of the sine wave generator.

The greater the limiting, the more square the resulting waveform, the greater the rise time of the pulses of the differentiated waveform, and the less the time jitter in the output of the subsequent discriminator. It was essential to have some source of time fluctuation in order to locate the mean of a peak to better than one PHA channel. The sine wave amplitudes were adjusted so that each peak had a full width at half maximum of about three channels. The time jitter was apparently Gaussian. In calculating the cable delays the mean for each peak was found by making a least-squares fit to this shape for the highest four or five channels.

It should be noted that for this experiment the use of calibrated cables was actually a redundant middle step in calibrating the TAC-PHA system. The setup of Fig. 16 can directly determine channels/nsec for the system by storing in the PHA memory two peaks whose separation corresponds to a known time difference. The two frequencies and the internal delays can be chosen so that these peaks fall approximately at the positions of the two particle peaks of interest. Calibration cables were used in the experiment because, unfortunately, the technique presented in this section had not been perfected when the time-of-flight data were taken.

As has been previously pointed out, one disadvantage in using cables is that the calibration routine can not rapidly alternate with data taking. With this suggested method a simple system of gating can rapidly switch the inputs of the TAC between the scintillation counters and the calibration network. An obvious choice of gating would be to synchronize with the cycling of the accelerator and calibrate during "off" times.

A second difficulty with the use of reference cables for calibrating

a TAC-PHA system is that there is no unique time delay for a cable. Because of attenuation and dispersion, the effective delay for a pulse depends on its initial rise time and on the discrimination level of the subsequent detector; thus it is a function of the modules at each end of the cable. For this reason care was taken that the same modules were used both in calibrating the system against the cables during data taking and in calibrating the cables themselves.

F. Comparison with the Spectrometer Measurement

We originally planned to determine the beam momentum with a magnetic spectrometer technique. Although the measurement was carried out, the results were not fully satisfactory. An auxiliary bending magnet, placed in the beam after A_6, deflected the beam through 80 deg. Four wire spark chambers with magnetostrictive readout were used. Two defined the entrance particle trajectory, and two the exit trajectory. Because the momentum of each particle was overdetermined, this arrangement would reveal the presence of systematic error. Unfortunately, it did just that: The mean momentum determined from the first three chambers was consistently about 0.3% higher than from the last three. One source of this discrepancy could have been error in surveying the positions of the chambers. There possibly were errors in the location of certain of the fiducial wires in the chambers.

Although the time-of-flight measurement was used to derive the lifetime from the beam attenuation, the spark chamber measurement was still a valuable check. The average of eight separate runs--four with each polarity--was 312.6 MeV/c. Individual runs were no more than 0.2 MeV/c higher or lower than the average. The time-of-flight measurement was made with the beam conditions which prevailed during the lifetime measurement. The spark chamber measurement was carried out much earlier in the experiment when counter M_4 was effectively 1/16-in. thinner. To compensate for the additional momentum loss in M_4, the appropriate value for the lifetime analysis is the measured spark chamber momentum reduced by 0.4 MeV/c. For each run the average of the momenta determined by the two combinations of chambers--first three and last three--was used. Because of the discrepancy it is felt that the uncertainty in the momentum

is at least $\pm 0.15\%$. The spark chamber value is then 312.2 ± 0.5 MeV/c. It is in agreement with the time-of-flight value, 311.89 ± 0.32 MeV/c.

In deriving the lifetime from the measured beam attenuation, there is an important theoretical difference between using time of flight and using a magnetic spectrometer. Because a function of the velocity must be evaluated, the lifetime derived from a momentum measurement depends on the pion mass. In practice, the pion mass is known to such a precision that in all lifetime experiments to date, this source of uncertainty is negligible compared to other errors. Thus a velocity measurement is as satisfactory as a momentum measurement.

If both measurements are made, however, the pion mass can be determined, although systematic errors make it difficult to achieve as great an accuracy as more direct experiments. Velocity and momentum measurements carried out for both signs of pion, as in this experiment, determine the difference between the π^+ and π^- masses. Measurement of this difference is affected by fewer systematic errors than measurement of the mass itself. With time of flight, calibration of the system is a significant source of error in determining an absolute velocity; a measurement of a velocity difference, however, needs only a nominal value of channels per nanosecond. In a magnetic spectrometer, precise knowledge of the system geometry and magnetic field is far less necessary for determining a momentum difference than an absolute momentum.

To evaluate the mass difference from the data of this experiment a convenient relation is

$$\frac{\Delta m}{m} \approx \frac{\Delta p}{p} - \frac{\Delta \eta}{\eta},$$

where $\eta = \beta(1 - \beta^2)^{-1/2}$ and Δ means the difference between the π^+ and π^- values. This equation is reasonable. The two quantities on the right

hand side are equal if the masses are the same. If $m_+ > m_-$ and $v_+ = v_-$, then $\Delta p > 0$ and $\Delta\eta = 0$. Lastly, if $m_+ > m_-$ and $p_+ = p_-$, then $\Delta p = 0$ and $\Delta\eta < 0$ since $v_+ < v_-$.

Four independent pairs of spectrometer measurements--a run under the same conditions for each beam polarity--gave $\Delta p/p$ values (in units of 10^{-4}) of -0.4, -3.4, 2.5 and 4.8. Three time-of-flight comparisons yielded $\Delta\eta/\eta$ values ($\times 10^{-4}$) of 0.5, 0.5, and -5.0. With the mean values $\Delta p/p = (1\pm4) \times 10^{-4}$ and $\Delta\eta/\eta = (-1\pm3) \times 10^{-4}$ the above equation shows $\Delta m/m = (2\pm5) \times 10^{-4}$.

This limit on the possible mass difference has a precision comparable to existing measurements, which imply $\Delta m/m = (2\pm4) \times 10^{-4}$. The earlier result is particularly impressive because it is derived from measurements of the two masses made by entirely different procedures. From the energy of x rays from transitions in pionic atoms, the π mass was calculated to be 139.577±0.013 MeV.[23] From an emulsion measurement of the momentum of muons from pion decays, Barkas determined 139.60±0.05 MeV for the π^+ mass.[24] (The calculation required the value of the muon mass and assumed the neutrino was zero.)

VI. ANALYSIS

A. Different Methods of Treating the Data

The data from the experiment could be analyzed in several possible ways. If there were no difficulties with systematic errors, the lifetime could be determined from either the π^+ data or the π^- data in a straightforward manner. One would expect the two values to be the same (within statistical error), although the goodness of fit for the positive lifetime might be worse since random gain changes in the movable counter affected the π^+ detection efficiency more than π^-. There was an important systematic error, however. The decrease in efficiency with counting rate caused the measured lifetime to be too short. The effect was greater for π^+, and thus the positive lifetime appeared shorter than the negative. If the rate dependence of the counter efficiency for π^+ and π^- were known precisely enough, the correct lifetime could still be found from the data for either sign of pion by using a modification of the original method. The method actually used in the analysis derived the lifetime from the combined data for π^+ and π^-, making use of known properties of the rate effect. These various methods will now be discussed.

The experimental data consist of many measurements, at each of the positions along the decay path, of the number of D coincidences for some number of M coincidences. The quantities to be fitted are the ratios D/M, to be called R, as a function of x, the distance from the first data position. In the absence of systematic errors, the appropriate analysis is a simple least-squares fit to $R(x) = A \exp(-Bx)$ to determine the parameters A and B. The lifetime is $1/\gamma\beta B$.

The efficiency of the monitor system for detecting pions does not enter the calculation. If a pion fails to make an M coincidence and

subsequently counts in the movable detector, no error is made; a D coincidence requires a particle to count in CP and satisfy the M coincidence. The value of R = D/M observed at distance x is the product of the CP efficiency and the ratio of the number of surviving pions at x to the number of M coincidences. Neither of these factors has to be known. The free parameter A is the product of the CP efficiency and the pion ratio at x = 0. Although the CP efficiency does not have to be known, this analysis assumes it is independent of x.

In practice the rate-dependent gain of the principal photomultiplier of CP made the counter efficiency vary with x. If the change in efficiency as a function of rate is known, the measured values of R can first be corrected and then fit to $R(x) = A \exp(-Bx)$ as before. The corrected values are those which would have been measured if the efficiency at every value of x were equal to some standard efficiency, that at x = 0 for example. Equivalently, the measured values of R can be fitted without change to $R(x) = A \exp(-Bx)f(x)$, where f(x) is a known function of x which takes into account the variation of efficiency. If the change in efficiency is linear with rate, a suitable expression is

$$R(x) = Ae^{-Bx}[1 - C(1 - e^{-Bx})],$$

where A and B are again determined by a least-squares fit, but C is given. The factor $1 - \exp(-Bx)$ is proportional to the difference between the counting rate at x = 0 and at an arbitrary value of x. The constant C specifies the magnitude of the rate effect. With this form there is no correction at x = 0; in other words, the efficiency at DP1 is taken as the standard.

For the run from which the lifetime was derived the magnitude of the rate effect was not known well enough to use the above procedure. Only

later in the experiment, when the importance of this systematic error was fully appreciated, were careful measurements made of the effect. The magnitude of the efficiency variation during the run of interest could not be deduced from the later investigation. Because of factors which changed from run to run--the Cerenkov radiator, the phototube, the discrimination level--measurements of the rate effect were valid only for the run in which the data were obtained. The later measurements did serve to demonstrate the linear relation between rate and the change in efficiency. During data taking the attenuation of the beam caused the rate to vary by about a factor of two from one end of the decay path to the other. The rate investigation showed that over an even greater range, a factor of five, the change in R was approximately linear with rate.

Because the constant C in the above equation was not known to sufficient precision, it might be treated as a free parameter like A and B. The fit then determines A (the normalization), B (the true attenuation factor), and C (the rate effect coefficient). This approach results in a much greater statistical error in the lifetime, however. As explained in the Introduction, for a decay path which is only a fraction of a lifetime, a systematic error such as the rate effect can alter the apparent lifetime without significantly impairing the goodness of fit. The fact that the uncertainty in the lifetime is greatly increased if the magnitude of the rate effect is a free parameter is simply a result of this situation. As illustration, for the π^- data the two-parameter fit gave 25.97±0.01 nsec, while the three-parameter fit gave 25.54±0.14 nsec. The increased error in the lifetime is a reflection of the uncertainty in the size of the rate effect. Indeed, the value of C determined by

the fit had a relative uncertainty of 33%.

Although the magnitude of the efficiency change caused by a given change in rate was not known very accurately for either sign of pion, the ratio of the change in π^+ efficiency to that for π^- could be deduced from the measured pulse-height spectra for the principal phototube of CP. By using this ratio and assuming that the true lifetimes of π^+ and π^- are equal, analysis of the data for both signs of pion determines the lifetime well. To illustrate the idea in a simplified example, suppose the measured π^+ and π^- lifetimes are τ_+ and τ_-, and the true lifetime is τ. If the systematic error in the π^- measurement is e and the π^+ error is r times as great, these quantities are related by $\tau_- = \tau - e$ and $\tau_+ = \tau - re$. Since r is known, the two equations determine the two unknowns, the lifetime and the π^- error.

To apply this approach to the data, a single fit was made to the measured values of R(x) for both π^- and π^+ using the forms

$$R_-(x) = A_- e^{-Bx}[1 - C(1 - e^{-Bx})] \text{ for the } \pi^- \text{ points and}$$

$$R_+(x) = A_+ e^{-Bx}[1 - rC(1 - e^{-Bx})] \text{ for the } \pi^+ \text{ points.}$$

A_-, A_+, B, and C were free parameters; r, the ratio of the changes in the π^+ and π^- efficiencies for a small change in rate, was specified. The "best" values of A_-, A_+, B, and C were those which minimized the χ^2 sum formed from the observed and fitted values of both R_- and R_+. The pion lifetime was determined from B as before. The quoted lifetime is based upon this method of analysis.

B. Analysis of Data for One Sign of Pion

The initial evaluation of the data was a least-squares exponential fit to measurements of either π^- or π^+. Measurements at all seven data positions gave $\tau_- = 25.970$ nsec and $\tau_+ = 25.895$ nsec with a statistical error of 0.013 nsec. The fit to the 193 π^- points had $\chi^2 = 187$, and for the 194 π^+ points, the value 257. The difference between τ_- and τ_+ was a result of the rate effect, and the poorer fit for π^+ reflected the greater sensitivity to variations in phototube gain of the movable counter efficiency for π^+ compared to π^-.

Figure 17 shows histograms for π^- and π^+ of the contributions to the χ^2 sum from the individual measurements. The distributions were reasonably smooth except for one point of each fit for which there was negligible probability the observed deviation was due solely to the statistics of particle decay. These two points were not used in the subsequent analysis. Omitting these points had little effect on the calculated lifetime. The goodness of fit improved, of course. χ^2 per degree of freedom became 0.95 for π^-, and 1.28 for π^+.

Although a simple exponential fit to the data for one sign of pion did not provide a valid value of the lifetime because of the rate effect, it aided in detecting systematic errors. The fit to the data at all seven positions for π^- and π^+ had a reasonable goodness of fit. Moreover there was no indication that measurements at any one position were inconsistent; some points at every position had large residuals. Because the decay path was only a fraction of a lifetime, however, a single fit to all the data was not a sufficient test for certain systematic errors. One such error was beam loss, surviving pions in the monitor missing the aperture of the movable counter. If there was loss at every position,

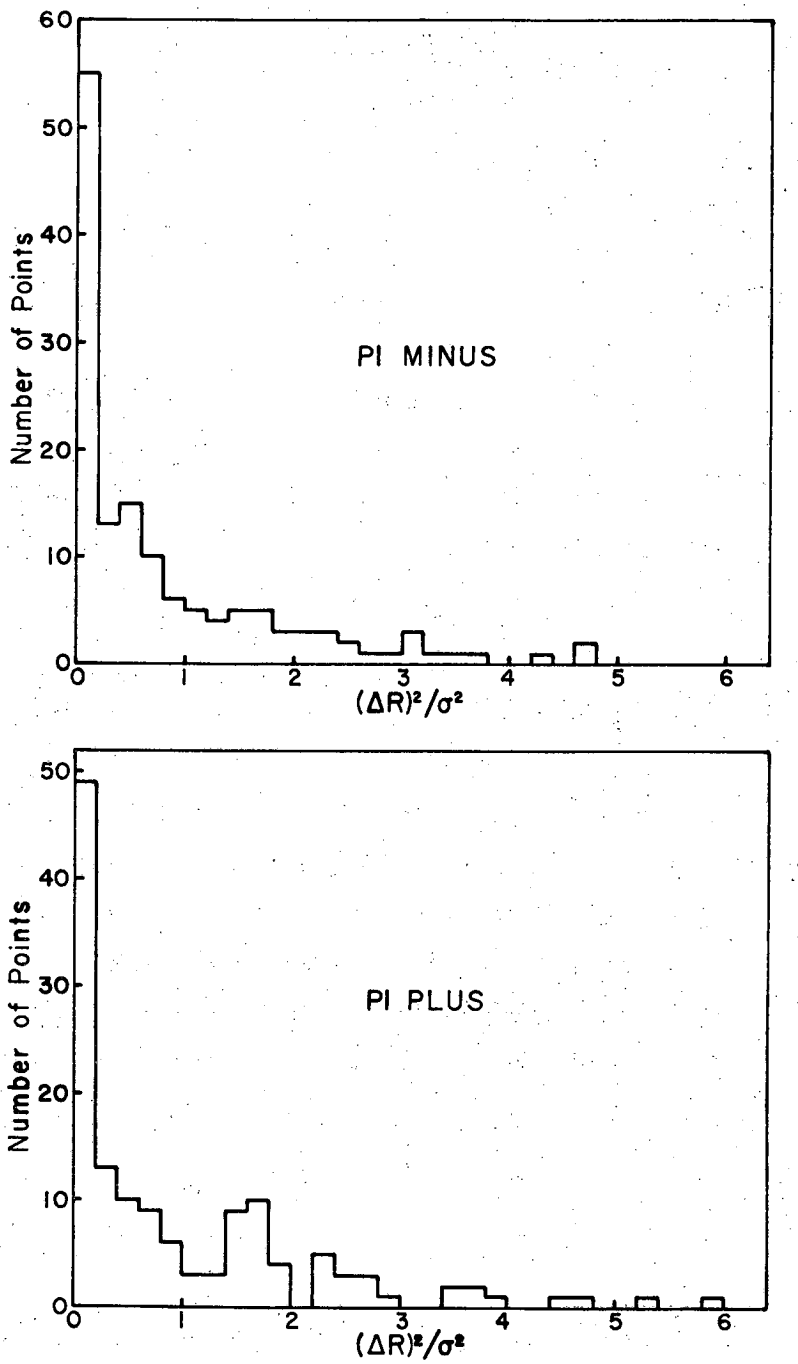

Fig. 17. Distribution of the contributions to the χ^2 sum from individual data points for fits to the π^- or π^+ data with DP7 omitted. ΔR is the R residual for the point, the difference between the observed and fitted values of D/M, and σ^2 is the variance of R. One π^- contribution at 8.5 and one for π^+ at 13.7 are not shown.

the error increasing with distance downstream, a satisfactory fit would still be obtained. Even if the loss was confined to the last position, the change in the calculated lifetime caused by this systematic error could exceed the statistical error yet not be indicated by the statistical tests used.

The more revealing test of beam containment involved making fits to the data for various subsets of the seven positions. If beam was lost only at the last one or two positions, error would be indicated by the fact that the lifetime computed from the downstream positions alone would be shorter than that computed from upstream positions.

The nature of the beam design ensured that any loss was confined to the last data positions. At DP1 the beam cross section was a well-defined circle of diameter 4.5 in., the shape of the hole in A_6. Since the cylindrical mirror of CP had a diameter of 7 in., there was certainly no loss at DP1.

Because the diameter of the beam envelope was smallest around DP4, loss at the middle data positions should have been negligible also. Beyond DP4 the beam size increased and, at a sufficiently great distance downstream, would exceed the counter aperture.

If pions scattered from the edge of A_6, but failed to produce enough scintillation light to count, they would contribute to beam loss. Loss from this source should also have been confined to the last data positions. Multiple Coulomb scattering is predominantly at small angles. Scattering from the edge of A_6 would have the effect of slightly broadening the angular distribution of beam particles. Although the beam envelope would be slightly larger than that expected for "clean" beam optics, the overall behavior of the beam cross section should be unchanged. Thus loss of

scattered particles should occur only at the far downstream positions, where the unscattered beam was already large.

Figure 18a gives evidence that there was a loss at DP7. The point labeled "1-7" indicates the π^- lifetime with statistical error derived from a fit to all data. The results of fits using only the first (last) 6, 5, 4, or 3 positions are shown by the other filled (open) circles. The different values clearly do not agree. To estimate the magnitude of the loss, the fitting procedure was repeated with D/M at DP7 increased, all other data unchanged. Figure 18b shows the results for a 0.2% increase. It is seen that a change in this one data position brings the various fits into agreement.

Because of the loss at DP7 this position could not be used in the lifetime calculation, and the consistency of DP6 was then tested in the same manner as DP7. Figure 19a shows that fits to various combinations of positions, none including DP7, agree within statistical error. To estimate how great a loss could escape notice, fits were made with D/M at DP6 decreased. In Figure 19b, D/M was decreased only 0.05%, yet the results suggest inconsistency between upstream and downstream measurements.

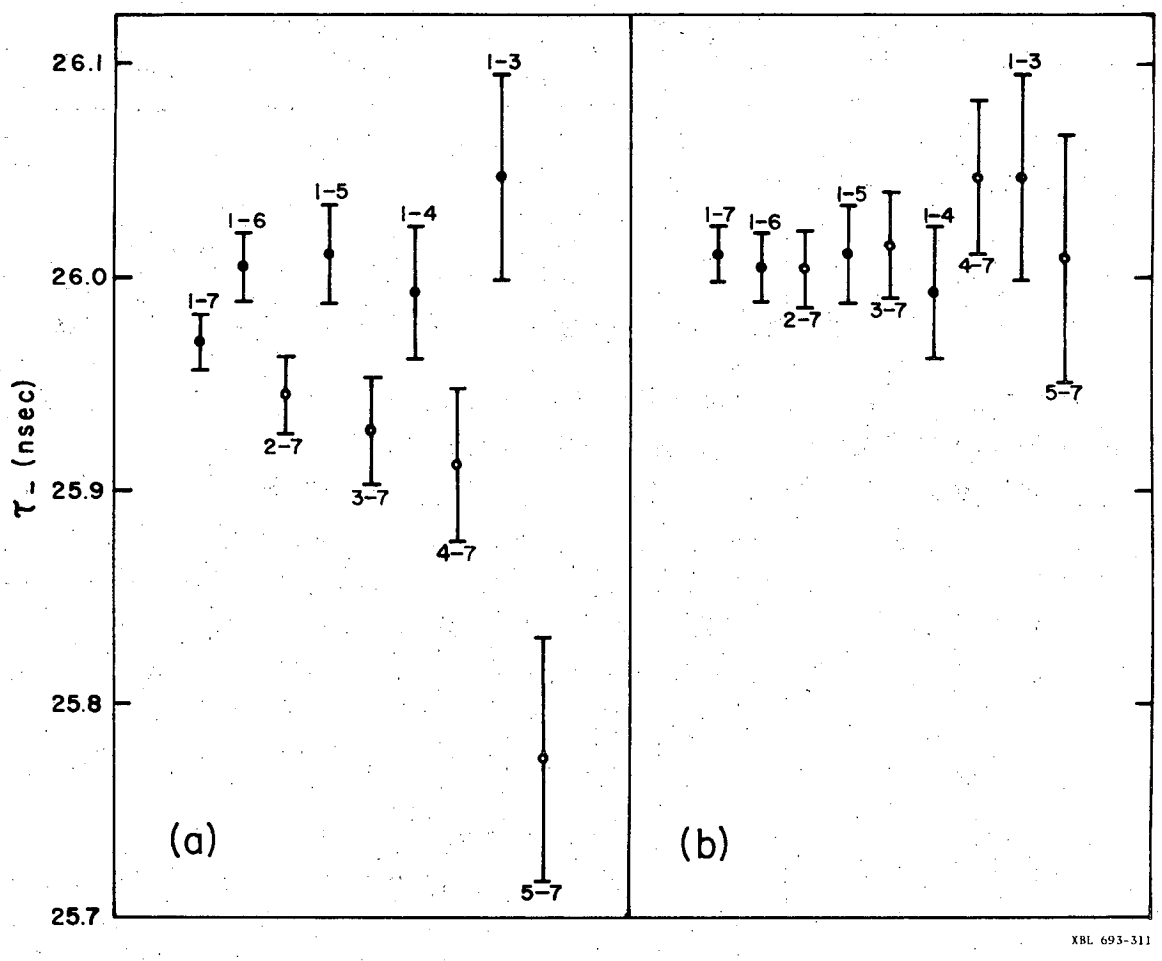

Fig. 18. The π^- lifetime determined from fits to different combinations of data positions. The notation "1 - 7" means all positions were used, "1 - 6" excludes DP7, and so on. The indicated errors are statistical.

(a) No changes in the data.

(b) D/M for DP7 increased by 0.2%.

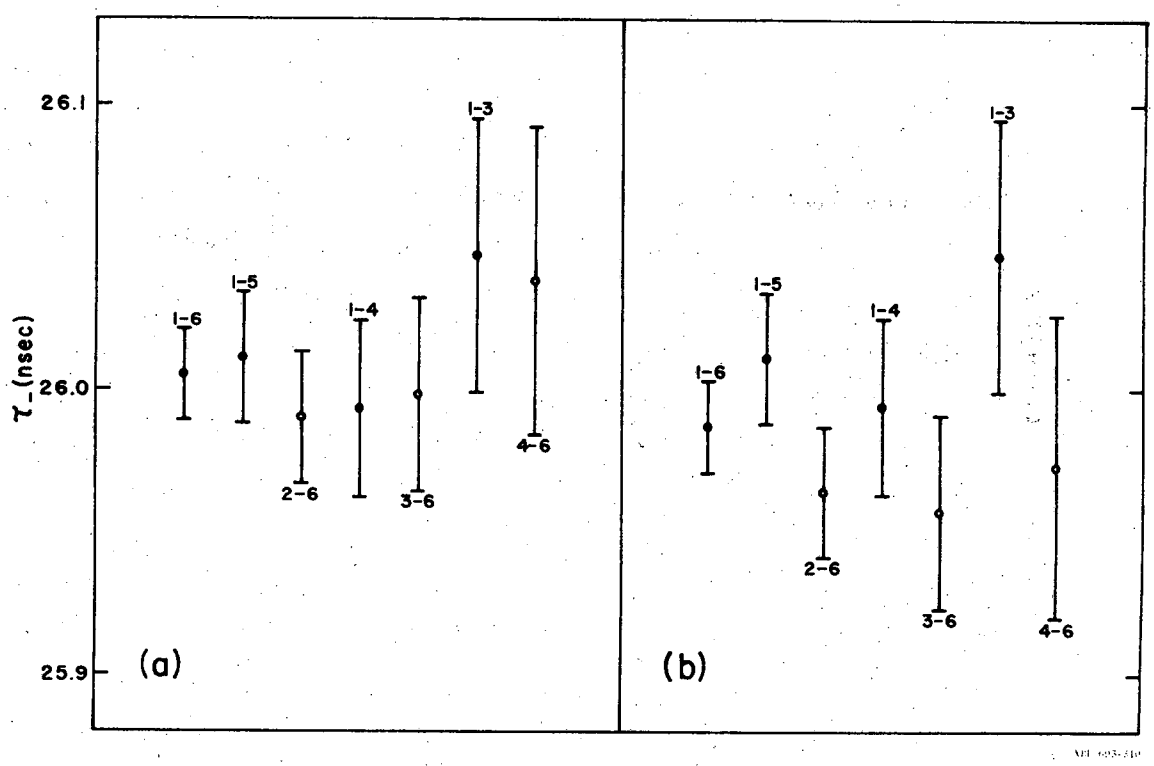

Fig. 19. The π^- lifetime determined from fits to different combinations of data positions, none including DP7.

(a) No changes in the data.

(b) D/M at DP6 decreased by 0.05%.

C. Containment of the Pion Beam

The procedure of comparing the lifetime determined from upstream data positions to that from downstream positions has indicated that there was some beam loss at DP7 and negligible loss at DP6. More direct evidence concerning beam containment was desirable, however, because conceivably statistical fluctuations caused the DP7 measurements to appear low although there was no loss of beam, or caused the DP6 measurements to appear valid although there actually was a loss.

Measurements of D/M with CP displaced with respect to the beam line gave information about the lateral distribution of the beam. (One such "beam profile" is shown in Fig. 9.) If the counter efficiency had been perfectly constant within some radius and zero beyond this radius, the extent of the beam could be found by determining the largest interval over which CP could be displaced without changing D/M. The width of the beam would simply be the effective diameter of CP minus the interval of uniform response. In practice the counter efficiency was not constant over its aperture, and the observed profile depended on both the beam distribution and the variation in counter efficiency.

For small displacements the observed variation in D/M was primarily an effect of the counter. For example, some deuterium runs showed a roughly linear variation of D/M (some 3% per inch of lateral displacement). The fact that other runs--with essentially the same beam but with changes in the counter--showed a more uniform response indicated that the asymmetry was in the counter and not in the beam. The sharp decrease in D/M for displacements exceeding two inches marked the point at which the envelope of the beam began to exceed the aperture of the counter.

As a test of beam confinement the profile technique had its limitations.

It could not be used to determine the last data position at which no beam was lost. At such a position the maximum beam dimension just equaled the effective CP aperture, and the profile had no flat central region. Thus the profile had the same appearance as at a position where beam was lost, and the two cases could not be distinguished. Another limitation was that an approximately uniform background of pions outside the main beam could not be detected. As the counter was displaced, it would gain as many particles from one side as it lost from the other, and thus D/M would remain unchanged, just as if there were no background.

To look for pions outside the main beam an additional, thin scintillation counter, one-inch square, was mounted just in front of CP. This counter, called M_6, moved along with CP as the Cerenkov counter was displaced. A particle satisfying a DM_6 coincidence had a known trajectory since it passed through M_6, and was presumably a pion since it counted in CP. Profiles of the beam measured using this technique showed a sharp decrease in the beam density after a distance which was in agreement with the D/M profiles. Beyond this distance, however, the apparent pion density did not go to zero; the particle density was several tenths of a percent of that at the center of the beam.

Decay muons had a distribution extending beyond the pion beam and provided an explanation for the observation. An MM_6 coincidence could occur if a pion satisfied M, and its decay muon counted in M_6. If this muon spuriously counted in CP, the DM_6 coincidence would be satisfied. A range measurement indicated that indeed the particles outside the pion beam were muons. It thus appears that the absence of one systematic error, poor beam containment, can be defended only by acknowledging the presence of another, poor rejection of decay muons by CP. This systematic

error is discussed in the next section.

The most elaborate study of the beam was a measurement of the beam distribution at each data position using a wire spark chamber with a useful area 12-in. square. The chamber had four planes, two grounded and two at high voltage, each with a magnetostrictive readout system. Spark position data were digitized and stored on magnetic tape using an on-line PDP-5 computer as a buffer. (With three other chambers this system had been used for the beam momentum measurement.) Since the detector was in effect two separate spark chambers, one immediately behind the other, spurious sparks in either half could be identified. The subsequent off-line analysis ignored any spark in one gap which was not accompanied by a spark in the other gap displaced laterally by less than 0.2 in. There were spurious sparks in another sense, however. The chamber was triggered for particles satisfying the M coincidence and counting in a large scintillator immediately behind the chamber. Just as in the case of the MM_6 coincidence, a monitor pion could decay and the muon pass through the scintillator with correct timing to make a coincidence. A second source of background arose from particles which may not even have satisfied the M coincidence or counted in the scintillator, but which traversed the chamber during its long sensitive time (25 μsec).

Although there was this background of undesired particles, events were mainly monitor pions and the chamber data provided a valuable comparison of the beam at different positions along the beam line. Figure 20 shows the distributions at DP6 and DP7. Each plot contains more than 21 000 points. A circle of the same diameter as the CP cylindrical mirror (7 in.) is shown for comparison.

In considering the question of containment of the pion beam, it proved

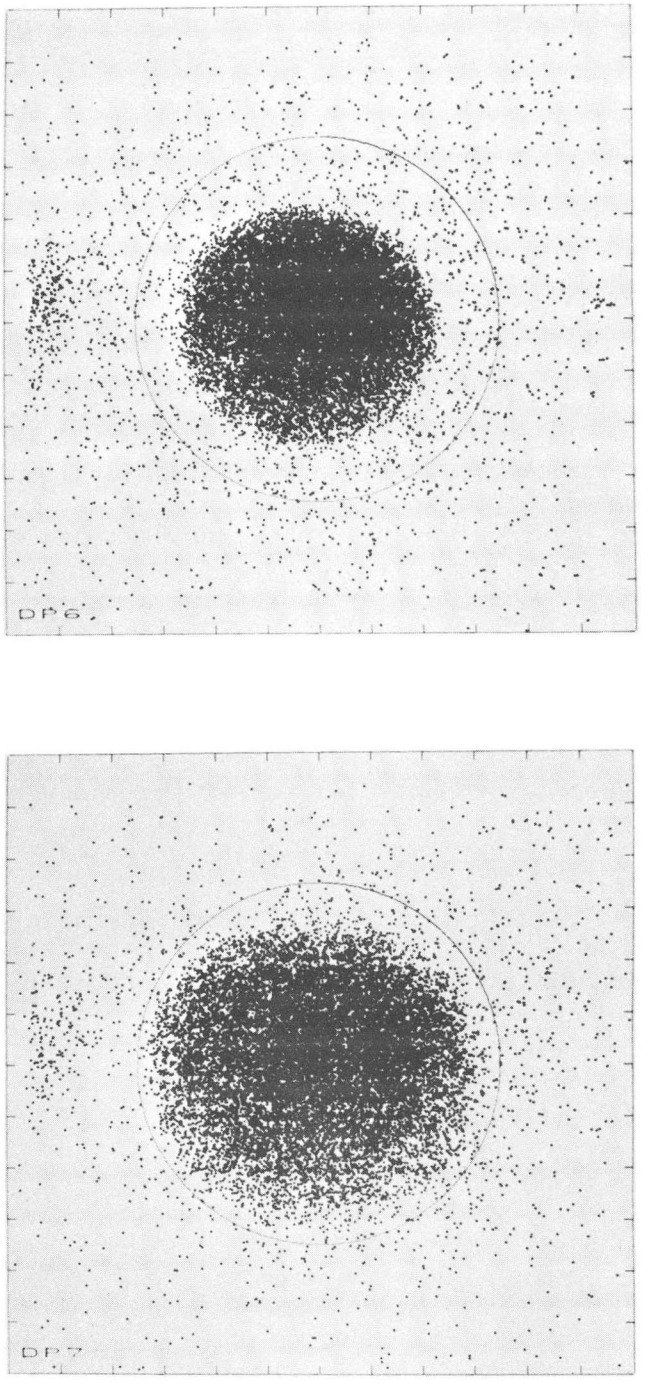

XBB 692-1409

Fig. 20. Distribution of particles detected by a spark chamber at DP6 and DP7. Each scale division is one inch. A circle of the same diameter as the CP cylindrical mirror (7 in.) has been added.

useful to display the spark chamber data at each position in terms of contour plots indicating constant particle density (number of particles per unit area). Such plots for the last six positions are shown in Fig. 21. The innermost contour is at 90% of the maximum density and the outer contour is at 10%. The contour interval is 10%. (The contours for DP4 are more ragged than for the other positions because only 2300 particles were recorded at DP4 but at other positions at least 9500.)

The significant feature of the contour plots is that, for every data position, the spacing between the outermost contour intervals is approximately constant. In other words the particle density decreased linearly with radius. The M_6 profiles also indicated this behavior. Both techniques, however, showed particles beyond the point at which the density should have gone to zero if a linear decrease with radius continued to hold.

There would be a serious systematic error in the lifetime measurement if a significant fraction of the particles at large radii were pions in the monitor coincidence. A possible cause of pions outside the main beam would be particles which were scattered by A_6, the last anticounter, but were not vetoed by this counter. Figure 21 gives evidence that there was little scattering of the beam. If there had been significant scattering, the variation of particle density across the beam would have been roughly Gaussian, rather than trapezoidal as observed. At the last data positions especially, scattering would be revealed by a greater interval between the 10% and 20% contours than between other adjacent contours.

In the main beam--the region for which contours were made--the particles recorded in the chamber were primarily pions in the monitor

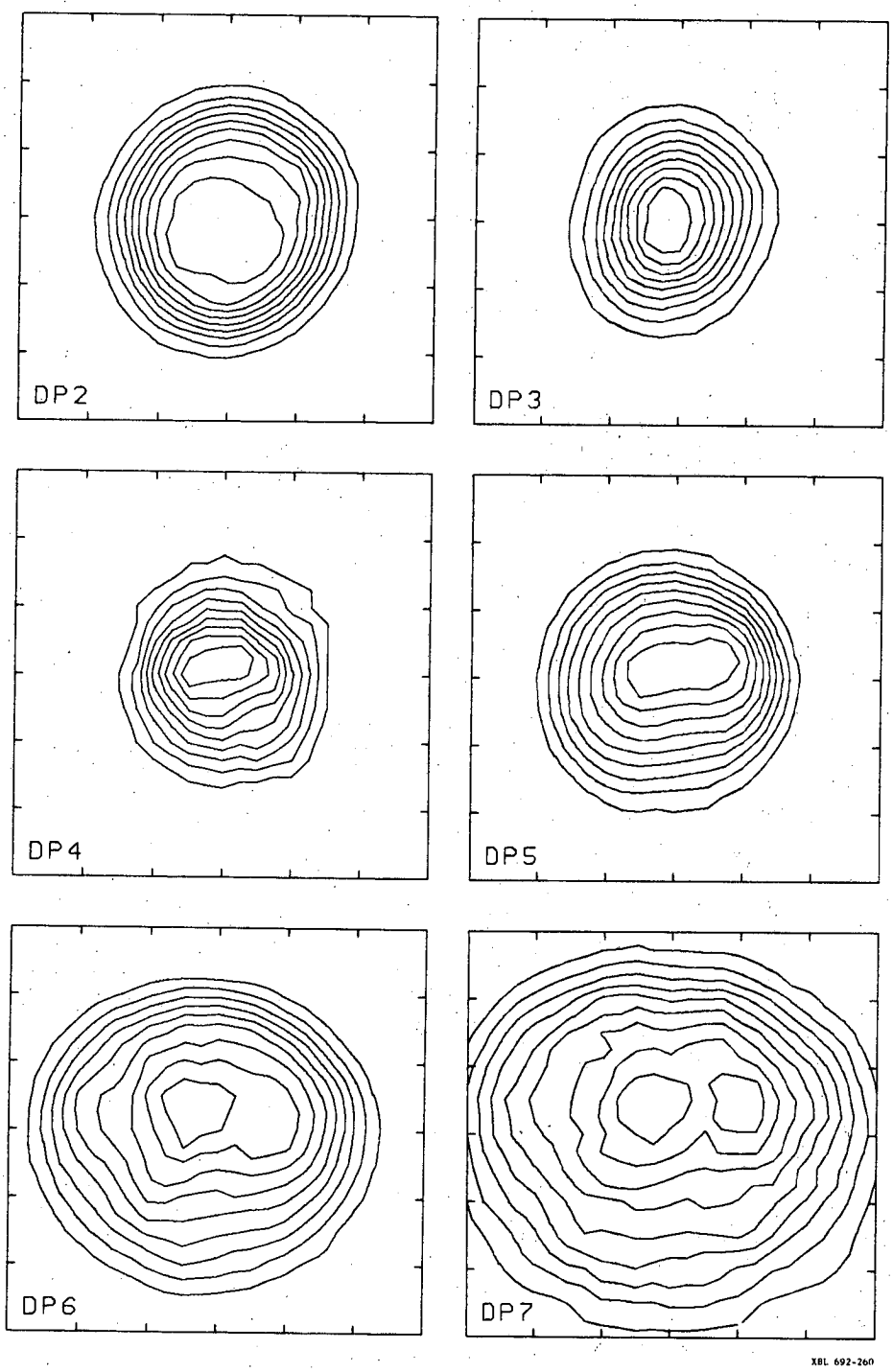

Fig. 21. Contours of constant particle density for the distribution of particles detected in the spark chamber. Each scale division is one inch.

coincidence. Because of this fact the outermost contours can be used to deduce the envelope of monitor pions. The envelope should have been a "0% contour" paralleling the 10% line with a spacing the same as that between the 10% and 20% contours. With this interpretation of the spark chamber data, all particles recorded outside this curve were from spurious sources such as decay muons.

These various measurements of the beam can now be put together to find the effective aperture of CP and to show that at all data positions except DP7 the beam was well contained within the counter. M_6 profiles, extrapolated linearly to zero beam density, indicated that the diameter of the beam at DP4 was 3.5 inches. The D/M profiles at this position (Fig. 9) showed that the counter could be moved laterally or vertically over a range of at least 2.5 inches without a significant change in efficiency. Thus the counter had uniform efficiency over a circle of diameter at least 6 inches. M_6 profiles at DP7 showed a beam diameter of 6 inches; thus DP7 was just at the limit of containment. At DP6 the beam diameter was at least an inch smaller, and there should have been no loss.

Between the time of the spark chamber measurements and the good data run, the anticoincidence counters in the monitor were modified. The changes had the effect of making the beam narrower. For this reason beam dimensions determined by M_6 profiles, rather than the spark chamber data, were used in the above argument. Note that the contour plot for DP6 indicates that it was a satisfactory position with the original, larger beam. With the smaller beam during the data run, there was even less question of beam loss.

D. Counting of Decay Muons

The error in the measured lifetime caused by the counting of decay muons depended on two factors: the efficiency of CP for counting decay muons and the variation from one data position to the next of the ratio of decay muons to pions entering the counter. Note that if the monitor counters were infinitely far upstream of CP, no error occurs even if all the decay muons which enter CP count. The reason is that in this case the spurious increase in D/M is strictly proportional to the pion contribution to D/M. There is no error in the calculated lifetime since the relative change of D/M with distance is the same. Error results only if the muon-pion ratio varies from position to position. A similar argument was previously applied to the CP efficiency for pions. The calculated lifetime is independent of this efficiency if it does not vary with distance.

The detection efficiency of CP for decay muons was difficult to determine. No direct test was possible. In contrast, the efficiency with which CP spuriously responded to beam electrons and beam muons was monitored by appropriate coincidence circuits. (See Sec. III-D.) Counting of decay muons was more complicated since these particles had a range of velocities and angles, and the efficiency of CP depended on both of these parameters. The efficiency as a function of velocity for paraxial particles was indicated by a momentum-response curve, such as the one for CM shown in Fig. 8. The variation as a function of angle for particles of the correct velocity was tested by rotating the counter about an axis perpendicular to the beam line.

The momentum-response curve and the measured efficiency for beam muons showed the rejection of off-velocity particles to be good. The rejection

of off-angle particles was less effective. One test with CP rotated 6.2 deg (the largest angle used) showed the efficiency to be 80% of that with no rotation. (This test was not made during the good data run; the results depend somewhat on the setting of the CP discrimination level during the particular run.) Muons emitted around 7 deg in the lab have the same velocity as pions. Extrapolation to 7 deg of the data with CP rotated indicated that at this angle the counter would still have more than 50% of full efficiency.

Forward muons and 7-deg muons were limiting cases in the sense that the former had correct angle and wrong velocity, while the latter had correct velocity and wrong angle. Large-angle muons were potentially more a source of error because they were numerous (half the decay muons had angles greater than 5 deg) and because CP had imperfect rejection of off-angle particles. On the other hand, the relative increase in D/M caused by these muons tended to be equal at all positions, since muons from decays far from the counter could not have large angles and still enter its aperture. Muons having a small angle in the lab, although less numerous, had the disadvantage of remaining in the beam and making a relatively larger increase in D/M at positions farther downstream. These muons, however, were rejected well by CP. Those emitted forward in the pion rest frame apparently counted with negligible efficiency, and those emitted backward had a velocity below Cerenkov threshold.

The best determination of the efficiency of CP for decay muons came from the beam studies with the one-inch-square scintillation counter M_6 used in conjunction with CP. If all the particles passing through M_6 were known to be decay muons, the efficiency was simply the ratio of MM_6 coincidences to DM_6 coincidences. In the center of the beam most particles

were pions; far from center it has been argued that any MM_6 coincidence arose from a pion which counted in M with its decay muon counting in M_6. In accord with this interpretation, MM_6/DM_6 should have been large on the beam center line (approximately D/M), and decreased with radial distance from center, reaching a constant at a distance beyond the envelope of monitor pions. The observed ratio had this general behavior. Measurements at DP2 at radii beginning near the limits of the pion beam and increasing in steps of 0.8 in. gave 0.74, 0.15, 0.14, and 0.12 on one side of the beam and 0.41, 0.11, and 0.06 on the other. The first measurement of each of these series was clearly at a radius where there was a significant fraction of pions. The weighted average of the remaining values was 0.11. The statistical accuracy of each measurement was not great. For 100 000 M coincidences, MM_6 and DM_6 were typically 100 and 10, respectively.

The major uncertainty in the measured decay-muon efficiency was systematic, not statistical. If some of the particles far from beam center were indeed pions, then the measured efficiency would be too high. The difference between the velocity-angle distribution of muons far from center and that for muons which actually entered CP during data taking could also cause the M_6 measurement to be high. Closer to beam center there were relatively more small-angle muons which CP rejected better than muons at large angles. With a conservative estimate of the uncertainty the muon efficiency was taken to be 0.11 ± 0.05.

The variation with distance of the ratio of muons to pions entering the counter will now be considered. Two independent factors caused the ratio to differ at the various data positions. First there was the finite distance between the data positions and the monitor coincidence

counters. A muon from a pion decaying after CM could complete a D coincidence, but if the decay occurred before CM there would be no M coincidence (and thus no possibility of a D coincidence). For data positions farther downstream there was a longer distance over which pions could decay and send muons into CP; thus the muon-pion ratio was greater.

The action of the anticoincidence counters in the monitor--the scintillators with holes in the center--also caused the ratio to increase with distance. The counters vetoed some decay muons which otherwise could have entered CP and counted. The variation in the muon-pion ratio resulted because the counters had less effect for data positions farther downstream. At such positions most muons entering CP arose from decays occurring after the anticounters; for these muons the counters had no effect. Muons originating before the last anticounter and entering CP at the far data positions necessarily had a small angle with respect to the beam line and were unlikely to intercept an anticounter. The effect of the counters was almost entirely confined to DP1 and DP2.

The muon-pion ratio was calculated from the decay kinematics and counter geometry. For simplicity the pion beam was initially assumed to have no lateral extent. If the finite distance between CM and DP1 (650 cm) is taken into account and the effect of the anticounters is ignored, the calculated ratio of decay muons entering CP to pions varied from 6.7% at DP1 to 6.9% at DP6. The ratio was almost constant because most muons entering CP arose from decays immediately in front of the counter. For example, all muons from decays closer than 70 cm entered; such muons were 0.6 of the total. For distances between 70 cm and 650 cm a constant fraction of the decay muons entered CP at all data positions. Because so few muons from decays at distances greater than 650 cm could

have entered the aperture, the finite distance between CM and DP1 did not cause a great variation in the ratio from position to position.

A greater effect was caused by the anticounters, particularly A_6, which was only 40 cm from CP at DP1. Only this one anticounter was considered. If the effect of A_6 was taken into account, the variation in the ratio was much greater. At DP1 the ratio became 6.2%, versus 6.9% at DP6.

The calculation was then carried out with a more realistic model of the pion beam, one with a constant circular cross section the size of the hole in A_6. Because more muons were vetoed by A_6, the ratio for each position was smaller: 5.7% at DP1 and 6.5% at DP6. Note that the difference between the values at DP1 and DP6 was greater. For a pion trajectory parallel to the beam center line, the greater the radial distance from center, the greater the probability its decay muon could enter CP at DP1 or DP2 yet be vetoed by A_6. Thus the calculated difference between the ratio at downstream and upstream positions was greater for the larger beam.

The counting of decay muons was taken into account in the lifetime analysis by correcting the observed values of R, the ratio of D coincidences to M coincidences, before making the fit. Considering R as a sum of contributions from pions and decay muons, one can write $R = e_\pi f + e_\mu \rho f$, where e_π and e_μ are the efficiencies of CP for pions and decay muons. For each data position f is the fraction of M coincidences for which pions reach the counter without decaying, and ρ is the ratio of muons to pions entering. The determination of e_μ and ρ has been discussed. The CP efficiency for π^- and π^+ was deduced from an analysis of pulse-height distributions presented in the next section. The pion

contribution to R could be expressed in terms of known quantities:

$$e_\pi f = \frac{e_\pi R}{(e_\pi + e_\mu \rho)} .$$

Precise values of the π^- and π^+ efficiencies were not needed. If the muon ratio did not vary with position, the lifetime calculation would not need these efficiencies at all. They provided the correct relative normalization of the muon and pion contribution to R. (Since the π^+ efficiency was less than π^-, the muon error for π^+ was slightly greater.) The dependence of the calculated lifetime on the pion efficiencies was slight because the muon error itself was small.

With a muon efficiency of 0.11 and values of ρ calculated from the model of the pion beam having a constant circular cross section, the muon correction reduced the originally calculated lifetime by 0.032 nsec. There were several sources of uncertainty in this value. The correction depended on the phase-space distribution assumed for the pion beam. It was concluded that the simple model used for the calculation was sufficiently representative of the true beam since the much less realistic model initially used--a beam with no lateral extent--yielded a correction differing by only 0.006 nsec. The primary uncertainty in geometry was the distance between A_6 and the cylindrical mirror of CP. If the value of 40 cm were in error by 10 cm, however, the correction would change by only 0.005 nsec. The major source of uncertainty was the muon efficiency, 0.11±0.05. In terms of the lifetime the error in efficiency corresponds to 0.015 nsec, the value to be used in the error analysis of the lifetime.

We had hoped the rejection of decay muons by the movable counter would be more effective. The optical system was capable of better

rejection. With sharp enough imaging of the Cerenkov light, the annular opening in the diaphragm could have been narrower and the anticoincidence ring more sensitive without impairing the response of the counters for pions. Dispersion in the Cerenkov radiator was apparently the source of difficulty. It was perhaps unfortunate that the two quartz windows and the entrance window of the RCA-4522 phototube extended the response to Cerenkov light in the ultraviolet region.

The movable counter rejected undesired particles in two ways. The particle could fail to count in CP (the central phototube) or, if it did count, it could be vetoed by CPA (the anticoincidence ring). The data from two of the secondary coincidences, simultaneously scaled during the experiment, gave indirect information about the rejection of beam muons and decay muons. One of these coincidences was M CP, equivalent to the D coincidence without the CPA signal. The other, denoted T, was the same as the monitor coincidence M without the CM $\overline{\text{CMA}}$ signal. Table IV shows the lifetime calculated using different scaler ratios: D or M CP as a numerator and M or T as denominator. (The method of analysis is that described in Sec. VI-F with no correction for the counting of decay muons.) One feature of the four calculated lifetimes is that the effects of the anticoincidence ring and the monitor Cerenkov counter were apparently independent. (The numbers in each row differ by 0.028, and the numbers in each column by 0.008.)

Table IV. The pion lifetime calculated using different coincidences (nsec).

Monitor Coincidence	Movable counter coincidence	
	D	M CP
M	26.057	26.085
T	26.065	26.093

Because the monitor Cerenkov counter efficiently rejected beam muons, removing this counter from the monitor coincidence revealed the effect of beam muons which spuriously counted in CP. The different lifetime fits imply that beam muons were primarily rejected by their failure to count in the central phototube: The lifetime calculated using T, instead of M, was greater by 0.008 nsec, whether the CPA signal was used or not. The increase in lifetime is consistent with the relative number of momentum-analyzed muons and pions in the beam and the measured efficiency of CP for these muons.

The calculated lifetime is greater by 0.028 nsec when the M CP coincidence is used in place of D. Because the anticoincidence ring had little effect on whether beam muons counted, we conclude that this increase is due to decay muons. The calculation in this section showed that an 11% efficiency for decay muons increases the apparent lifetime by 0.032 nsec. If rejection of decay muons had been primarily the result of vetoing by CPA, omitting this anticoincidence requirement would have greatly increased the decay-muon detection efficiency and increased the calculated lifetime by many times 0.032 nsec. The fact that the lifetime changed only 0.028 nsec indicated that most decay muons, like beam muons, were rejected by their failure to count in the central phototube.

E. Analysis of the Pulse-Height Distribution

The method of treating the data giving the most accurate value of the lifetime required knowledge of the ratio of the relative changes in π^+ and π^- efficiencies for a given change in counting rate. This ratio (the parameter r introduced in Sec. VI-A) was determined from pulse-height spectra of the CP central phototube measured for π^+ and π^-. The spectra also enabled the absolute efficiency of CP to be calculated.

To make use of the spectrum its origin must be understood. The pions contributing to the spectrum consisted of two classes: those which traversed the entire radiator without interacting and those which did interact. In the absence of statistical fluctuation, the noninteracting pions would have produced a narrow peak at one pulse height. Because pulse height was proportional to the depth at which interaction occurred, and the number of interactions at a given depth was approximately constant, interacting pions produced an almost uniform pulse-height distribution extending from zero to the pulse height of noninteracting pions. Actually the exponential attenuation of the pion intensity with depth caused the distribution to decrease slightly with pulse height.

Statistical fluctuation caused a broadening of this hypothetical distribution. Variation in the number of photoelectrons liberated by a given number of incident photons was the principal source of fluctuation. Variation in the number of photons reaching the photocathode and in the number of secondary electrons emitted at each dynode also contributed to the broadening. When statistical fluctuation is taken into account, the delta function in pulse height contributed by noninteracting pions becomes a Gaussian distribution.

Figure 22 shows the pulse-height distributions for interacting pions

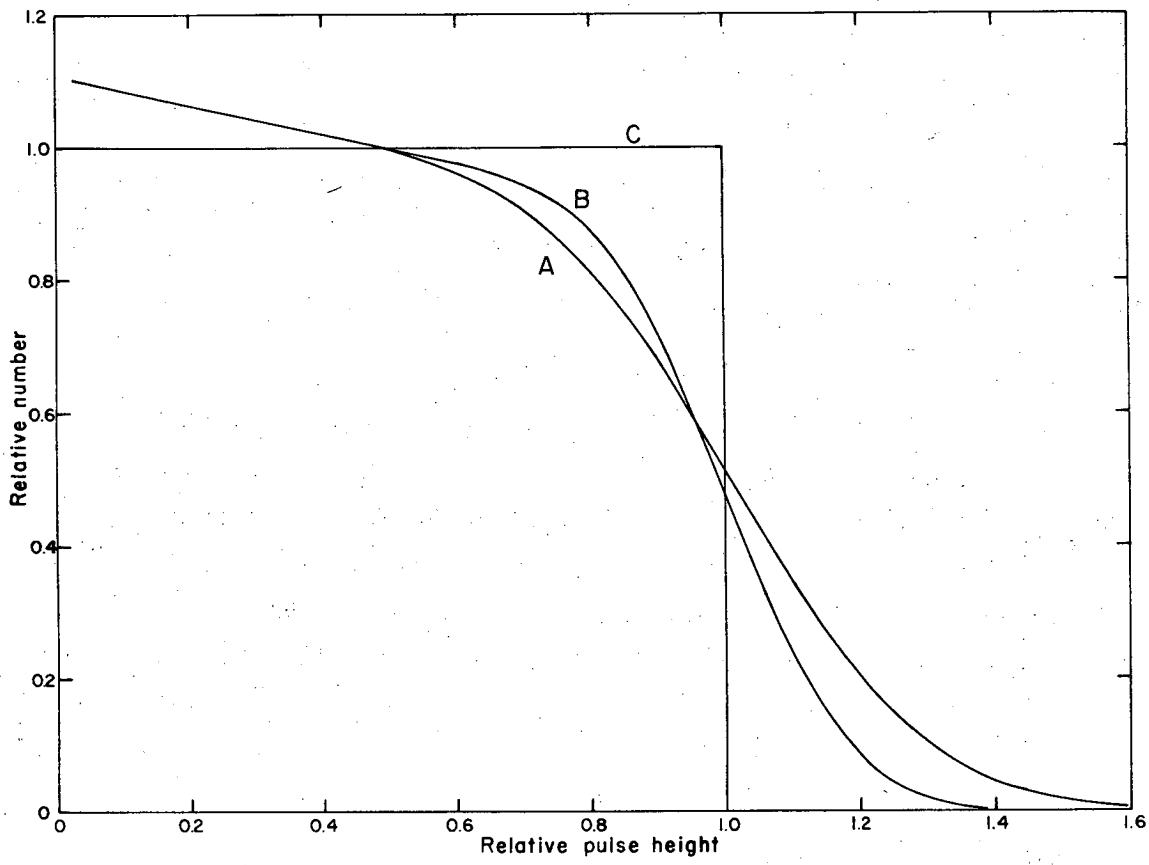

XBL 694-373

Fig. 22. Predicted pulse-height distributions for positive pions which interact before completely traversing the radiator. The statistical fluctuations were determined by a binomial distribution assuming a quantum efficiency of 0.3 and either 15 photoelectrons (curve A) or 35 (curve B). Curve C would result if the collision length were very large and there were no fluctuations. The three distributions have the same normalization.

predicted by a simple model in which statistical fluctuation results only from photoelectron production. The number of photoelectrons liberated was determined by a binomial distribution with a probability of "success," the quantum efficiency, of 0.3. The number of photoelectrons produced by a complete traversal of the radiator was 15 for curve A and 35 for B. The pion attenuation assumed a collision length of 120 cm (appropriate for π^+) and a radiator length of 25 cm. The two curves have the same normalization as the rectangular distribution C which would result if the number of pions interacting was independent of depth (large collision length) and there were no fluctuations.

Other factors affected the distributions actually obtained during running. The pulse-height analyzer was normally gated to record CP pulses corresponding to either a D or M coincidence. Since a D coincidence could result only if the CP pulse height exceeded a discrimination level, a D spectrum was zero below this minimum pulse height. An M spectrum extended below the threshold pulse height and for this reason included pulses other than those produced by pions. Decay muons were not excluded by the method of gating. If a pion made an M coincidence and decayed before reaching the movable counter, the muon had the proper timing to be analyzed. Most of the pulse-height distribution for these muons was below threshold, and did not appear in a D spectrum. Above the discrimination level the portion of the distribution contributed by muons was small because far more pions entered the counter than muons and only a fraction of entering muons counted.

An M spectrum obtained for positive pions is shown in Fig. 23. To illustrate the origin of the distribution a six-parameter fit was made to the observed points. The distribution was represented as a sum of three

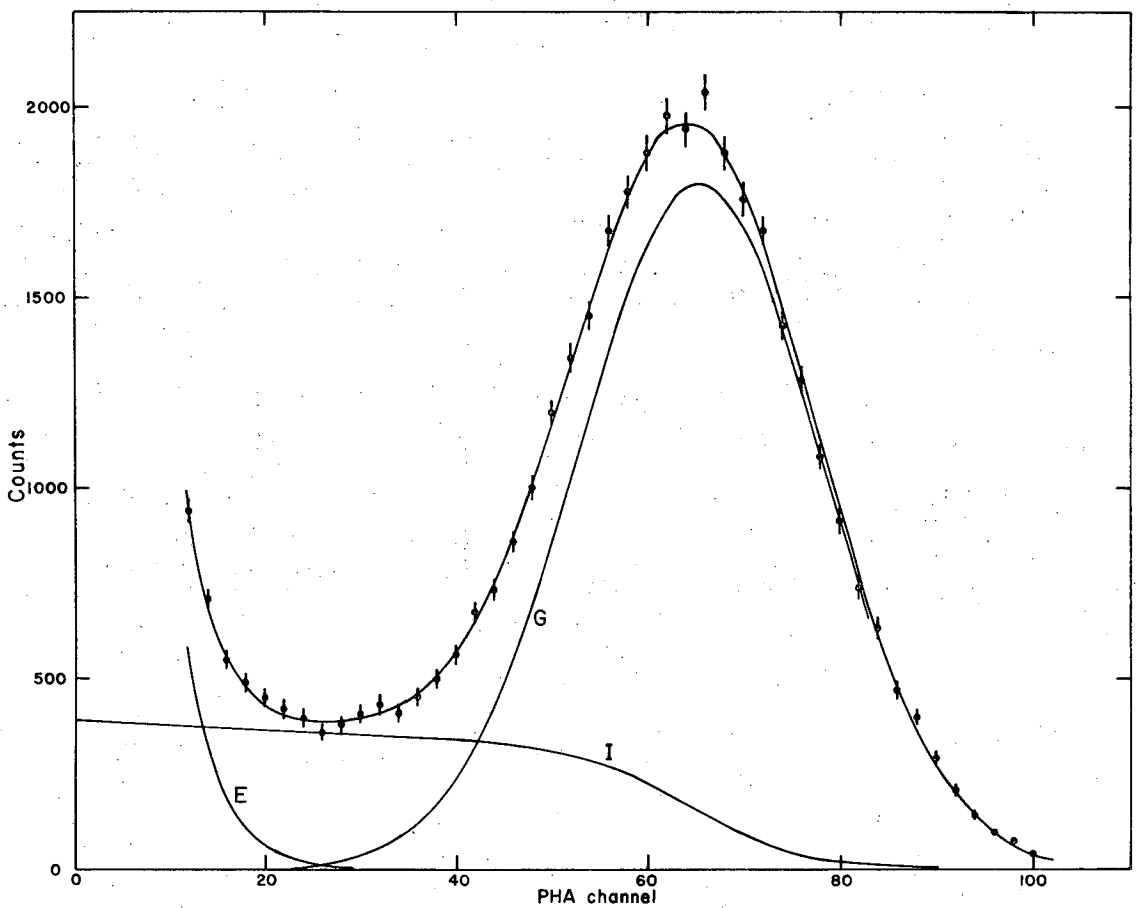

XBL 694-375

Fig. 23. Pulse-height distribution for CP observed with the positive beam and M-coincidence gating. (For clarity only every other channel is shown.) The fitted distribution is the sum of the three labeled curves: a Gaussian term G, an exponential term E, and a distribution describing interacting pions I.

terms. The first was a Gaussian contribution for noninteracting pions; the width, mean, and normalization were free parameters. The second was the contribution from interacting pions. The relative magnitude of this term was the only parameter; the shape was that shown in Fig. 22 for 35 photoelectrons. (The results were not very different if 15 photoelectrons were assumed.) To simplify the computation, the discrete distribution calculated from the model was approximated by a continuous function of the channel number C having the form

$$\frac{\exp(C/A)}{1 + \exp[(C - C_o)/B]} .$$

C_o is the channel that, in the absence of fluctuations, corresponds to the pulse height from noninteracting pions. A and B are constants which best approximated the desired distribution. The third term was the contribution from sources other than pions, such as decay muons and accidental coincidences with tube noise pulses. Although the exact shape of this part of the distribution was not known, it had the general behavior of a decaying exponential. The normalization and decay constant for this term were free parameters.

Figure 23 shows the experimental points used in the fit, the fitted curve, and the three contributions whose sum is the fitted curve. The goodness of fit was satisfactory: There were 89 points and the χ^2 sum was 71. Of equal significance the description was physically reasonable. The implied fraction of pions interacting, 29%, was in adequate agreement with the known total cross section. (The fraction could not be predicted with great precision because of the nonuniform geometry of the radiating volume--a dome at one end and slanting boundary at the other--and because of uncertainty in the true zero channel of the PHA.) The nature of the

exponential term was also reasonable. It was essentially zero above the threshold pulse height, in agreement with the fact that relatively few D coincidences were from decay muons and accidental coincidences.

The variation in efficiency caused by a change in counting rate was equivalent to a change in the discrimination level. From run to run the discrimination level was not at the same point of the pulse-height distribution, and the distribution itself was altered if, for example, a different phototube was used. Thus the calculation of changes in efficiency had to be carried out with the distributions obtained during the one run of interest. These were D spectra measured at DP1 for both π^+ and π^- and an M spectrum for π^+. The calculation was made more involved by the lack of a π^- M spectrum.

If the discriminator had a perfect step-function response--never an output if the input level was less than threshold and always one if the input was greater--then a D spectrum would have been sufficient for the calculation. The decrease in efficiency for a small increase in the discrimination level would simply be proportional to the height of the distribution just above threshold. Actually there was a range of pulse height, corresponding to about 10 channels, for which the discriminator sometimes produced an output. The observed number of counts in any channel was the product of the discriminator response for the corresponding pulse height and the number of pulses having that amplitude. This discriminator response function was found by comparing the M and D spectra for π^+.

Calculation of changes in the π^- efficiency required an M distribution for π^-. This spectrum was deduced from the available spectra as follows. First the two D spectra were normalized to correspond to the

same number of M coincidences. This step could be done accurately because the ratio of D and M coincidences for π^+ and π^- was well known from the scaler data. (It was the basic data of the lifetime measurement.) The correct normalization was such that the integral of the π^+ spectrum was 0.927 times the π^- integral. For the same number of M coincidences there were fewer D coincidences for π^+. The next step made use of the fact that the difference between the two D distributions was independent of the contributions from decay muons and possible accidental coincidences. For a given number of M coincidences the same number of decay muons entered the counter for either sign of pion; accidentals were the same since the M rates were kept equal. The difference distribution was then a function only of the spectrum for pions. Noninteracting pions contributed a Gaussian term. (The difference between two Gaussians with the same mean and width is another Gaussian.) Interacting pions gave rise to a term approximately like the distribution for interacting pions of either sign. A fit was made to the difference distribution, the free parameters being the mean, width, and normalization of the Gaussian term and the normalization of the term describing interacting pions. The purpose of the fit was to extrapolate the difference distribution below the point at which the D spectra went to zero. The final step was to extend the π^- D spectrum below threshold--thus generating the desired π^- M spectrum--by using the measured π^+ M spectrum and the fitted difference distribution.

Figure 24 shows the observed D spectra for π^+ and π^- with the correct relative normalization. The π^+ distribution has fewer counts at large pulse height and more counts at low pulse height than the π^- distribution. The dotted lines show the expected distribution below the discrimination

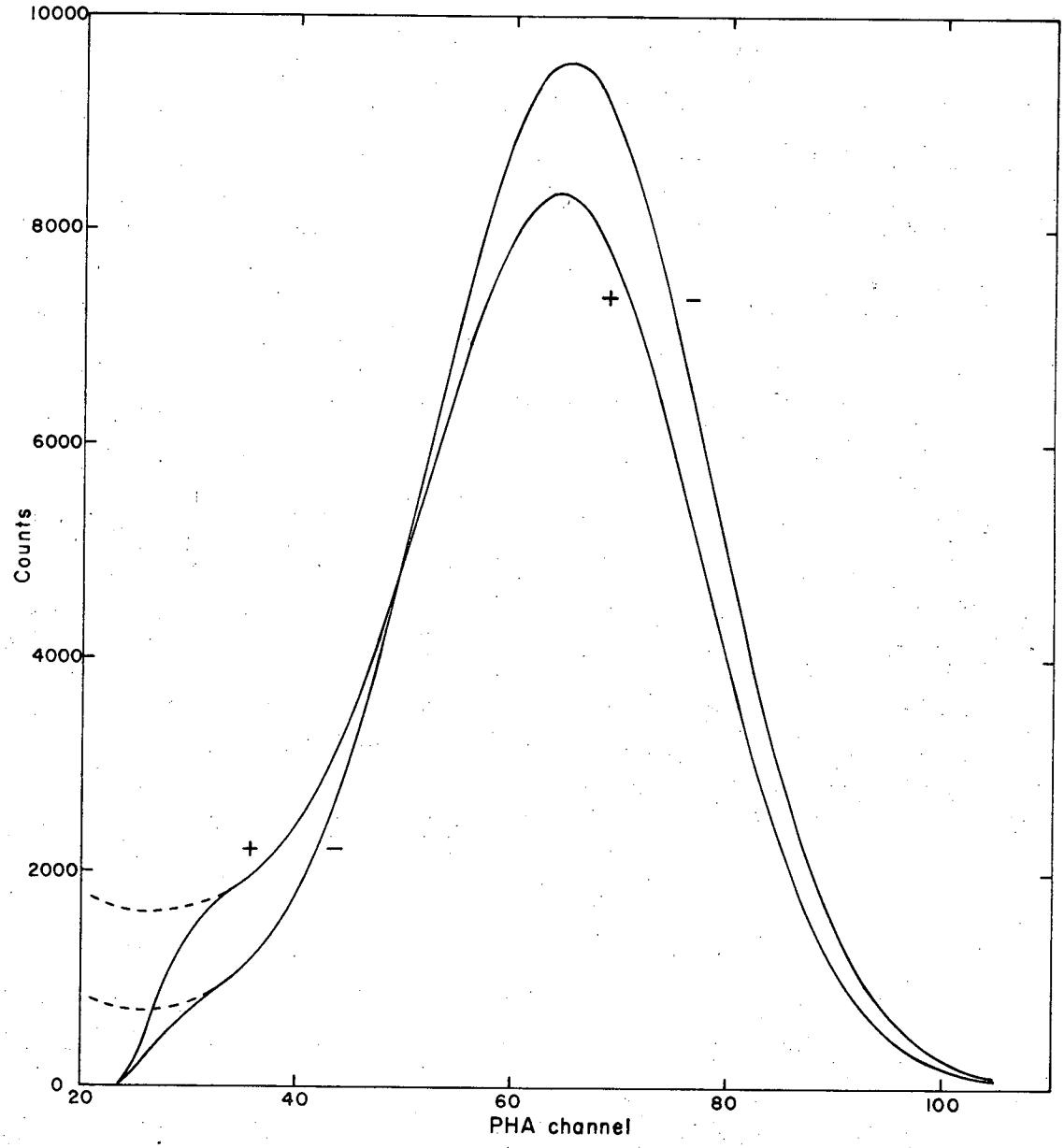

XBL 694-374

Fig. 24. Observed π^+ and π^- pulse-height distributions for CP for D-coincidence gating. The two distributions are normalized for the same number of M coincidences. The dotted lines show the expected distribution below the discrimination level.

level. For π^+ the extension was determined from the observed M spectrum. The π^- extension was calculated as described above.

The M spectra for π^+ and π^- were used to find the parameter r, the ratio of the relative changes in the π^+ and π^- efficiencies for the same change in discrimination level. For a particular value of the discrimination level, the efficiency was proportional to the sum of the contents of the channels in the M spectrum above some threshold channel. More accurately, since the discriminator response was not a step function, the efficiency was proportional to the sum, for all channels, of the product of the channel contents and the discriminator response for the channel. The experimental spectra were measured at DP1. At other data positions the counting rate was lower, and the tube gain was less. To calculate the change in efficiency the discriminator response function was shifted one or more channels higher with respect to the M distributions. For a one-channel increase in the discrimination level, the relative decrease in efficiency was 0.56% for π^+ and 0.23 for π^-; thus r was $0.56/0.23 = 2.4$.

The calculated value of r depended to a degree on the magnitude of the assumed change in threshold. For a larger increase in discrimination level, r was slightly lower. (Because the plus and minus distributions were more similar in shape at larger pulse height, the ratio of the changes in efficiency was closer to unity.) The desired value of r is that calculated for a change in discrimination level corresponding to the gain change which occurred in the experiment. The final analysis will show that the relative change in π^- efficiency between DP1 and DP6 was 0.12%, equivalent to a change in threshold of less than a channel. Thus the value of r calculated above for a one-channel change was appropriate.

Note that the method of calculating the lifetime using r treats this parameter as a constant, independent of x, the distance along the decay path. Actually it was a function of x because the change in efficiency increased with x. This simplification was permissible, however. The variation of r was a higher order effect on the efficiency since the correction itself was small.

For each sign of pion the D and M spectra were used to calculate the CP efficiency. If, for a given number of M coincidences, the number of pions which entered the counter at any position had been known, the efficiency could be found by simply dividing the number of D coincidences by the number of pions. Even at DP1, however, for every M coincidence a pion did not enter. A pion could make an M coincidence and then decay at some point after M_4. To an extent the anticoincidence scintillators eliminated such events from the monitor coincidence: If a muon from a pion which decayed after M_4 counted in one, the event was vetoed. Nevertheless it was possible for a muon to miss the anticounters, in which case there would be an M coincidence, yet no pion would reach the decay path.

In terms of the pulse-height distributions, the efficiency was the ratio of the integrals of the D spectrum (almost entirely pions) and the pion contribution to the M spectrum. For low pulse height the M spectrum included contributions from extraneous sources such as decay muons. The pion contribution was deduced using the predicted distribution for interacting pions, which has been discussed. The π^- efficiency was found to be 0.952 and π^+, 0.873.

One check of the analysis was to derive the true pion fraction in the beam at DP1, the fraction of M coincidences which resulted in a pion

entering the counter. This fraction was the observed value of D/M divided by the calculated efficiency. At DP1 the π^- fraction was 0.678/0.952 = 0.712 and π^+ was 0.629/0.873 = 0.721. The ratio of the π^+ and π^- fractions, 1.013, is to be compared to 1.022, the value deduced from runs with the counter filled with liquid deuterium. With this radiator the plus and minus efficiencies were the same, and thus the ratio of D/M for plus and minus gave directly the ratio of the pion fractions. The agreement with the deuterium value was satisfactory; the small difference was consistent with uncertainty in the true zero of the pulse-height distribution, the lower limit of the integrals. The reason the pion fractions for plus and minus were not equal was that some pions counted in M_4 and interacted just before emerging. Scattered positive pions often intercepted a subsequent anticounter and were vetoed. Negative pions, however, could charge exchange; the emerging neutral pion could not be similarly vetoed. Thus the positive beam had a slightly higher fraction of pions.

F. Simultaneous Fit to the π^- and π^+ Data

The results of the preceding five sections were applied to the data from the good hydrogen run. The measured ratios R = D/M were first corrected for the counting of decay muons. If R was the observed value, the corrected value was

$$\frac{e_\pi R}{e_\pi + e_\mu \rho} .$$

The ratio ρ of decay muons to pions entering the counter at a given data position was calculated from kinematics and counter geometry. The average efficiency for counting decay muons e_μ was deduced from data taken with CP displaced from the beam center line. For each sign of pion the efficiency e_π was derived from analysis of the CP pulse-height spectrum.

The corrected ratios for the data at distance x were fit to

$$A_- e^{-Bx}\left[1 - C(1 - e^{-Bx})\right] \text{ for } \pi^-$$

and

$$A_+ e^{-Bx}\left[1 - rC(1 - e^{-Bx})\right] \text{ for } \pi^+.$$

These expressions assume that π^+ and π^- have the same lifetime and that the CP efficiency is some constant (different for π^+ and π^-) plus a term linear with rate. The magnitude of the rate-dependent term is r times as great for π^+ as for π^-. The value of r, 2.4, was determined from pulse-height spectra. The parameters A_-, A_+, B, and C were varied to minimize the χ^2 sum for both sets of data.

Only data at the first six data positions, where the pion beam was well contained within the counter aperture, were used. Each readout of the scalers provided a data point, the ratio of the numbers of D and M

coincidences accumulated since the previous readout. Two points with unreasonably large deviations from their fitted values were omitted. There remained 331 points, corresponding to a total of 130×10^6 M coincidences. χ^2 for the fit was 316. To illustrate the fit the weighted average and statistical error were found for the 12 to 24 data points obtained each of the two times the movable counter was at each position. The residuals for these average values are shown in Fig. 25.

The lifetime was computed from $\tau = 1/\gamma\beta B$. The D/M fit determined B and the time-of-flight measurement provided $\gamma\beta$. There were only three significant sources of uncertainty in the lifetime. The statistical error was 0.031 nsec. The experimental error in $\gamma\beta$ corresponds to 0.027 nsec in τ. Lastly, it was shown that uncertainty in the correction for the counting of decay muons was 0.015 nsec. With these three errors the lifetime is 26.02±0.04 nsec (26.024±0.044 nsec before rounding). Other possible sources of error, which proved to be negligible, will be discussed.

Uncertainty in the position of CP along the decay path was not significant. The movable counter was positioned by aligning its carriage with respect to marks on the tracks on which it traveled. The calculated lifetime depended primarily on the distance between DP1 and DP6. A 0.1% error in τ corresponded to an error of 0.9 cm in this distance. The distances between positioning marks were known to much greater precision.

Accidental coincidences were not a problem. The greatest fraction of accidentals was in the coincidence between CM and the pulse for coincidence of all the remaining monitor counters. The coincidence rate with the CM signal delayed 51 nsec (the fine-structure period of the cyclotron) was less than 0.1% of the rate with CM in time. Not only was this

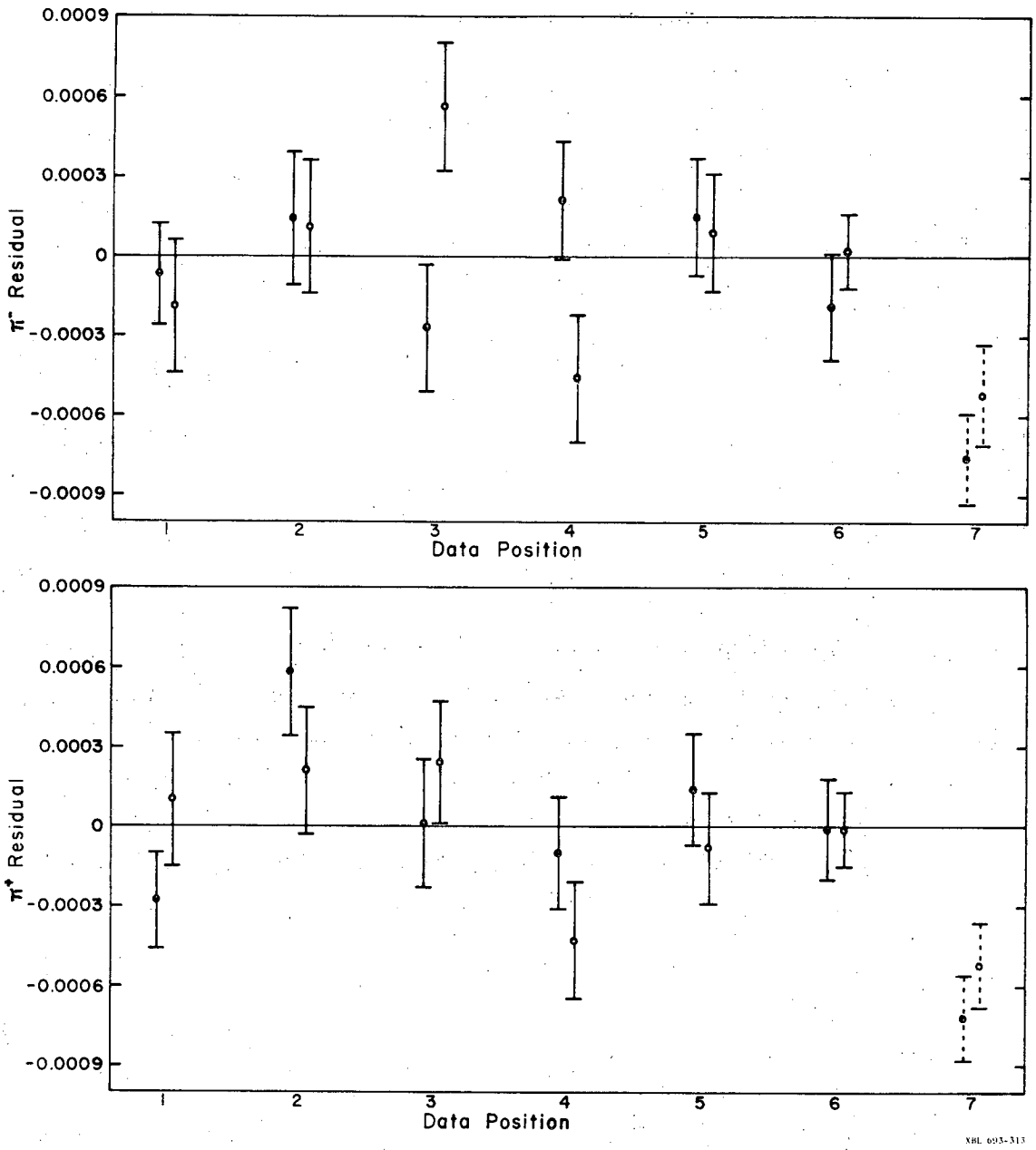

Fig. 25. D/M residuals (differences between observed and fitted values) for the simultaneous fit to the π^- and π^+ data. The solid circles indicate the first measurement at each position; the open circles, the second. (The pairs of points have the same abscissa and are displaced from one another for clarity.) Data Position 7 was not used in the fit. The indicated errors are statistical.

accidental rate low, but as explained in the Introduction, an accidental rate strictly proportional to the monitor rate causes no error in the lifetime.

The values of the five free parameters determined by the fit were a function of the constant r. Figure 26 shows the variation with r of quantities proportional to two of these parameters. One, determined by B, is the lifetime; the other, determined by C, is the relative decrease in the π^- efficiency of CP for a given reduction in counting rate. (From the definition of r the π^+ decrease is r times as great.) The derived value of r changed if the assumed pulse-height distribution for interacting pions was varied. The resulting error in the lifetime was negligible, however. The uncertainty in r was less than 0.1; such a change altered τ only 0.004 nsec.

Two features of the magnitude of the rate effect determined by the fit should be noted. Like the lifetime, the value was not strongly dependent on the parameter r. Secondly, the predicted rate dependence of the efficiencies for π^- and π^+ was not unreasonable. Agreement with the rough measurements made during the run was not as good as expected, however. For comparison, all data were expressed as the relative decrease in efficiency for a 50% decrease in counting rate. With r = 2.4 the lifetime fit predicted an effect of 0.15% for π^- and 0.37% for π^+. Three measurements for π^+ made during the run--0.12%, 0.09%, and 0.22%--were all lower than the predicted value.

There is a possible explanation for the high predicted value. The fit to the lifetime data assumed that the variation in efficiency as the counter was moved from one position to another depended only on the D rate, the rate at which surviving pions in the monitor entered the movable

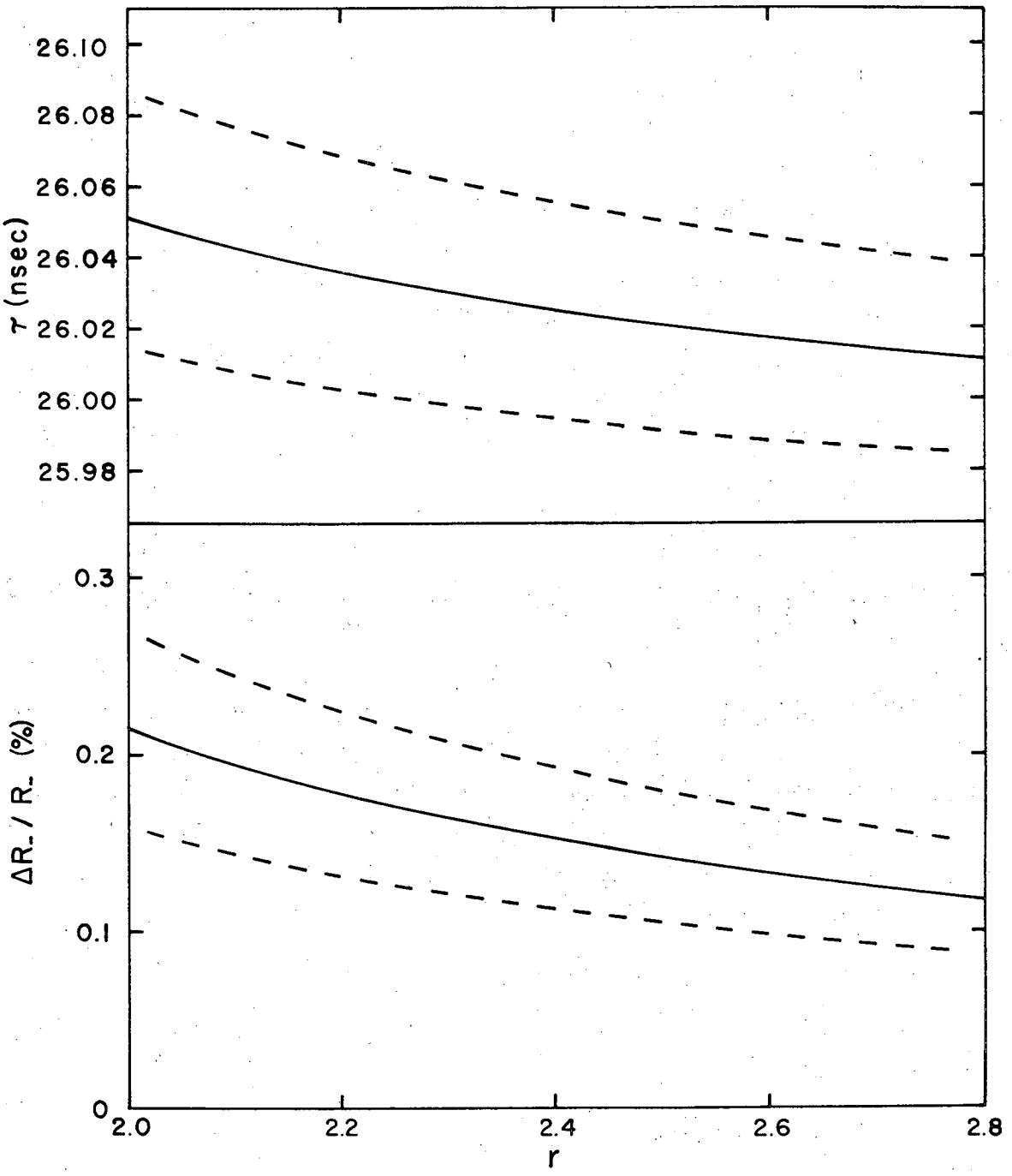

XBL 694-372

Fig. 26. The dependence on r of two quantities determined by the simultaneous fit to the plus and minus data. τ is the lifetime and $\Delta R_-/R_-$ is the relative decrease in the π^- efficiency of the movable counter for a 50% reduction in counting rate. The dotted lines indicate the statistical error in the fitted value.

counter. Because of the origin of the rate effect, efficiency variation was correlated with the total flux of Cerenkov light reaching the CP phototube, not just that from pions which had satisfied the monitor coincidence. In fact most particles physically in the beam were not monitor pions. The rate of pulses from CP which exceeded threshold (CP in coincidence with no other counters) was about five times the D rate (CP in coincidence with the monitor signal.)

At upstream data positions many of the pions entering the counter had been vetoed by the beam-defining anticounters. These pions were vetoed because it was likely that they would miss the counter at the downstream positions. Thus, as the counter was moved downstream, the effective decrease in rate was due not only to decay of pions, but also to the reduction in the relative number of those pions which entered the counter and were not in the monitor. The functional form describing the efficiency variation omitted this second source of rate variation, and the fit, by attributing an excessively large effect to the first source, yielded a high value for the parameter C.

The fraction of pions which entered CP yet were not in the monitor decreased monotonically with distance, as did the fraction of monitor pions entering. The precise distance dependence of this omitted source of efficiency variation was surely not the same as the exponential dependence assumed in the lifetime calculation. To test the effect on the derived lifetime caused by the functional form used for the efficiency, the calculation was repeated assuming the relative decrease in efficiency was linear with distance, rather than exponential. The calculated lifetime differed from the original value by only 0.005 nsec. Because the decay path was only a fraction of a mean decay length, there was negligible

difference between an exponential and a linear dependence on distance. For once, the short length of the decay path was an advantage!

In the analysis of the experimental data the largest correction to the calculated lifetime was for the variation of CP efficiency with distance. Fitting the D/M data for one sign of pion to A exp(-Bx) neglects this effect. With the final data selection (i.e., DP7 omitted) such an analysis gave π^- and π^+ lifetimes shorter than the corrected lifetime by 0.05 and 0.13 nsec, respectively. In comparison, the muon correction was only 0.03 nsec. Because of the magnitude of the efficiency-variation correction, it was fortunate that the two essential assumptions of the correction were well established: the equality of the lifetimes of π^+ and π^-, and the constant ratio between changes in the π^+ and π^- efficiencies of CP caused by gain variation.

VII. DISCUSSION

The result of this experiment, $\tau = 26.02 \pm 0.04$ nsec, can be compared with others shown in Table I. Our measurement is by far the most precise among those using pions in flight and is in good agreement with the recent measurements with stopping pions. The test of special relativity calculated by Rédei consists of comparing the lifetimes measured with pions in these two states of motion. In Rédei's model the lifetime measured in the laboratory frame of reference for pions of momentum p is $\gamma\tau[1 + (\alpha p/\hbar)^2/5]$, where τ is the lifetime in the pion rest frame and α is the fundamental length. In terms of $\lambda\!\!\!^{-} = \hbar/mc$, the pion Compton wavelength divided by 2π, the expression is $\gamma\tau[1 + (\beta\gamma\alpha/\lambda\!\!\!^{-})^2/5]$. With no violation of relativity, $\alpha = 0$ and the measured lifetime is $\gamma\tau$. If the deviation between the observed lifetime and that expected from the usual time-dilation formula is no greater than $\Delta\tau$, then

$$\alpha^2 < \frac{5\lambda\!\!\!^{-2}}{\beta^2\gamma^3}\frac{\Delta\tau}{\tau} .$$

An upper limit on α can be determined from this experiment and that of Eckhause et al.[2] The difference between the two measurements of τ is 0.00 ± 0.06 nsec. With $\Delta\tau = 0.06$ nsec and values of β and γ corresponding to our momentum of 312 MeV/c, the above inequality gives $\alpha < 3 \times 10^{-15}$ cm.

For the type of relativity violation originally proposed by Blokhintsev,[10] this experiment is the most stringent test of the existence of a fundamental length. Inhomogeneity of space-time should also lead to violations of the conservation laws of energy and momentum. Present data are not at high enough energy and lack the precision to give a limit smaller than that found in this experiment.[9]

It is hoped that future experiments can place an even smaller limit on the fundamental length. An appropriate goal is the characteristic length of the weak interaction $\sqrt{G/\hbar c} \approx 6 \times 10^{-17}$ cm, since the particles whose lifetimes can be measured by a beam technique are those which decay via this interaction. The above relation between α and $\Delta\tau/\tau$ shows that a stronger limit on α can be obtained if the precision in the two lifetime measurements is greater (smaller $\Delta\tau/\tau$) or if the particle energy in the beam measurement is greater (larger β and γ). Unfortunately these approaches are contradictory to an extent. Recall that the relative error in a beam measurement of the lifetime is inversely proportional to the number of mean decay lengths over which the measurement is made. Since the decay length is $\gamma\beta c\tau$, for a given measurement distance $\Delta\tau/\tau$ increases as $\gamma\beta$ increases. Also, the higher the momentum, the less suitable is the time-of-flight technique for measuring $\gamma\beta$.

Measurements with kaons, instead of pions, might provide a stronger test of relativity. Because of the shorter lifetime and greater mass, the mean decay length for a kaon is 0.13 times that for a pion of the same momentum. Thus the use of a beam with high momentum is less detrimental to the precision of the lifetime measurement. The theoretical interpretation of the experimental results is more difficult for kaons because the decay interaction is less well understood. (Rédei has applied his model of relativity violation only to pions and muons.) The results of the most precise experiments with kaons are as follows:

Fitch et al.[25]	12.443±0.038 nsec	stopping kaons
Boyarski et al.[26]	12.31±0.11 nsec	
Lobkowicz et al.[27]	12.272±0.036 nsec	kaons in flight
Ford et al.[28]	12.21±0.11 nsec	

The most precise measurements of each type are in serious disagreement with each other. If only one of these two experiments is considered (Ref. 25 compared with Ref. 28, or 26 with 27), the discrepancy is less significant. In any event the results do not indicate a violation of relativity of the type described in Rédei's theory, for the lifetime measured in flight is shorter, not longer, than that measured at rest.

Measurements with pions are perhaps best for this test of relativity. In any future experiment similar to ours, the problem of rate-dependent efficiency of the movable detector can presumably be avoided. In the data analysis of this experiment, this systematic error was properly taken into account by virtue of the difference in its effect on π^+ and π^-. (For this reason it was no loss that a contemplated high-statistics run with one beam polarity was not carried out or that the beam momentum for the deuterium runs was not known sufficiently well.) The validity of the result of this experiment requires that the difference between D/M for π^+ and π^- arose as assumed--via the rate-dependent gain and the difference in π^+ and π^- pulse-height distributions--and not, for example, because of some difference in the momenta or spatial distributions of the two beams. The analysis assumed π^+ and π^- have the same lifetime, in accord with the CPT theorem. It was fortunate that a parallel goal of this experiment was to test this equality. Analysis of the deuterium data showed $\tau_+/\tau_- = 1.00055 \pm 0.00071$.[1] The fact that the deuterium runs indicated equality showed that the origin of the apparent lifetime difference in the hydrogen runs was indeed the result of the different pulse-height spectra and that there were no other significant plus-minus biases.

It is doubtful that a simple solution will be found for the other

limitation of the movable counter, the counting of decay muons. An improved technique for measuring the efficiency for such spurious counting would be of value. Subsequent experiments, however, may be of the type using a detector which does not distinguish between these muons and pions. No matter what novel experimental method is employed, the beam momentum must be known. Unless refined techniques for determining particle momenta are developed, this requirement will be a limitation on the precision of any future lifetime experiment using particles in flight.

ACKNOWLEDGEMENTS

This experiment necessarily was a group effort. It was made enjoyable and educational for me by my collaborators, Drs. David S. Ayres, David O. Caldwell, Allan M. Cormack, Virgil B. Elings, Robert W. Kenney, and Rollin J. Morrison, and Mr. William P. Hesse. The initial interest in this investigation and the application of focusing Cerenkov counters to the measurement are due to Dr. Caldwell. The success of the experiment owes much to Dr. Ayres, whose thesis was the lifetime-ratio analysis of the data.

I appreciate the continued interest and encouragement of Professors A. Carl Helmholz and Burton J. Moyer.

The experiment benefited from the cooperation of the cyclotron staff and the efforts of many support groups, particularly those involved in counter construction, cryogenic operations, and electronics. Among the great many individuals who provided technical assistance I wish to thank Mr. Cordon R. Kerns for his help with photomultiplier operations.

I am grateful to Miss Miriam L. Machlis for her assistance in preparing and typing this thesis.

This work was supported by the U. S. Atomic Energy Commission.

APPENDICES

A. The Effects of the Width of the Momentum Distribution

Since pions having a lower momentum have more time to decay before traveling a given distance, the momentum distribution of the beam at any downstream position is skewed toward higher values compared to the initial distribution. This fact has two consequences relevant to this experiment. If the width of the beam momentum distribution is sufficiently great, momentum analysis at a downstream point must be corrected to find the distribution existing at the start of the decay path. In addition, the attenuation of the pion beam with distance will differ from that expected for a beam with a unique momentum.

Assume that the normalized momentum distribution function at the start of the decay path ($x = 0$) is

$$f(q) = \frac{1}{\sigma\sqrt{2\pi}} \exp\left(-\frac{q^2}{2\sigma^2}\right) ,$$

where $q = p - p_o$ and p_o is the mean momentum at $x = 0$. Because the number of pions having momentum p decreases with x as $\exp(-mx/p\tau)$, the distribution for arbitrary x is proportional to

$$f(q) \exp\left(-\frac{mx}{(p_o + q)\tau}\right) .$$

To firstforder in the small quantity q/p_o, the normalized distribution at x is $f(q)(1 + nq/p_o)$, where $n \equiv mx/p_o\tau$. The change in mean momentum after n decay lengths is then $\langle q \rangle = \int q\, f(q)(1 + nq/p_o)\, dq = n\sigma^2/p_o$. In this experiment the time-of-flight momentum determination was carried out at $n = 1.14$. By comparing the widths of the electron and pion distributions it is estimated that $\sigma \approx 0.8$ MeV/c. With $p_o = 312$ MeV/c the increase in the mean momentum over the flight path is 0.002 MeV/c, an insignificant

shift.

The second effect of the spread in beam momenta is even less serious. If the momentum distribution at x = 0 is f(q), the fraction of surviving pions at distance x is

$$R(x) = \int f(p - p_o) \exp\left(-\frac{mx}{p\tau}\right) dp.$$

Changing the variable of integration to $q = p - p_o$ and expanding the exponential, we have

$$R(x) = \int f(q) \exp(-n) \left[1 + n\frac{q}{p_o} + \frac{n(n-2)}{2}\frac{q}{p_o} + \ldots\right] dq,$$

with $n = mx/p_o\tau$ as before. Assuming the simple Gaussian form for f(q), we find

$$R(x) \approx \exp(-n) \left[1 + \frac{n(n-2)}{2}\left(\frac{\sigma}{p_o}\right)^2\right] .$$

Since n = 0.5 for our data, the width of the momentum distribution caused a relative increase in the attenuation of no more than 2×10^{-6}.

B. Sources of Rate-Dependent Photomultiplier Gain

Variations of phototube gain associated with changes in counting rate can arise from several sources. The most well-known and most reproducible factor causing changes in gain involves shifts in the voltage levels applied to the dynodes of the tube. More subtle are the changes occurring inside the tube which lead to "fatique"; gain changes from these sources depend upon the previous operating conditions of the tube, as well as the present circumstances.

In a typical photomultiplier base a voltage-divider network allows a single power supply to produce the voltage levels for all dynodes. Problems arise from the fact that the current in the divider string, not only provides the resistive voltage drop which generates the dynode voltages, but also serves as the current source for the secondary electrons produced at each dynode. As the average secondary-electron current increases, the current remaining to continue down the divider string decreases, and the inter-dynode voltages in the last stages decrease. The gain of a stage is diminished because the secondary-emission ratio is lower at a lower voltage.

The greatest internal current is that from the last dynode to the anode, and it is this dynode-anode voltage which is most affected by rate changes. This last stage provides no additional gain: The anode simply collects the secondaries emitted by the last dynode. At high rate, however, this stage can diminish the overall tube gain. As the voltage between the last dynode and the anode decreases, the anode current becomes space-charge limited, and pulse amplitude decreases.

The change in voltage between last dynode and anode can not be considered alone, for a decrease in this voltage must be accompanied by

TECHNICAL INFORMATION DIVISION
LAWRENCE RADIATION LABORATORY
UNIVERSITY OF CALIFORNIA
BERKELEY, CALIFORNIA 94720